

NBSIR 88-3083

AIRCRAFT FIELD DEGRADATION AND ELECTROMAGNETIC COMPATIBILITY

Kenneth H. Cavcey
Dennis S. Friday

National Bureau of Standards
U.S. Department of Commerce
Boulder, Colorado 80303-3328

January 1988

-QC
100
U56
#88-3083
1988
c.2

NBSIR 88-3083

AIRCRAFT FIELD DEGRADATION AND ELECTROMAGNETIC COMPATIBILITY

Kenneth H. Cavcey
Dennis S. Friday

Electromagnetic Fields Division
Center for Electronics and Electrical Engineering
National Engineering Laboratory
National Bureau of Standards
Boulder, Colorado 80303-3328

January 1988

Sponsored by
U.S. Army Aviations Systems Command (AVSCOM)
St. Louis, Missouri 63120-1798



U.S. DEPARTMENT OF COMMERCE, C. William Verity, Secretary

NATIONAL BUREAU OF STANDARDS, Ernest Ambler, Director

CONTENTS

	Page
LIST OF TABLES	v
LIST OF FIGURES	v
ABSTRACT	1
1. INTRODUCTION	1
2. TEST CONFIGURATION	3
3. EXPERIMENTAL DESIGN CONSIDERATIONS	4
4. READING THE PLOTS	7
5. OBSERVATIONS and DISCUSSION	8
6.1 KIOWA	9
6.2 COBRA	10
6.3 BLACKHAWK	11
6.4 CHINOOK	12
6.5 MOHAWK FIXED WING AIRCRAFT	12
6.6 THE THREE HUEYS	13
7. CONCLUSIONS	14
8. REFERENCES	17

LIST OF TABLES

	Page
Table 1. Aircraft Tested	18
Table 2. Active Frequencies for CAAF	19
Table 3. A comparison of noise floors in dBm taken . . with the inside E-field monopole(helicopters running)	20

LIST OF FIGURES

	Page
Figure 1. Field Test Configuration	21
Figure 2. Block Diagram of Electronic System Hardware used for Data Acquisition	22
Figure 3. Transfer Function for the Receiving Up-Converter measured at 1000 Hz	23
Figure 4. Kiowa Helicopter	24
Figure 5. Kiowa Helicopter	25
Figure 6. Kiowa Helicopter	26
Figure 7. Kiowa Helicopter	27
Figure 8. Kiowa Helicopter	28
Figure 9. Kiowa Helicopter	29
Figure 10. Kiowa Helicopter	30
Figure 11. Kiowa Helicopter	31
Figure 12. Kiowa Helicopter	32
Figure 13. Kiowa Helicopter	33
Figure 14. Kiowa Helicopter	34
Figure 15. Kiowa Helicopter	35
Figure 16. Kiowa Helicopter	36
Figure 17. Cobra Helicopter	37
Figure 18. Cobra Helicopter	38
Figure 19. Cobra Helicopter	39
Figure 20. Cobra Helicopter	40
Figure 21. Cobra Helicopter	41
Figure 22. Cobra Helicopter	42
Figure 23. Cobra Helicopter	43
Figure 24. Cobra Helicopter	44
Figure 25. Blackhawk Helicopter	45
Figure 26. Blackhawk Helicopter	46
Figure 27. Blackhawk Helicopter	47
Figure 28. Blackhawk Helicopter	48
Figure 29. Blackhawk Helicopter	49
Figure 30. Blackhawk Helicopter	50
Figure 31. Blackhawk Helicopter	51
Figure 32. Blackhawk Helicopter	52
Figure 33. Blackhawk Helicopter	53
Figure 34. Chinook Helicopter	54
Figure 35. Chinook Helicopter	55
Figure 36. Chinook Helicopter	56
Figure 37. Transfer Function for a Small Size H-field Current Clamp - Serial No. 156.	57

Figure 38.	Transfer Function for a Small Size H-field Current Clamp - Serial No. 143.	58
Figure 39.	Transfer Function for a Medium Size H-field Current Clamp - Serial No. 539.	59
Figure 40.	Transfer Function for a Medium Size H-field Current Clamp - Serial No. 55	60
Figure 41.	Transfer Function for a Large Size H-field Current Clamp - Serial No. 22	61
Figure 42.	Chinook Helicopter	62
Figure 43.	Chinook Helicopter	63
Figure 44.	Chinook Helicopter	64
Figure 45.	Chinook Helicopter	65
Figure 46.	Chinook Helicopter	66
Figure 47.	Chinook Helicopter	67
Figure 48.	Mohawk Airplane	68
Figure 49.	Mohawk Airplane	69
Figure 50.	Mohawk Airplane	70
Figure 51.	Mohawk Airplane	71
Figure 52.	Mohawk Airplane	72
Figure 53.	Mohawk Airplane	73
Figure 54.	Mohawk Airplane	74
Figure 55.	Mohawk Airplane	75
Figure 56.	Mohawk Airplane	76
Figure 57.	Mohawk Airplane	77
Figure 58.	Mohawk Airplane	78
Figure 59.	Mohawk Airplane	79
Figure 60.	Mohawk Airplane	80
Figure 61.	Mohawk Airplane	81
Figure 62.	Mohawk Airplane	82
Figure 63.	Mohawk Airplane	83
Figure 64.	Huey Helicopter No. 1	84
Figure 65.	Huey Helicopter No. 2	85
Figure 66.	Huey Helicopter No. 2	86
Figure 67.	Huey Helicopter No. 2	87
Figure 68.	Huey Helicopter No. 2	88
Figure 69.	Huey Helicopter No. 3	89
Figure 70.	Huey Helicopter No. 3	90
Figure 71.	Huey No. 2	91
Figure 72.	Huey No. 3	92
Figure 73.	A comparison of the NOISE floor for Hueys No. 2 and No. 3	93

AIRCRAFT FIELD DEGRADATION AND ELECTROMAGNETIC COMPATIBILITY

Kenneth H. Cavcey and Dennis S. Friday
Electromagnetic Fields Division
National Bureau of Standards
Boulder, Colorado 80303

This paper discusses the first tests undertaken to study the problem of field degradation in army aircraft (helicopters and one fixed wing airplane) due to the deterioration of electronic and electrical systems. The electromagnetic compatibility (EMC) of such systems was investigated by passive measurement of the aircraft as a collection of radio frequency sources. Methods for detection of these sources were developed that included sensitivity to both stationary and nonstationary noise that existed.

The collected data were studied to see if there existed any obvious factors derived from the data that one could use to correct potential problems that might affect flight safety. Emphasis was placed upon making such test methods appropriate, inexpensive, and easily performed by army field personnel. In addition, applications to quality control or acceptance testing, as related to the Environmental Stress Screening (ESS) program, are examined.

Key words: bandwidth; data acquisition; electromagnetic compatibility (EMC); electromagnetic interference (EMI); electromagnetic spectrum; field probes (or antenna); noise floor; noise sources; spectrum analyzer.

1. INTRODUCTION

The problem of aircraft (helicopter) field degradation due to deterioration of the aircraft's electrical and electronic systems was studied via experimental field testing. Radiated emissions from the aircraft under test were detected over the spectrum of frequencies ranging from 100 Hz to 500 MHz using three different kinds of sensing probes. The data that were taken suggest a possible future technique that if successful could alert U.S. Army product assurance personnel of potential problems. Correction of these electrical and/or electronic systems would mitigate the interference thus assuring aircraft integrity and safety.

The problem of field degradation of electromagnetic compatibility (EMC) can be studied from several viewpoints. An aircraft's electronic hardware system should function independent

of other outside or inside sources of electromagnetic radiation that might impair its ability to complete its basic mission. This is of course based upon the premise that its original design is such that each subsystem will not affect any of the others irrespective of the number and type activated (example: communications and fire control). In almost all aircraft electrical systems, the design is such that specific components can be added or deleted without affecting the overall EMC integrity. As discussed later, this has not always been the case.

Noise from cables and connectors were studied by Shands and Woody [1]. They found that intermodulation (IM) noise as strong as 40 dBm was generated when a cable network was radiated with EM energy in the 22 to 425 MHz region. Connectors were found to be the major offenders when subjected to mechanical vibration. Noise can also be generated by defective ground or multiple tie points. In a later study, the same investigators [2] found that Metal-Insulative-Metal (MIM) junctions produced even more noise than the cable system. Watson [3] studied the same phenomena with relation to naval radio systems. He also found MIMs induced noise on ships which may be mitigated by:

- 1) cleaning, reassembly and welding short flexible shorting straps across the junction or
- 2) applying a special chemical compound to quench the rectifying action of the MIM.

Other investigators [4] have used acoustics and other forms of radiation, but the work was limited to laboratory efforts on simulated structures with results that are not directly comparable to the work of this report.

This report covers work that was performed on seven helicopters and one fixed wing aircraft to see whether EMC degradation could result from:

- a) penetration from outside known or unknown sources;
- b) interaction of subsystems from a static and dynamic test (avionics on - engines off or on);
- c) sources with and without the presence of the aircraft;
- d) the generation of unknown sources due to radiation from any known source impinging on the airframe skin due to faulty connections (ground or otherwise).

All of these potential problems were studied to determine a method or technique of locating potentially dangerous electromagnetic emissions. This interference leads to system EMC degradation. If it can be detected by U.S. Army Product Assurance

Personnel and be corrected, the corrective action will insure electrical/electronic systems integrity and aircraft safety.

The tests were performed at the U.S. Army Aviation Development Test Activity Center (AVNDTA) located at Carins Army Air Field (CAAF), which is part of Ft. Rucker, Alabama. This report covers the measurement techniques, the test configuration and the experiments that were conducted. Data that were collected (spectrum plots and time series) are presented and interpreted in light of the constraints placed upon those tests. In addition, the validity of the methods are discussed and suggestions for further work are proposed.

2. TEST CONFIGURATION

All of the measurements at Carins Army Air Field were made at a location known as "Chinook Hill". The hill is an elevated flat grassy hill overlooking the flight line and field where most of the helicopters are parked and are flown. Figure 1 shows the relative location of the van containing the measurement electronics, interconnecting cables, and the aircraft under test. The figure also shows the relative locations of the electromagnetic field probes and current clamps. Except for the probe directly in front of the aircraft nose (kept at a constant 1 meter distance), the other field probes and field cable clamps were located as permitted depending upon the specific aircraft under test.

Figure 2 shows a block diagram of the electronics hardware used for all tests. Data acquisition was accomplished as follows:

- a) A commercially available package written in BASIC version 3.0 for the MS-DOS operating system was used for obtaining the spectrum plots.
- b) A special program written in the "C" language and linked to the object code written for the IEEE-488 interface card in the computer was used for obtaining the time series data.

The hardware performed the two tasks corresponding to (a) and (b) above. In the task under (a), an additional piece of hardware was built so that frequencies below 50 kHz (the lower limit of the spectrum analyzer) could be covered. This hardware was built so mechanical vibrations, that might result in low frequency radiation, could be sensed. To accomplish this measurement, a 100 kHz up-converter was used that provided an 8 dB gain. Figure 3 shows the voltage input to output transfer function of the converter at a frequency of 1 kHz. The unit is linear in response and allows coverage down to frequencies of 200 Hz or less. The local oscillator in this circuit has to be stable

and spectrally pure so that frequency determination is accurate and spurious products from the mixer are minimized. The circuit that was used incorporates a crystal oscillator, filter and buffer with the second harmonic (200 kHz) being attenuated over 40 dB with reference to the fundamental. The higher harmonics are attenuated in excess of 60 dB.

The mixer part of the circuit uses a commercial integrated circuit (designed for radio communications) that results in a linear voltage transfer function. For example, switching in the convertor after setting up the spectrum analyzer to cover 100 kHz to 600 kHz results in a frequency coverage range of nearly dc to 500 kHz with a span of 50 kHz per division. In the range 200 kHz to 150 MHz the mixer provides an additional gain of 8 dB over the gain of the spectrum analyzer.

Under (b) which is the second task (time series) the data were acquired in the following manner. First, the signal of interest was tuned in with the spectrum analyzer at a selectable bandwidth up to 1 MHz (at lower frequencies this bandwidth must be less). Next, the 10 MHz IF signal (obtainable from the spectrum analyzer) is detected or converted from ac to a time varying dc value. Finally, by means of a system digital voltmeter the dc signal is sampled as programmed and transferred through the IEEE-488 bus to the computer. It is important to note that the spectrum analyzer is used in the zero swept mode, when taking time series measurements at a predetermined tuned frequency.

The data were taken in strings of 7 ASCII characters up to 9000 points in length (63 kB) and then stored in the virtual "D" memory space of the computer. The data files were then transferred onto floppy disks for analysis at a later time.

3. EXPERIMENTAL DESIGN CONSIDERATIONS

It must be emphasized that this study was exploratory in nature and the intent was to acquire whatever information was present in the electromagnetic fields being emitted from the aircraft. A crucial consideration in designing these experiments was that they not be compromised by any bias toward any prior theories on the nature of the emissions. This approach was validated as our data exhibited information in ways that we had not preconceived, nor theorized. More on this later in the report.

The experimental procedures changed between the first aircraft (Kiowa) and later aircraft. Preliminary examinations of the data provided insights by which the procedures were modified to obtain the information more efficiently. This was a prime consideration since some of the aircraft were available only for limited times. Testing for all of the aircraft was performed in

as uniform a manner as possible, considering all of the constraints under which the tests were performed.

Three different types of probes were used for sensing the aircraft's electromagnetic emissions: E-field probes, H-field probes and H-field current clamps. The E and H probes were placed in and around the aircraft and the current clamps were attached to strategically located wiring harnesses inside the airframe.

Three loop H-field probes were used at first. One probe, which is referred to as "the large H-field probe," was approximately 0.763 meter in diameter and operated over a single frequency band. The remaining two loops were smaller, and are referred to as the small H-field probes. These were adjustable over eight smaller frequency bands. Five H-field current clamps were used; one of which was large (0.067 meter in diameter) and somewhat heavy. It could be used only where adequate space, cable size and physical support were available. Two of the clamps were of medium size (0.032 meters in diameter) and two were relatively small (0.019 meters in diameter). These dimensions are the inside dimension of the toroidal shaped clamps and indicate the largest size of cable they can be attached to. In the text to follow they are referred to as the large, medium and small clamps respectively. Placement of the probes inside the aircraft was constrained by the geometry of the aircraft by the need for a pilot (and sometimes a copilot) to operate the aircraft, and by safety considerations. The safety requirement dictated the aircraft and surrounding area be free of any loose cables, probes, or other equipment when the rotors or propellers were turning.

Two E-field probes were used in the experiment. Each probe was a broad band vertically mounted monopole of adjustable length. The larger one (1.00 meter maximum length) was used only for monitoring the field external to the aircraft because its large base and length, when extended, prevented its use in several of the aircraft. The small E-field probe (0.356 meters maximum length) was selected for internal use and was mounted on a small block of foam. It was difficult to find a consistent location on all the aircraft for placement of the internal probes because of the differing aircraft geometries.

In the cases of the three Hueys, the Chinook, and the Blackhawk helicopters, there was a large personnel/cargo area behind the cockpit, and the small E-field probe was mounted vertically on the floor, or on a seat, as far away from surrounding conductive surfaces as possible. In the cases of the Cobra helicopter and the Mohawk airplane, the cockpit was extremely confined and there was no personnel/cargo area. On the Cobra the E-field probe was placed on a shelf behind the pilots seat (the rear of the two tandem seats). On the Mohawk the

cockpit was so constrained that it was not possible to place the probe in the same cavity as the crew. This was also the case for the other aircraft. There were a series of chambers in the main part of the fuselage, which were inter-connected by openings in the longitudinal walls. The internal E-field probe was placed centrally in this cavity. The Kiowa was the only aircraft tested without an internal E-field probe.

The large E-field probe was placed on the ground in front of the aircraft, on center, exactly 1 meter from the end of the pitot tube or, the extreme point of the nose. This monopole was fully extended for all of the tests. With the varying topologies of the aircraft this was a location which could be replicated. The probe had to be fixed (probes were not allowed to be moved around an operating aircraft) for safety reasons. A more important feature of this location was that all of the aircraft had plexiglass canopies or bubbles in the forward fuselage. This was often the major skin material in this region. Any fields generated inside the aircraft cavity would therefore be likely to leak through the acrylic plastic ports and be stronger in this region than at any other location relative to all of the aircraft.

The choice of location of the H-field probes was similarly constrained. The large H-field probe was placed centrally in the relatively small personnel/cargo area. Since there were two small identical H-field probes (electrostatically shielded loops), we decided to use one internal and one external to the aircraft. The placement of two such probes in electrically distinct locations inside all of the aircraft was not always possible. The large H-field probe (another loop) was used only internally. Its light weight and large size and surface area rendered it unsafe for external use anywhere within or near the radius of the rotor blades. This probe was used only on the Kiowa when later it was determined that the same information was better obtained from the small E-field monopole. The small external H-field probe was mounted on a wooden tripod 30 meters in front of the aircraft. This probe was high enough that it had to be out of range of the rotors and the resulting air downwash. Placing it in this location put it in the same optimal region relative to the helicopter as the external E-field probe.

The H-field current clamps, the third type of probe, were used on all of the helicopters in different configurations. Their placement was constrained by cable location, cable size, the space surrounding the cable, the weight of the current clamp and safety considerations. Within these limitations, the clamps were dispersed, as much as possible throughout the airframe on different cables. The objective was to identify any strong localized emissions from sources interior to the aircraft.

Functional labeling of the harnesses was nonexistent and electronic technicians on the base had only limited knowledge of the function of some of the harnesses. Distributing the clamps to accessible harnesses in different regions of the aircraft was the only reasonable alternative within these limitations.

4. READING THE PLOTS

Important to the understanding of this report is the correct interpretation of each spectrum plot included herein. The following discussion is to assist the reader in this task.

For example, refer to plot D06067 (Figure 20) acquired at time 14:09:48 on December 6, 1986. The top contains information on the reference level, the center frequency of the frequency range (abscissa) and the span or frequency per horizontal division.

If, in the text of this report, the up-converter is not used, figure 20 is read in the following manner:

Plot D06067 (Figure 20)

- 1) All horizontal scale lines start at the top at a reference level of -60 dBm.
- 2) One division down would be -70 dBm as stated by the VERT DISPLAY statement of 10 dB/div in the lower left hand corner of the plot.
- 3) In this example the ordinate range is from -60 dBm at the top to -140 dBm at the bottom. Note that the average noise floor is about -93 dBm for this plot.
- 4) The span is 5 kHz/div, the center frequency of 125 kHz is shown in the top center, and the abscissa range is from 100 kHz to 150 kHz.
- 5) The video filter (VID FILTER) is off and the RES BANDW (or bandwidth of the spectrum analyzer) is set to 10 kHz. This information is important because the amount of noise recorded is a function of the received bandwidth.
- 6) The bottom statement of 0-1.8 FREQ RANGE can be ignored because it is just a statement of range for the instrument (the 1.8 is GHz). This is somewhat misleading because in reality the lowest frequency that can be covered without a loss in gain is 50 kHz according to the specifications of the instrument.

When the up-converter was switched on (for all aircraft observed

after the Kiowa) the two things that changed were the frequency range and the gain. The purpose of the convertor is to up-convert from lower frequencies. Subtract 100 kHz from all horizontal readings. Statement (4) now reads as follows:

- 4a) The span is 5 kHz per horizontal division, and the abscissa range is from 0 to 50 kHz. In addition, since the up-convertor exhibits an 8 dB gain, the RF ATTN statement should read +8 instead of 0 as is shown and the REF LEVEL would be interpreted as -52 dBm.

At higher frequency spans the 100 kHz conversion frequency is insignificant. At lower frequencies the interpretation is reversed. Consider figure 7 and its abscissa. For plots like this, subtract the 100 kHz; thus the 95 to 105 kHz range is shifted to -5 to 5 kHz range, folded about zero in frequency, similar to a double sided Fourier spectrum plot. Plots like this are read only on the right side of zero frequency. Remember that the up-convertor was used on all aircraft after the Kiowa.

5. OBSERVATIONS and DISCUSSION

Over 700 spectral and time series observations were recorded during a seven-day testing period on the various aircraft available. It should be stated that this study is not an exhaustive one. The large amounts of data recovered were a first look at radiated emissions in and around the aircraft under all the given test conditions.

As testing progressed, experimental conditions were changed in an effort to eliminate redundancy and obtain the most relevant data. Equipment configurations as well as antenna and probe selection and placement played an important part in obtaining usable results. As might be expected in this type of evolutionary process, other factors will be considered in future tests, now that the first study has been completed.

The sequence of helicopters tested was determined by the base flight operations group. Each is discussed separately except for the three Hueys which are discussed as a group. Consequently, the report will depict what was measured in a chronological fashion. Discussion of the Hueys is carried out jointly because their data may exhibit similarities due to their common geometry.

In the measurement scheme or experimental plan we hoped that several helicopters of the same type but of differing age and/or flight time could be tested so that one could look for EMC degradation as a function of use. As the discussion progresses it should become obvious that this plan was not fully achieved due to circumstances beyond our control. However, this did not deter the basic exploratory goals of the test.

Table 1 is a list of every aircraft tested and is arranged in the order they were made available for testing. Table 2 is a list of radio frequencies that the army uses and that were observed across the electromagnetic spectra. Examination of the plots referenced in the aircraft topics should be made keeping these frequencies in mind.

6.1 KIOWA

This was the first aircraft tested, and we stepped through the entire frequency domain (dc-500 MHz) in small increments without the avionics or engine running to acquire a look at the ambient background noise and to observe those radio services that were supposed to be present in the environment. The probe used for this purpose was the external E-field unit located off the aircraft's nose. A typical plot recorded from this series is that of figure 4 which shows the 50-100 MHz region with local FM radio stations clearly visible above a -82 dBm background. This is a typical plot. Only plots of special interest are shown, because of the many that were taken.

On all aircraft, plots were taken under the following conditions: (1) quiet, or (2) engine and avionics on. Two small and one large H-field loops were used to acquire the data. Comparing data acquired by the H-field loops and the E-field probes implies that the loops were unnecessary. In addition the loops are bandwidth limited and required tuning when switching between frequency ranges. Since they were physically large compared to the monopoles and somewhat insensitive, their use was discontinued on all aircraft after the Cobra.

The first unidentifiable signal detected in the spectrum measurements was referred to by our army liaison officer as a classified low frequency source. This signal as depicted in figures 5, 6, 7 and 8 appears as a cluster of pulses moving through the lower frequencies varying in both frequency and amplitude. This signal was first seen on the external E-field probe. It was later decided to see whether the aircraft itself would pickup any signals by way of it's conductive surface. A coaxial cable was attached from the nose of the Kiowa via the Pitot tube and another was attached to a tie-down bracket located on the tail boom. The cables were connected to the spectrum analyzer via a 4:1 balun. As seen in figure 9 (helicopter running) the airframe itself is an excellent antenna. This phenomenon helped explain plots on other aircraft in which this same signal was present on certain cables, wiring between systems, and an internal E-field antenna that was added on the Cobra helicopter. It is believed that the physical mechanism responsible for the coupling to the field is either by ground connections to cable shields (in which radiated currents can flow) or capacitive coupling (as in the case of any conductor

located close to the airframe) or by physical contact with a suitable dielectric.

The Kiowa was considered to be an electrically noisy aircraft when compared to the others tested. Even though an internal E-field probe was not used until later, data from the H-field probes and the external E-field monopole confirm this fact. Noise can be categorized under several different definitions which have been observed in the electromagnetic spectrum. The most general noise definition is a non-stationary process emitted from either a known or unknown source of a random amplitude and bandwidth. In the case of the Kiowa, the noise detected seemed to depend on whether or not the avionics were turned on. Figures 10 and 11 from the external E-field probe suggest a repetitive process which may be an electronic switching circuit associated with the on-board power supplies. These plots show the noise extending up to 6 MHz. Figures 12, 13 and 14 are from the medium size H-field current clamp located on a cable near the left front windshield. Figures 15 and 16 show the noise on a small cable located in the left rear bay of the aircraft (0-1 and 0-5 kHz). Even though the noise floor is relatively low (-110 dBm in figure 15) the actual signal variation is plus or minus 10 dB for a 100 Hz bandwidth. This would show a higher level of noise if the bandwidth were increased. This increase in bandwidth was implemented later in the testing process. As the work continued, measurement techniques were changed, but references were chosen and adhered to for comparison purposes.

6.2 COBRA

An internal E-field probe was first used on the Cobra. Since the cockpit is a tandem arrangement, placement of the probe was restricted to a location behind the pilots seat. Figures 17, 18 and 19 are spectra taken with this probe showing the OP communications transmitters on board the helicopter at 36.4, 138.8 and 242.1 MHz. Note that due to the strong near field, 30 dB of rf attenuation was switched in at the spectrum analyzer to avoid overloading.

The spectral plots for the E-field probes did not reveal any significant EMI with the exception of the low frequency jamming signal (previously discussed) present on the internal probe (figure 20).

Two medium clamps were located in the rear section of the cockpit. Only one showed a change between the helicopter running and quiet. Behind the pilot's seat, a clamp was placed near three control boxes marked in one location as attitude control. Figure 21 displays electronic switching noise 10 dB higher than the noise floor with a repetition rate of approximately 275 kHz.

Figure 22 shows the quiet or ambient noise floor. All other features appeared normal.

The Cobra was the last ship to use the H-field loop probes. The small external loop displayed the same noise floor at a 10 kHz bandwidth as the other probes (-95 dBm). When the same kind of probe was placed internal, the first apparent feature was shielding from outside sources such as the ADF signal at 560 kHz (see Figures 23 and 24 for comparison purposes). Other plots seemed to be normal.

6.3 BLACKHAWK

All of the E-field plots seemed normal with the exception of those viewed in the 10 to 50 MHz region. The noise shown in figures 25 and 26 indicates that for some reason the environment itself was the problem since the noise was most apparent on the external probe.

Inside the aircraft, the H-field current clamps revealed another picture. On the large clamp to the left behind the copilot, electronic switching noise was detected with a repetition rate of about 75 kHz. The spectrum affected ran from about 1.8 to 9.5 MHz. The noise peaks were raised 25 dB in the running case as compared to the common noise floor of -90 dBm. These results can be viewed on figures 27 and 28. The medium clamp located behind the right side of the instrument panel showed the same general result with a slightly lower amplitude change (figures 29 and 30). Another interesting observation was made with the clamp located behind the left instrument panel. A signal or noise was observed when the avionics and or engines were shut down. Figure 31 shows the signal as some type of switched electronic source over the 1 to 10 MHz region. A check of the external E-field probe at the time when the noise was detected inside the airframe proved negative (no signal; see figure 33). No conclusion can be made whether the signal should or should not be present under what appeared to be reversed conditions. Up to this point, noise and/or helicopter generated signals were detected under "avionics on or engine running" conditions. The signal was also detected on a medium sized field clamp located under the right side of the instrument panel. Because the amplitude was reduced by about 30 dB we might conclude that the clamp was located further away from the source than the previous clamp (see Figure 29). The signal is again seen on figure 27 which is the output from a large clamp that was positioned behind the left copilot's seat. Here the signal is stronger than that seen behind the right instrument panel, but still weaker than the left instrument location. When the helicopter was powered up, the amplitudes in the same frequency region dropped considerably as seen in figure 30. Further comments on what was seen in this figure will be made later.

6.4 CHINOOK

The spectra collected by the E-field probes (both internal and external) showed very little information with the helicopter running or quiet. As a result, the discussion will concentrate on the H-field current clamps.

The medium sized clamp located under the left cockpit instrument panel demonstrated an increase in the noise floor (0-50 kHz) with the helicopter running. The average noise power can be calculated from equation (1) with reference to 1 milliwatt. This calculation is done with reference to the 50-ohm input impedance of the spectrum analyzer.

$$\text{dBm} = 10 \log_{10} \left[\frac{P(\text{watts})}{0.001} \right] \quad (1)$$

As shown in figures 34 and 35 the noise floor increases only 10 dB from -105 to -95 dBm. The noise power at this level is equivalent to 3.162×10^{-13} watts. In reality this is a very weak field and the measurement system exhibits sensitivity in making the measurements and its ability to see all emissions. Examination of figure 36 shows the noise up to frequencies of 600 kHz.

In the front cockpit a small clamp was attached to a cable entering the compass. The noise floor over the spectrum of 500 kHz to 10 MHz increased 10 dB or so with the helicopter running. Above 10 MHz little of interest was observed. All of the H-field clamps operate over only a specific range of frequencies. All the H-field clamps used in these tests cut off at the high frequency end at approximately 100 MHz. Figures 37-41 are the transfer functions (transfer impedance in dB as a function of frequency in MHz) for the five clamps used.

The CH-47HC Chinook was built primarily for transporting troops and material. In the main bay in the right forward section of this volume, circuitry was found near a heating unit. Here the large H-field clamp was slipped over a large cable bundle. In the dc to 50 kHz region the noise floor was found to be over 40 dB higher when the heating unit was activated. From 50 kHz up to 900 kHz the noise floor dropped by 30 dB. From 900 kHz to 5 MHz the noise continued to drop until it leveled off at -90 dBm. Compare figures 42, 43, and 44 with figures 45, 46 and 47. The source feeding this heater or nearby circuitry is unknown. The spectrum plots clearly indicate a potentially harmful source of EMI.

6.5 MOHAWK FIXED WING AIRCRAFT

When the engines and avionics were activated, the noise in

the rear belly bay jumped considerably as detected by a large H-field current clamp. This clamp was attached to some power cabling. The base line or noise floor was observed to be 40 dB higher than the ambient, when measured at a 1 kHz bandwidth (see figures 48 and 49). Figure 50 (-0.045 kHz to 0.900 MHz) shows the same phenomena and the ADF at 560 kHz can be seen on figure 51.

Figure 52 which covers 0.9 MHz to 9.9 MHz shows electronic switching noise that appears to change at a 10 kHz rate. The noise is 30 dB stronger than the quiet base line as seen in figure 53. A strong local AM radio station at 1560 kHz can be seen through the noise. At higher frequencies the noise drops off with little difference being seen as shown in figures 54 and 55. The same noise was observed on another current clamp. This medium size clamp was located in the rear bay and coupled to a cable of a smaller physical diameter (see figures 56 and 57).

In the cockpit small diameter H-field current clamps were attached to both sides of the instrument panel. The same noise seen previously was observed on the left side as seen in figure 58. On the right side the signal was not as strong over the spectrum (Figure 59). The local AM radio station mentioned before was 10 dB higher (figure 60) than that seen in the belly bay due to the acrylic plastic windows in the nose of the aircraft. Generally these external signals are suppressed because of the design of the H-field current clamps. RF currents flowing in the wire bundles where the clamps are attached create the fields in the toroidal cores of the clamps which are coupled by a separate winding. This means that in the case of an external source, impingement onto the aircraft's skin and radiation through acrylic plastic windows on to exposed wire bundling is sufficient to create the signals observed. Small coaxial cabling attached throughout the airframe is not excluded from this general problem. As long as there are conductive surfaces exposed to external radiation, rf circulating currents will be generated if improper termination exists.

Figures 61 and 62 show that the previously mentioned low-frequency jamming signal is also present on some of the aircraft's wiring. Figure 63 is a magnified view of this signal frozen in time for detailed observation purposes. This plot was obtained by increasing the vertical sensitivity to 2 dB per division. These plots were acquired from a small H-field clamp located under the left hand side of the instrument panel. In comparison to the previous aircraft, nothing unusual was seen on the E-field probe.

6.6 THE THREE HUEYS

These three aircraft were obtained at various times from the flight line when available. Since the Huey UH-1H helicopter is

the primary aircraft for training at CAAF, more of them were available. They were easier to acquire, but they were not identical in the way they were equipped from a systems wiring viewpoint.

Each helicopter demonstrated individual characteristics as far as detectable noise was concerned. In addition, the noise floor for each spectrum segment was generally the same except for the third or last aircraft. The first Huey showed electronic switching noise at around 100 kHz and was relatively weak at -80 dBm. The signal was picked up on the small H-field current clamp located on the left side under the instrument panel (see figure 64).

In the second Huey, noise was detected in the 3 to 4 MHz region (Figure 65) when the engine was running. This noise was detected on a small H-field clamp located on a cable in the right rear bay of the aircraft. Noise, at 330 kHz at -88 dBm, was detected on a medium H-field clamp located in the left rear bay (see Figure 66). In the same time frame that data were being collected on the clamps, the internal E-field monopole detected a noisy environment of -62 dBm for frequencies from 15 to 40 MHz. Some of the same features showed up in the quiet plots taken (see Figures 67 and 68). As a result, the only statement that can be made is that the noise in the spectral region is most likely external and the source or sources could not be identified. When the third Huey was tested all of the noise floors were higher with the engine and avionics running than in the first two. The major source of switching noise detected in Huey no. 3 was determined to be in the low frequency spectrum at around 235 kHz as detected inside the right rear panel by a small H-field current clamp. This noise was measured at -67 dBm plus or minus 18 dB (see Figures 69 and 70). No other signals were found but, due to the high ambient noise floor, others may exist.

7. CONCLUSIONS

Noise detected in the range of frequencies studied (dc to 500 MHz) can originate from various sources. The topic of noise has been investigated for many years and several general categories have been defined in an attempt to describe the process based upon the source.

EMC degradation is by definition a condition which is brought on by man-made noise even though unintentional. Propagation of the interfering signals can occur by unknown paths. In some cases, multiple paths can exist complicating the task of noise signal elimination. In general, investigators [5] have found that the amplitude of man-made noise decreases with increasing frequency and varies considerably with geographic location. Propagation is from power lines, ground waves and ionospheric reflection at frequencies below the maximum usable

frequency. Measurements of the noise indicate that peak levels are not proportional to received bandwidths for bandwidths greater than 10 kHz. This was often found to be the case in this study when the starting point in the spectrum was higher than approximately 1 MHz.

The propagation mechanism of what is believed to be unwanted signals in the aircraft tested is still not clear. Exact source locations were not determined for any of the signals detected due to the constraints of the experiment. Studies of the spectrum plots have indicated that the noise can either be periodic or nonstationary.

An example of a periodic process is that of electronic switching noise which is characterized by its regular change in amplitude as a function of frequency. Most of the time these types of signals were found to exist on H-field current clamps attached around wire bundles associated with aircraft power circuits. Sometimes they were strong enough to be detectable by the internal E-field monopole, which indicates a radiated near-field situation. This radiation may take place because of poor wiring practice due either to ground loops or nonexistent grounds on cables where they should exist. This is an area for further study in light of what maximum signal levels can be considered to be tolerable. To explore the situation would probably require a comprehensive matrix approach similar to that employed by some aircraft manufactures using EMI techniques with EMI instrumentation.

Random or nonstationary category noise was also studied for each aircraft tested. The internal E-field signal was observed as a noise floor plus amplitude variations riding on it. In this way of observing noise, with the aircraft quiet or running, we assume that the aircraft makes a contribution to what is seen through either a source consideration or an incident field modification process. Table 3 is a comparison of noise floors for the various aircraft tested and the nonstationary variation riding on that floor with the engines and avionics running.

Several facts can be deduced from the data shown on table 3. Over the five frequency segments covered, with specific exceptions as noted in the discussion for periodic noise, all of the aircraft except for one exhibited the same amount of generated noise. Levels ran from -82 to -112 dBm for received bandwidths of 1 kHz to 1 MHz. The only aircraft that appeared to be noisier than the rest was the third Huey tested. With 10 dB of attenuation switched in at the spectrum analyzer, the noise floor was measured to be about 10 dB higher on average over the same range of frequencies than the other aircraft. The amplitude variations were also twice as large. A common practice used in the location of broadband noise sources is to determine the highest frequency detectable because, with most man-made sources,

the amplitude is an inverse function of the frequency. If the geographical location of the source is approached, the near field of higher spectral components are penetrated until the source location is discovered.

The noise data for Huey no. 3 suggest that, even though the source locations were not found, they were associated with the helicopter since high frequency noise components did exist. As an example, figure 71 (Huey no. 2, 1-100 MHz) was overlaid on figure 72 (Huey no. 3, same frequency range). The result, figure 73, depicts graphically what table 3 indicates with the numbers. When viewing this plot remember that 10 dB of attenuation was switched in on Huey no. 2 beneath would not have easily been identified. It is also interesting to note that Huey no. 3, identifies itself by way of its serial number as the oldest of the three tested. The data may indicate that structural degradation is occurring and that further testing should be done.

Each Huey was found to be different from an electrical system viewpoint so we must be careful not to make specific conclusions at this time regarding the findings just presented. The additional noise found and the way it manifested itself does support and justify the need for further research and testing. The experimental technique, although not perfected at this time, also demonstrates the ability to detect possible EMC degradation of sources through the reception and interpretation of noise floor data. As a result, it suggests that more work be performed building upon the knowledge gained from these tests.

From an EMI environmental viewpoint, a system matrix study performed in an electromagnetically quiet location as a function of aircraft geometry and spectral frequency now appears to be a next new starting point. The results should then be directly convertible into hardware that quality assurance could use in the Environmental Stress Screening (ESS) program.

8. REFERENCES

- [1] Shands, T.G. and Woody, J.A., Investigation of Intermodulation Products Generated in Coaxial Cables and Connectors, Rome Air Development Center, Air Force Systems Command, Griffiss Air Force Base, N.Y. 13441, Final Technical Report RADC-TR-82-240, September 1982.
- [2] Shands, T.G. and Woody, J.A., Metal-Insulator-Metal Junctions as Surface Sources of Intermodulation, Rome Air Development Center, Griffiss Air Force Base, N.Y. 13441, Final Technical Report RADC-TR-83-31, February 1983.
- [3] Watson, A.W.D., Improvements in the Suppression of External Nonlinearities (Rusty Bolt Effects) Which Affect Naval Radio Systems, IEEE International Symposium on Electromagnetic Compatibility, Arlington, Va., August 1983.
- [4] Denney, H.W., Acree, D.W. and Mantovani, J.C., EMC Measurement Techniques for Aircraft, Rome Air Development Center, Griffiss Air Force Base, N.Y. 13441, Final Technical Report RADC-TR-83-166, July 1983.
- [5] Reference Data for Radio Engineers, Sixth Edition, Howard W. Sams & Co. Inc., Indianapolis, In., 1979.

TABLE 1 Aircraft Tested

<u>Date Received</u>	<u>Aircraft</u>	<u>Serial No.</u>
12-04-86	OH-58A Kiowa	70-15612
12-06-86	JAH-15 Cobra	77-22766
12-06-86	UH-1H Huey	72-21574
12-07-86	UH-60A Blackhawk	86-24507
12-07-86	UH-1H Huey	66-17080
12-08-86	CH-47C Chinook	68-15862
12-08-86	UH-1H Huey	66-850
12-09-86	OV-1D Mohawk	68-16992

TABLE 2 Active Frequencies for CAAF

<u>Radio Service</u>	<u>Frequency for CAAF</u>
ADF	560 KHz
OP	36.4, 138.8 & 244.8 MHz 242.1 MHz
VOR	111.2 MHz
GCA	125.4, 125.8, 128.55 MHz 133.45, 133.75, 134.1 MHz 229.6, 232.5, 234.4 MHz 237.5, 242.6, 370.3 MHz
TWR	121.9, 127.0, 127.95 MHz 241.0, 242.1, 248.20 MHz 347.5 MHz
IFF	1200 MHz
RADAR	1030, 2762, 2800 MHz 9080 MHz

TABLE 3. A comparison of noise floors in dBm taken with
the inside E-field monopole (helicopters running).

<u>FREQUENCY RANGE</u>	<u>BLACKHAWK</u>	<u>CHINOOK</u>	<u>COBRA</u>	<u>MOHAWK</u>
0 - 50 kHz	-105 ± 9	-105 ± 10	- 94 ± 7	-104 ± 9
50 kHz - 1 MHz	- 99 ± 7	- 99 ± 6	-100 ± 7	- 98 ± 4
1 MHz - 10 MHz	- 90 ± 6	- 90 ± 5.5	- 99 ± 5	- 90 ± 4
10 MHz - 100 MHz	- 82 ± 6	- 83 ± 4.5	- 99 ± 5	- 82 ± 4
100 MHz - 500 MHz	- 82 ± 4	- 82 ± 4.5	-101 ± 4	- 82 ± 3

<u>FREQUENCY RANGE</u>	<u>HUEY NO. 1</u>	<u>HUEY NO. 2</u>	<u>HUEY NO. 3</u>
0 - 50 kHz	-104 ± 10	-112 ± 10	- 93 ± 18
50 kHz - 1 MHz	-103 ± 7	-103 ± 7.5	- 90 ± 14
1 MHz - 10 MHz	-103 ± 7	- 90 ± 5	- 80 ± 8
10 MHz - 100 MHz	-105 ± 5	- 82 ± 5	- 73 ± 6
100 MHz - 500 MHz	-114 ± 5	- 83 ± 4.5	- 73 ± 6

NOTE: Kiowa data not included because the up-converctor was not used making
the noise figure different and therefore the data uncomparable.

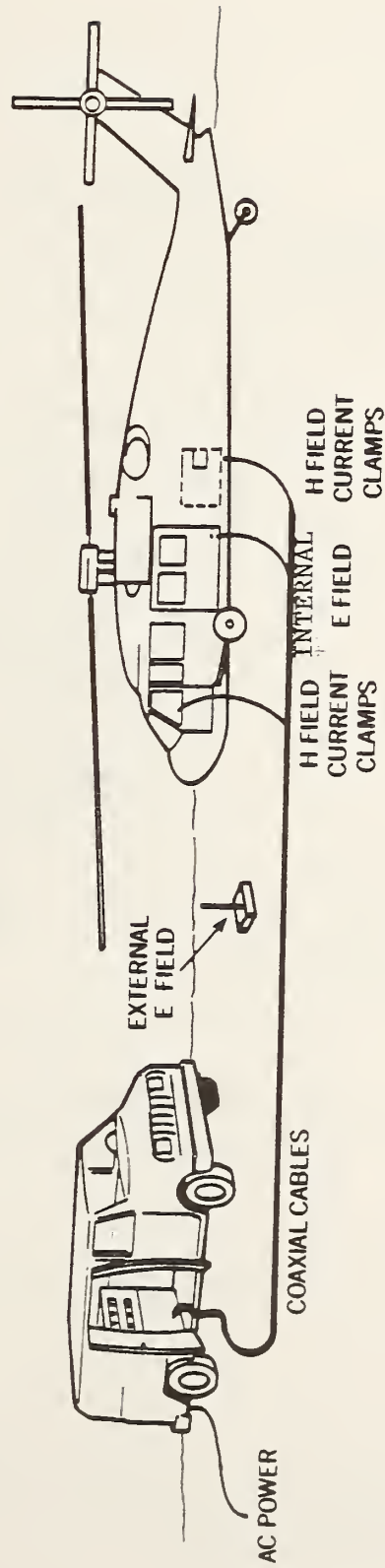


Figure 1. Field Test Configuration.

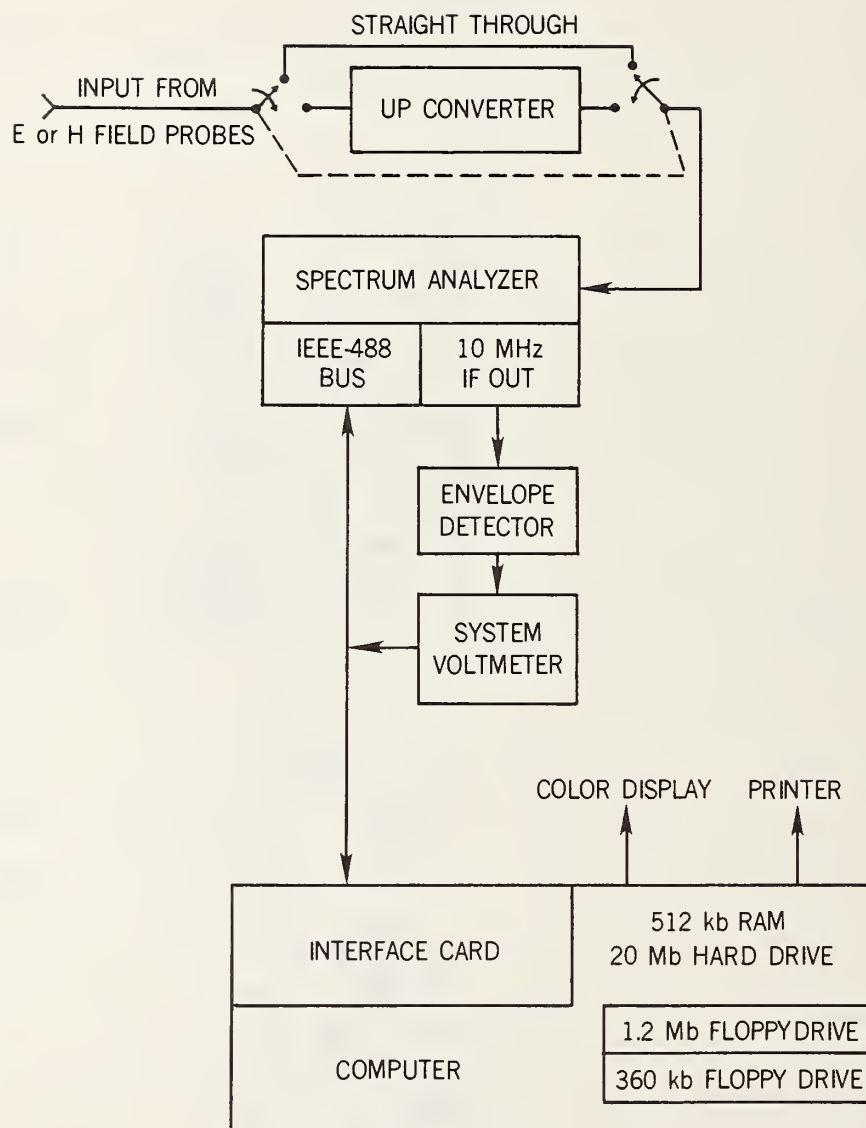


Figure 2. Block Diagram of Electronic System Hardware used for Data Acquisition.

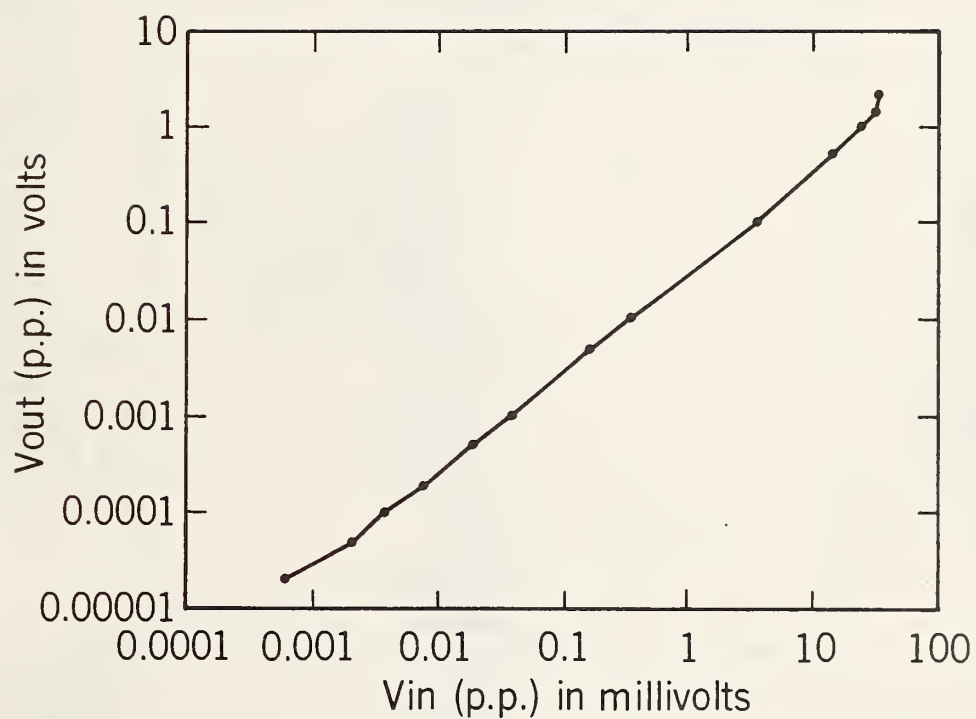


Figure 3. Transfer Function for the Receiving Up-Converter measured at 1000 Hz.

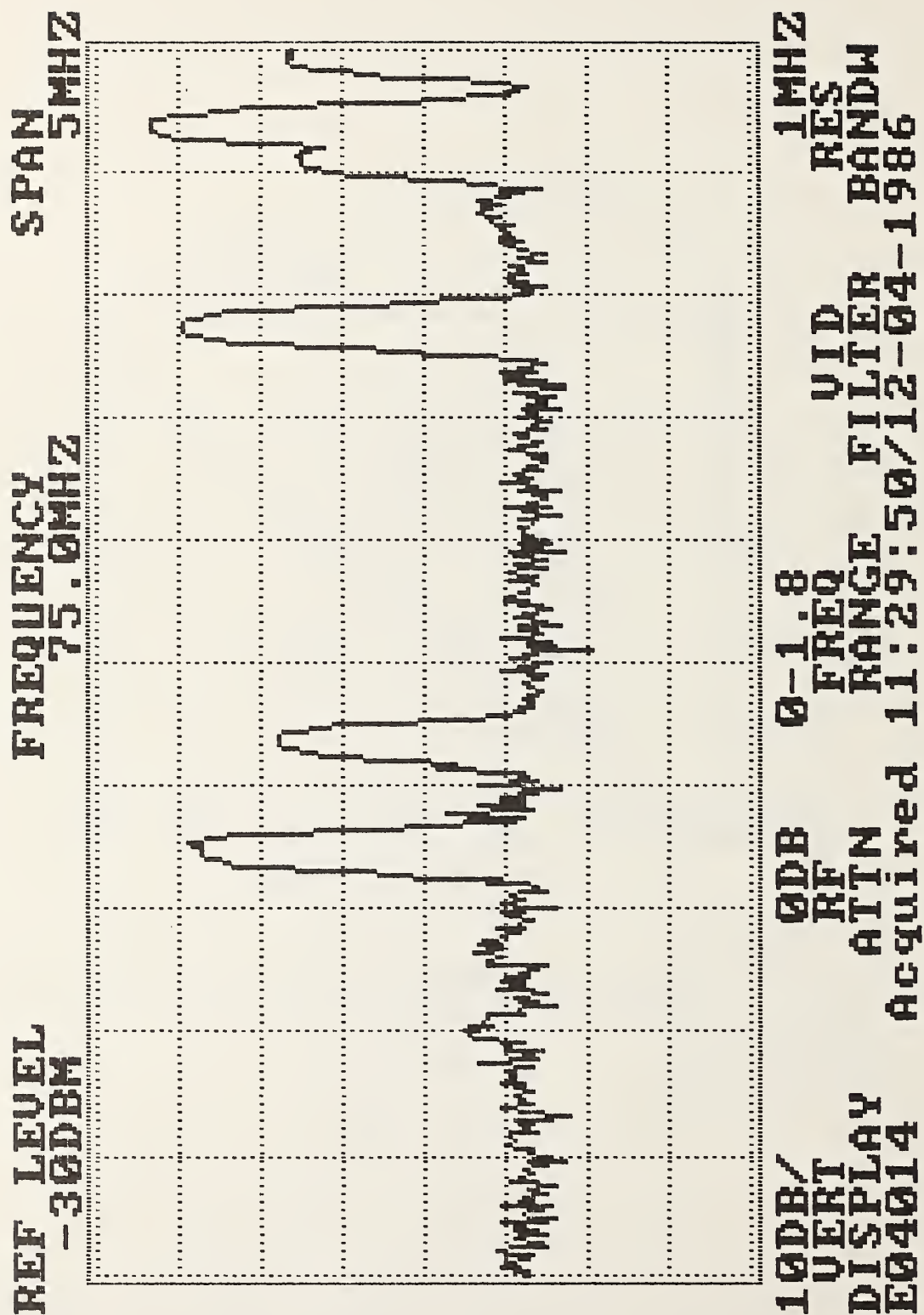


Figure 4. Kiowa Helicopter.

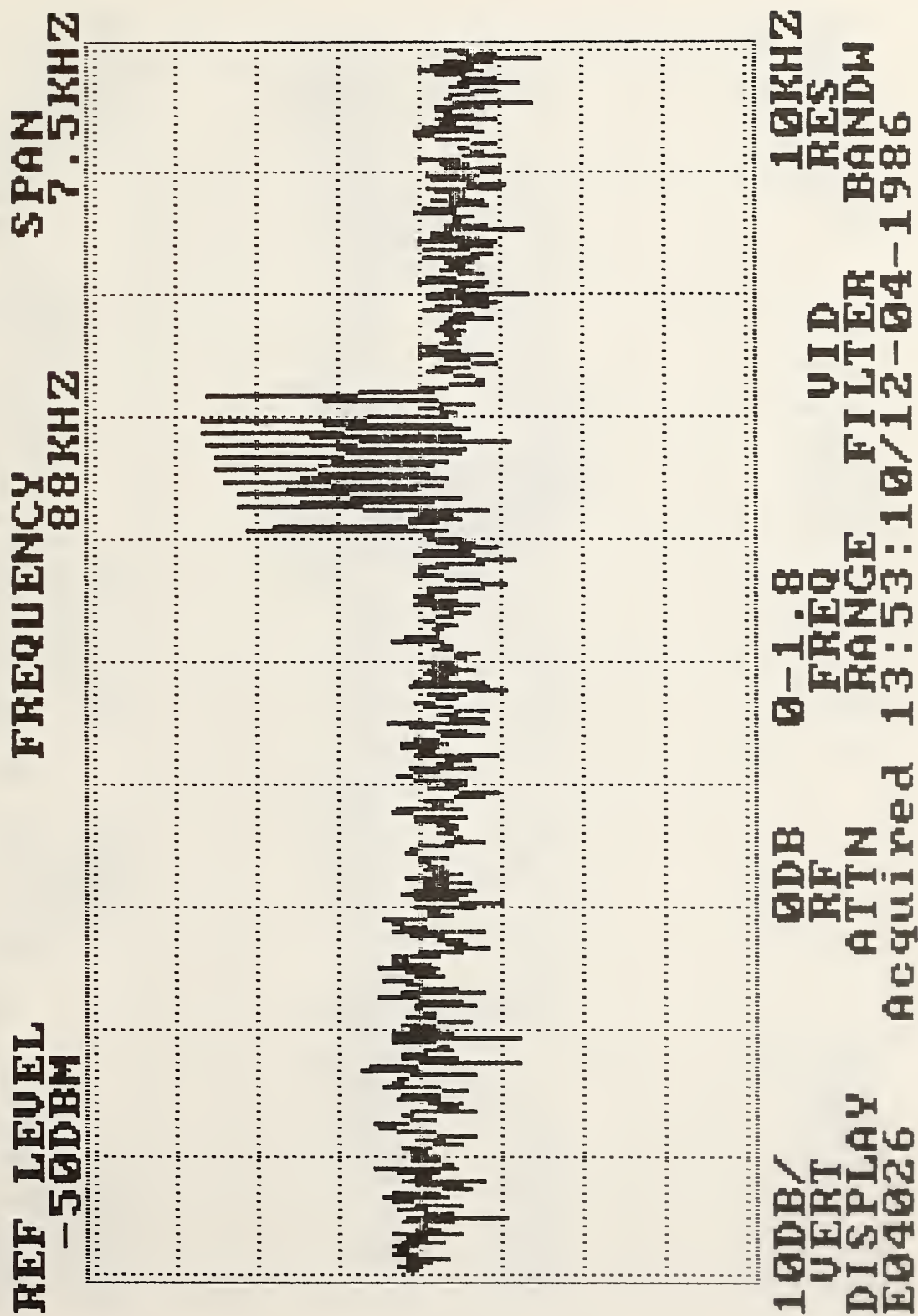


Figure 5. Kiowa Helicopter.

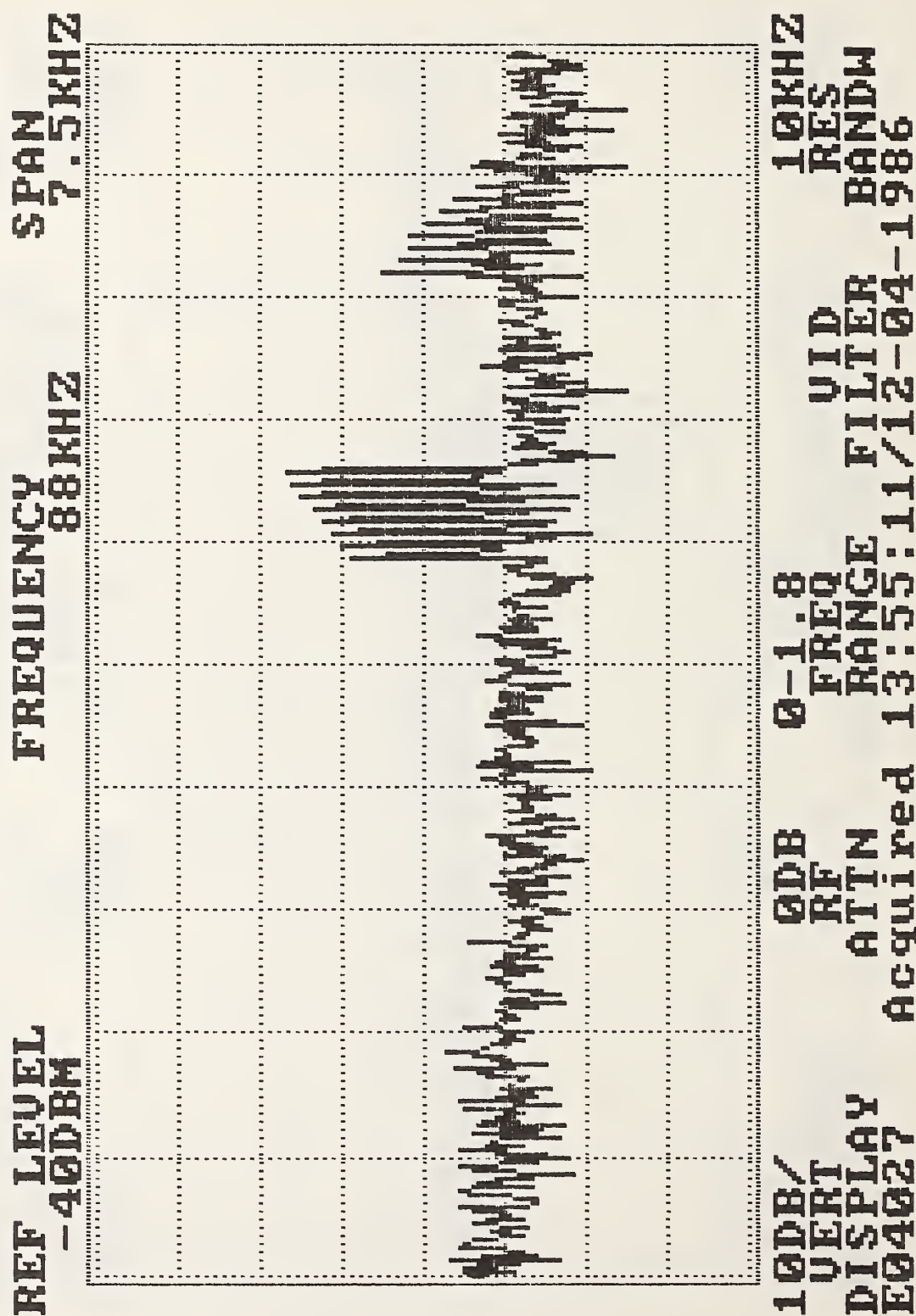


Figure 6. Kiowa Helicopter.

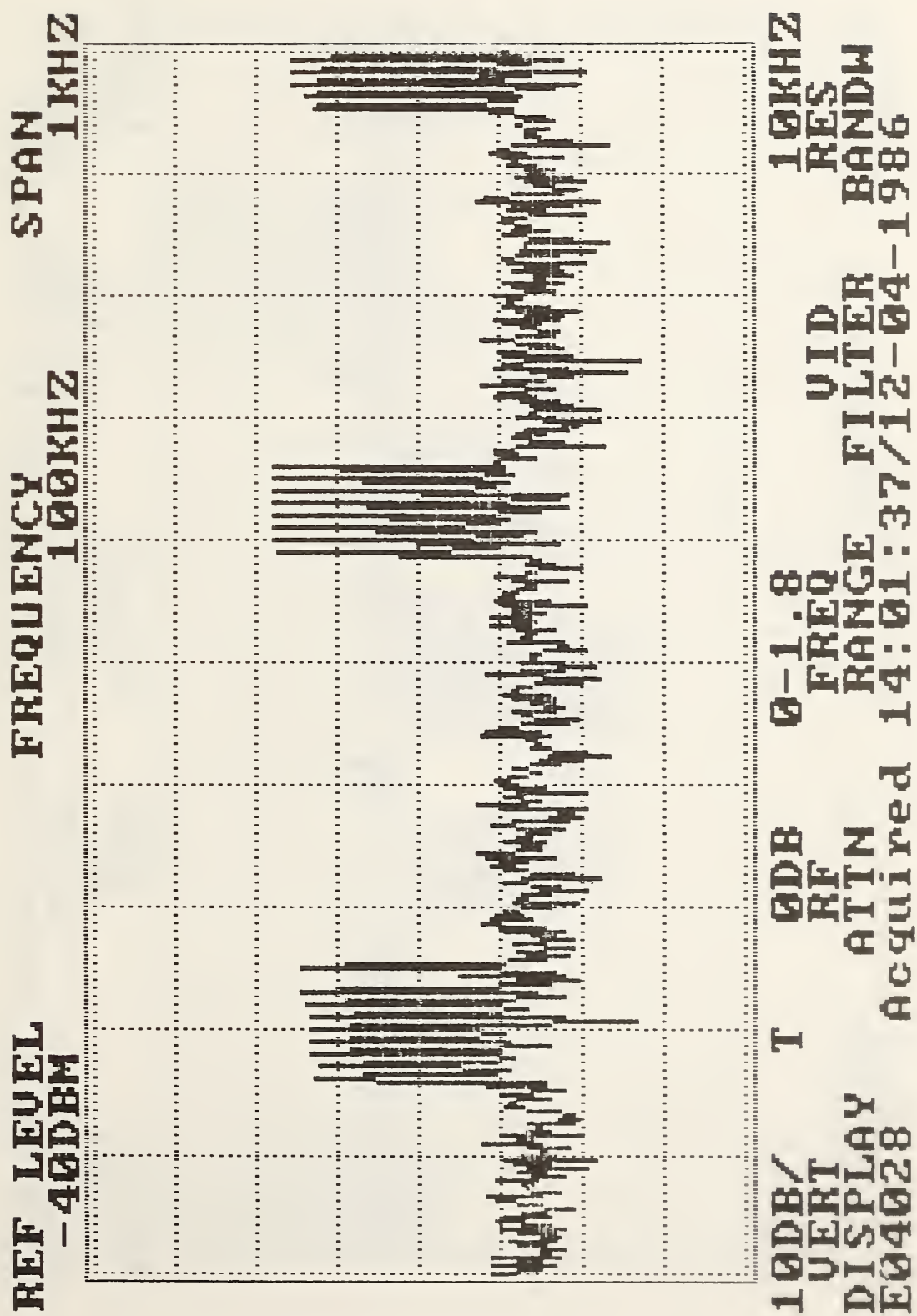


Figure 7, Kiowa Helicopter

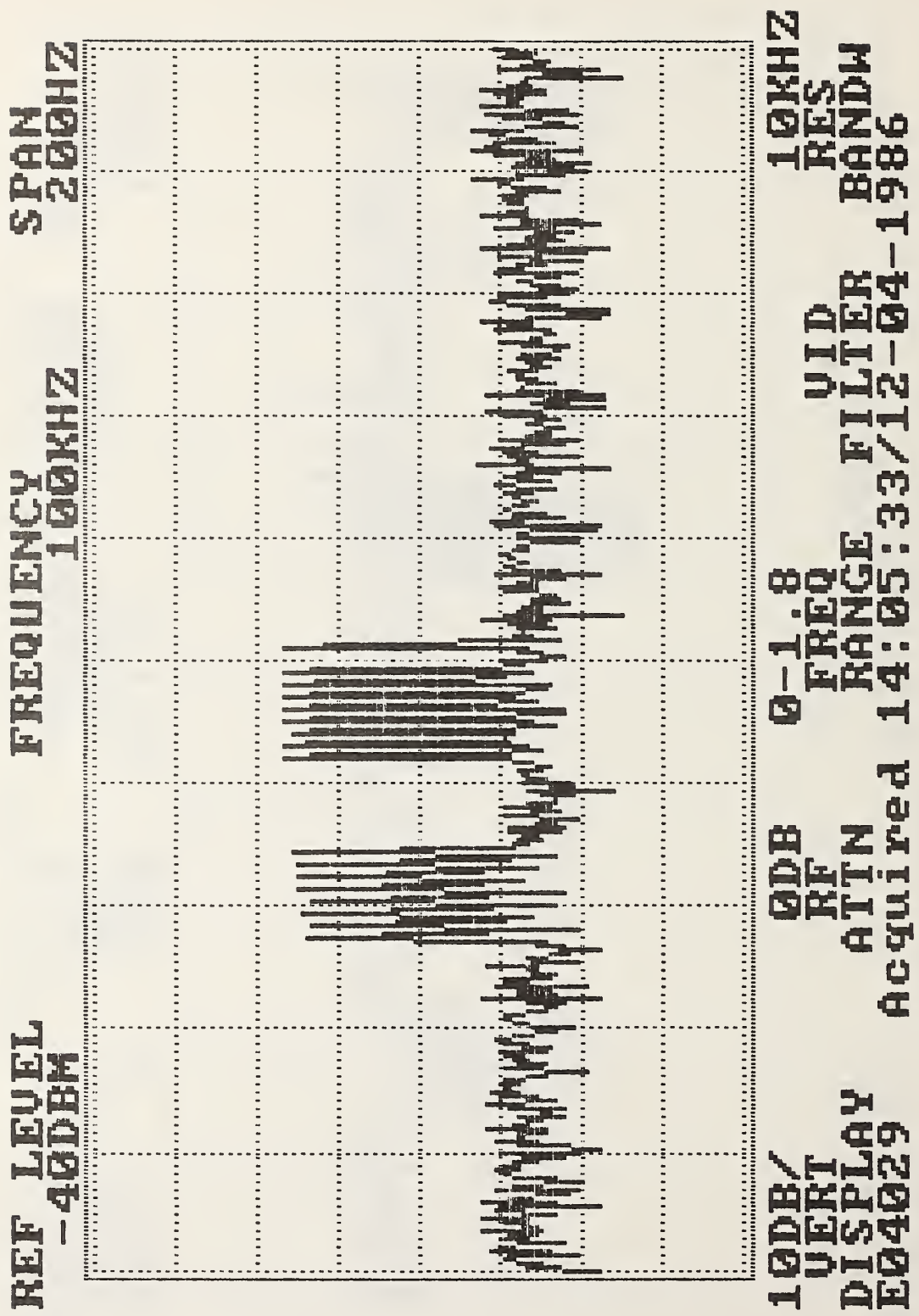


Figure 8. Kiowa Helicopter.

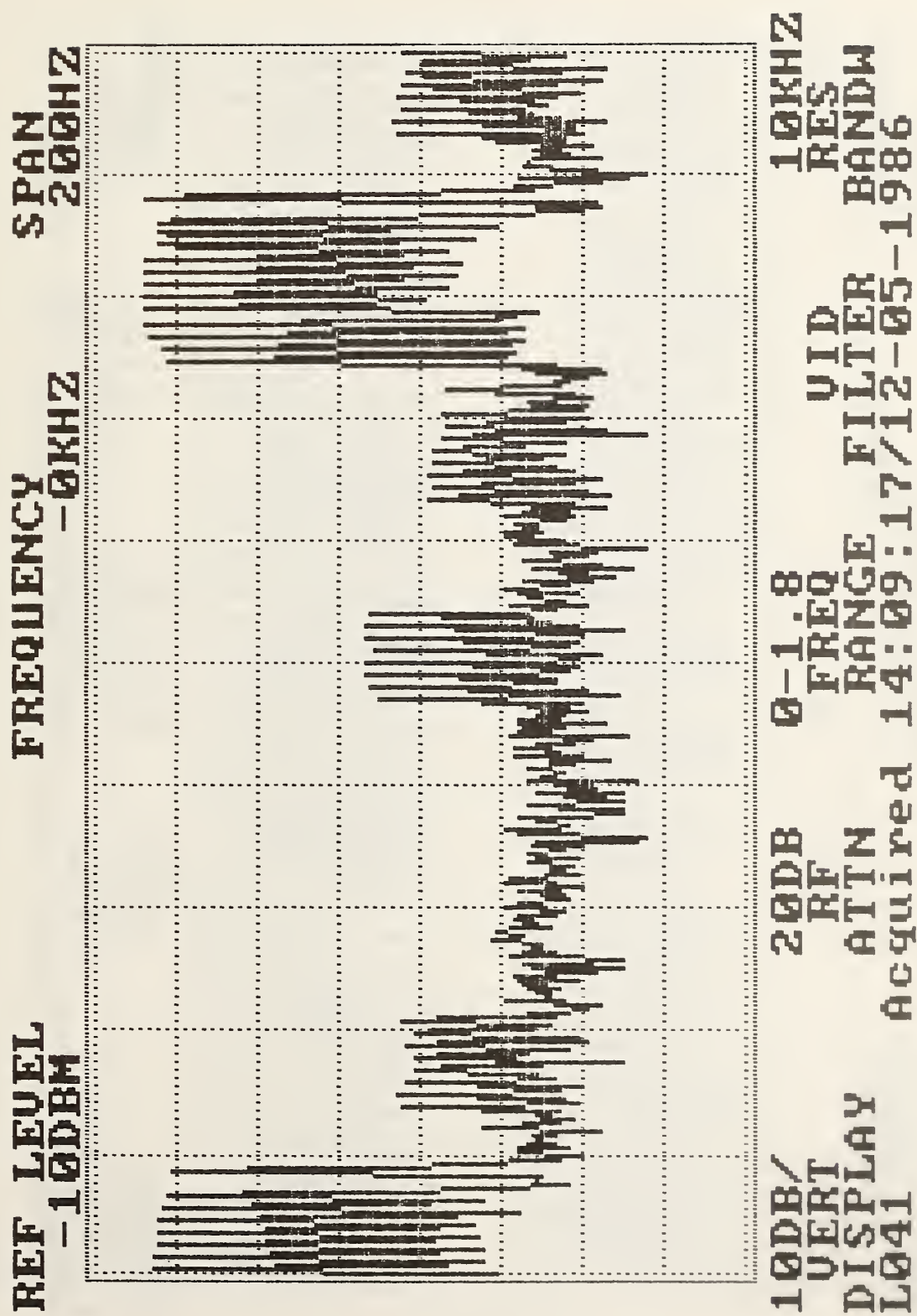


Figure 9. Kiowa Helicopter.

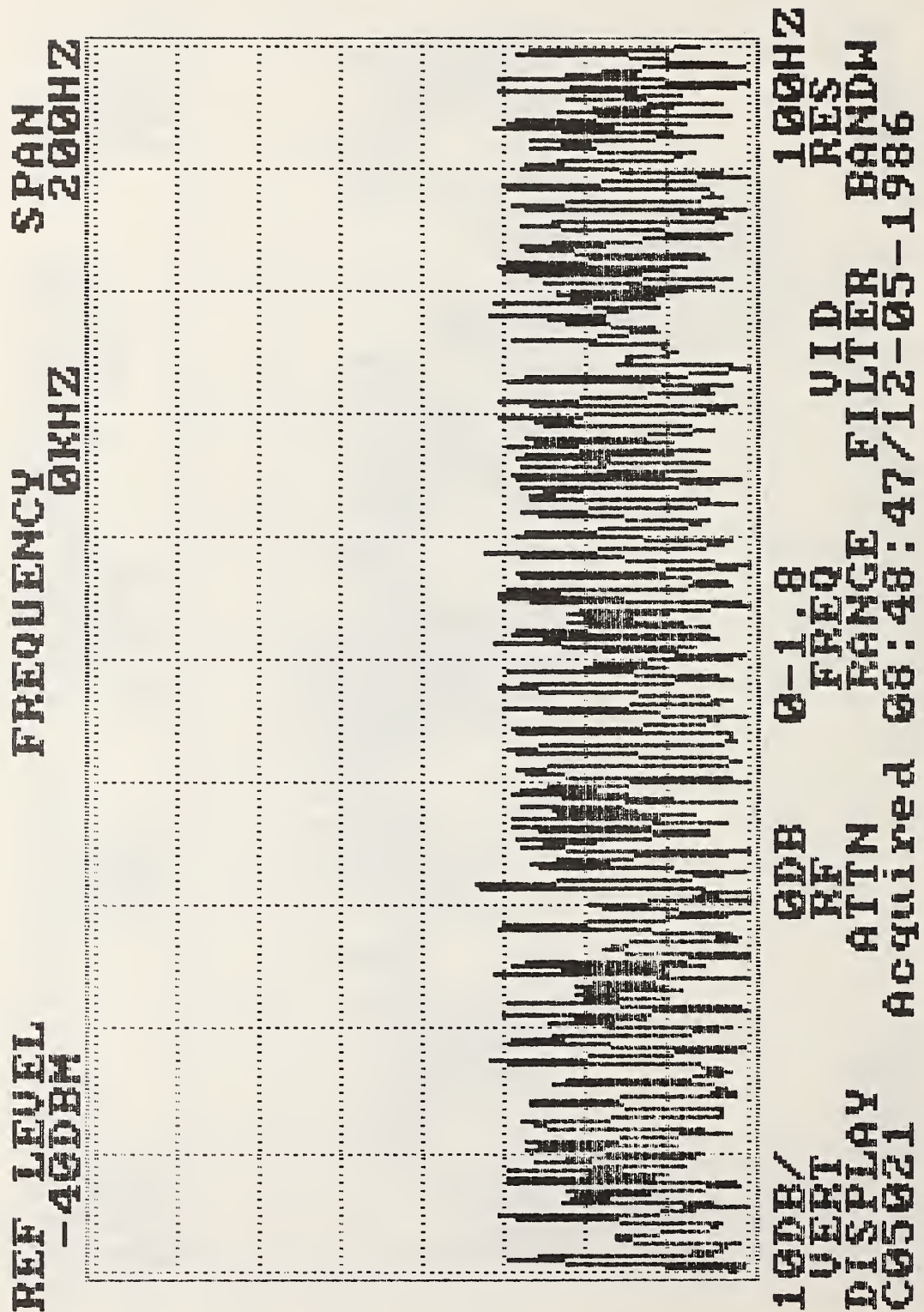


Figure 10. Kiowa Helicopter.

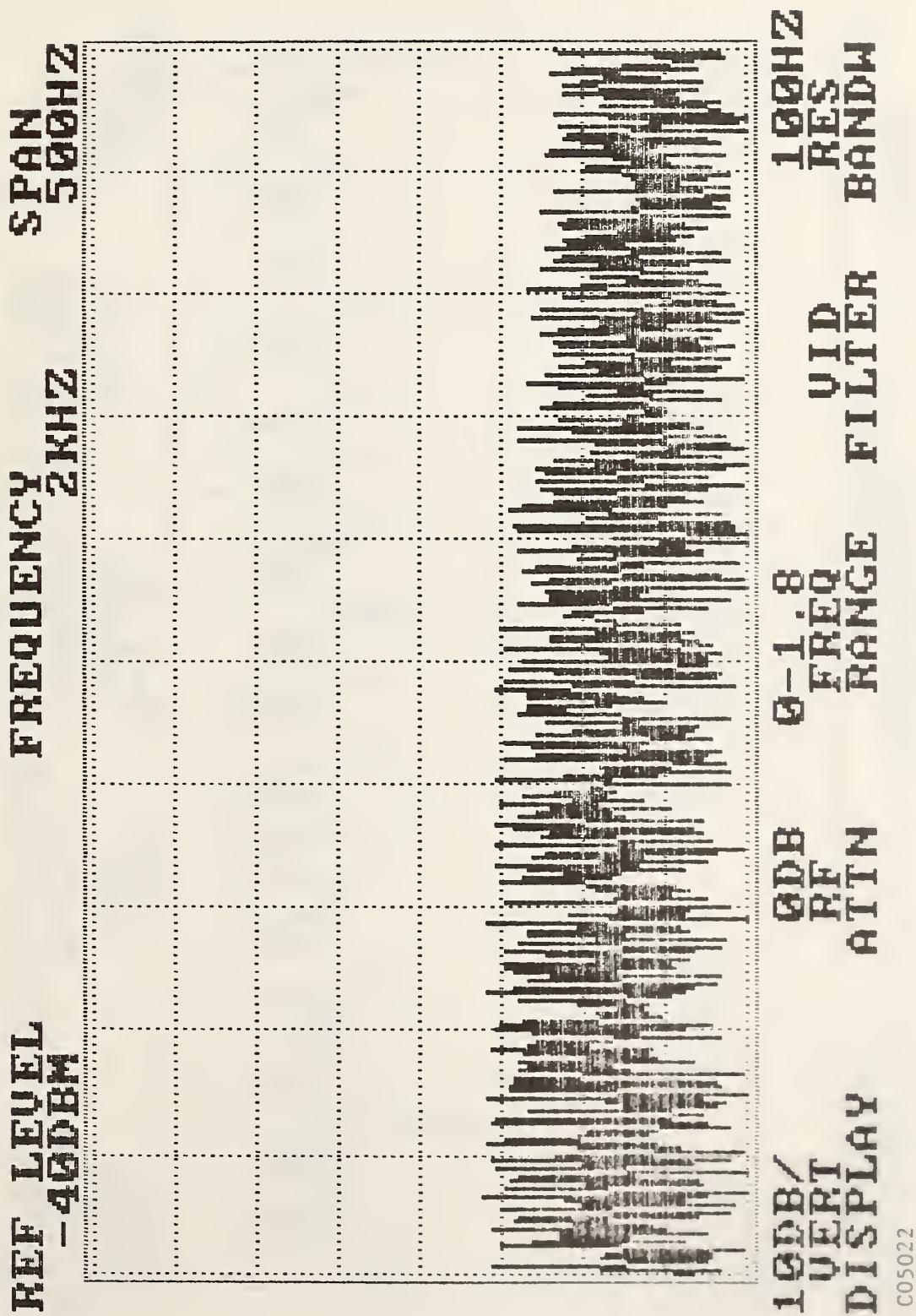


Figure 11. Kiowa Helicopter.

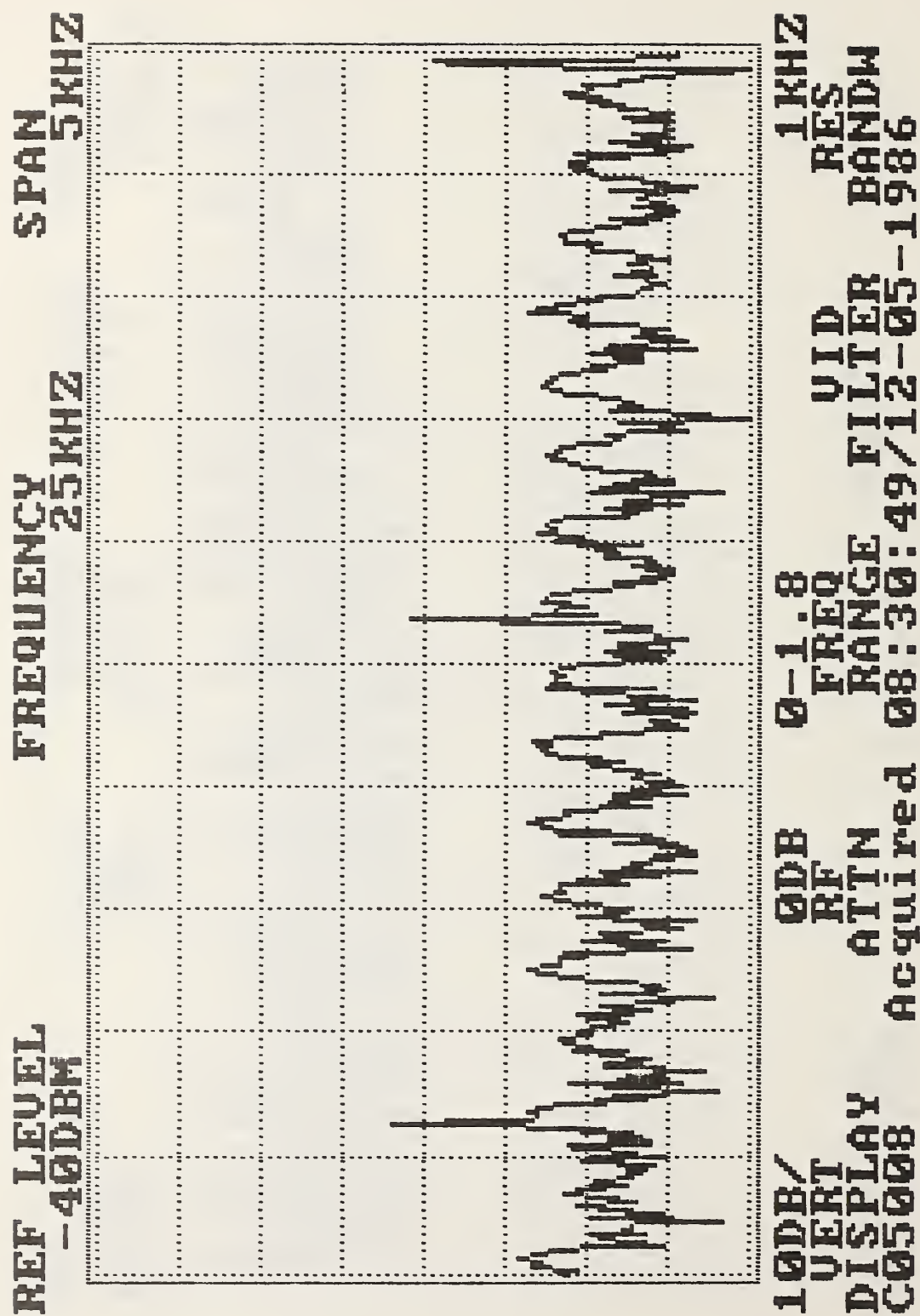


Figure 12. Kiowa Helicopter.

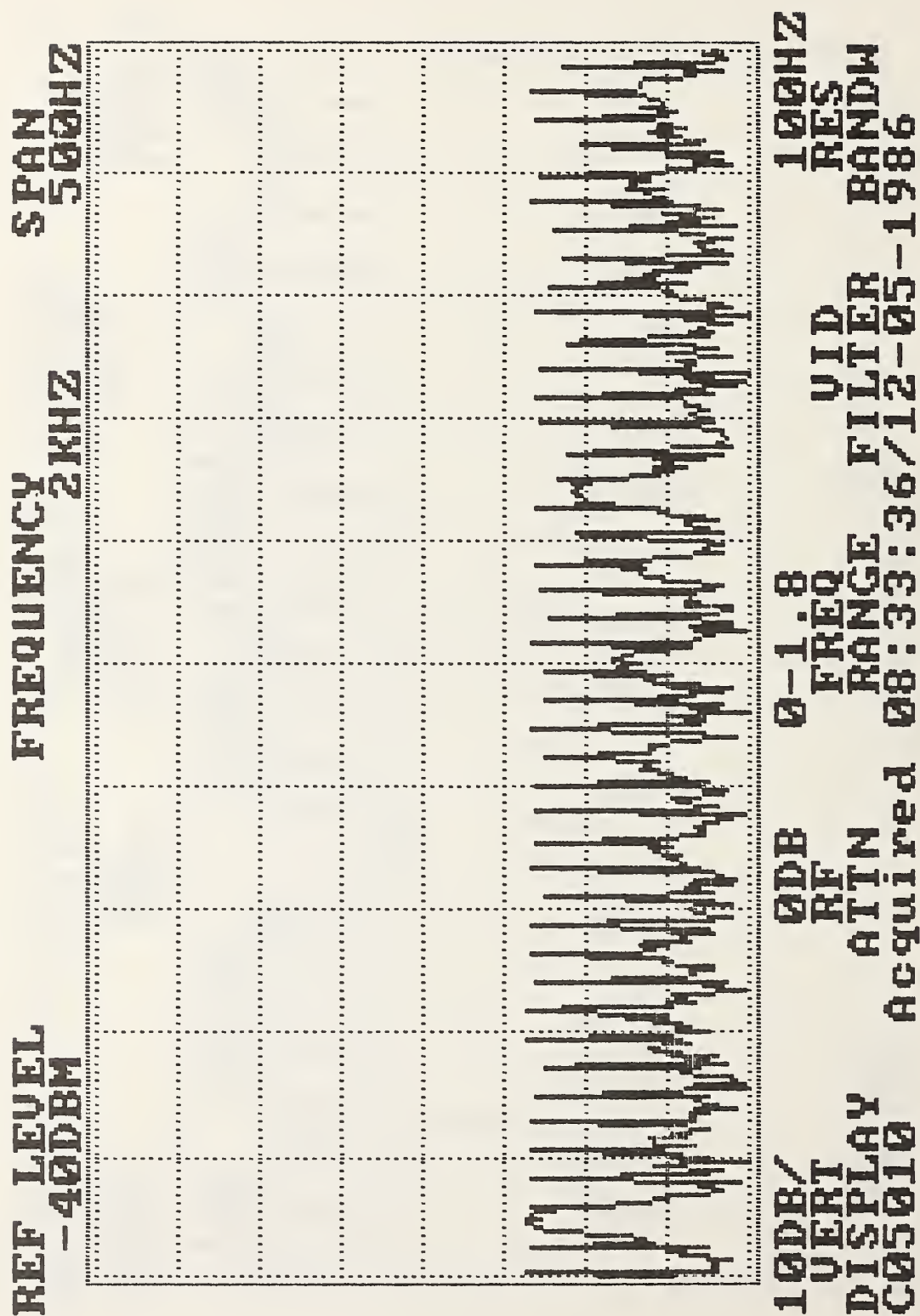


Figure 14. Kiowa Helicopter.

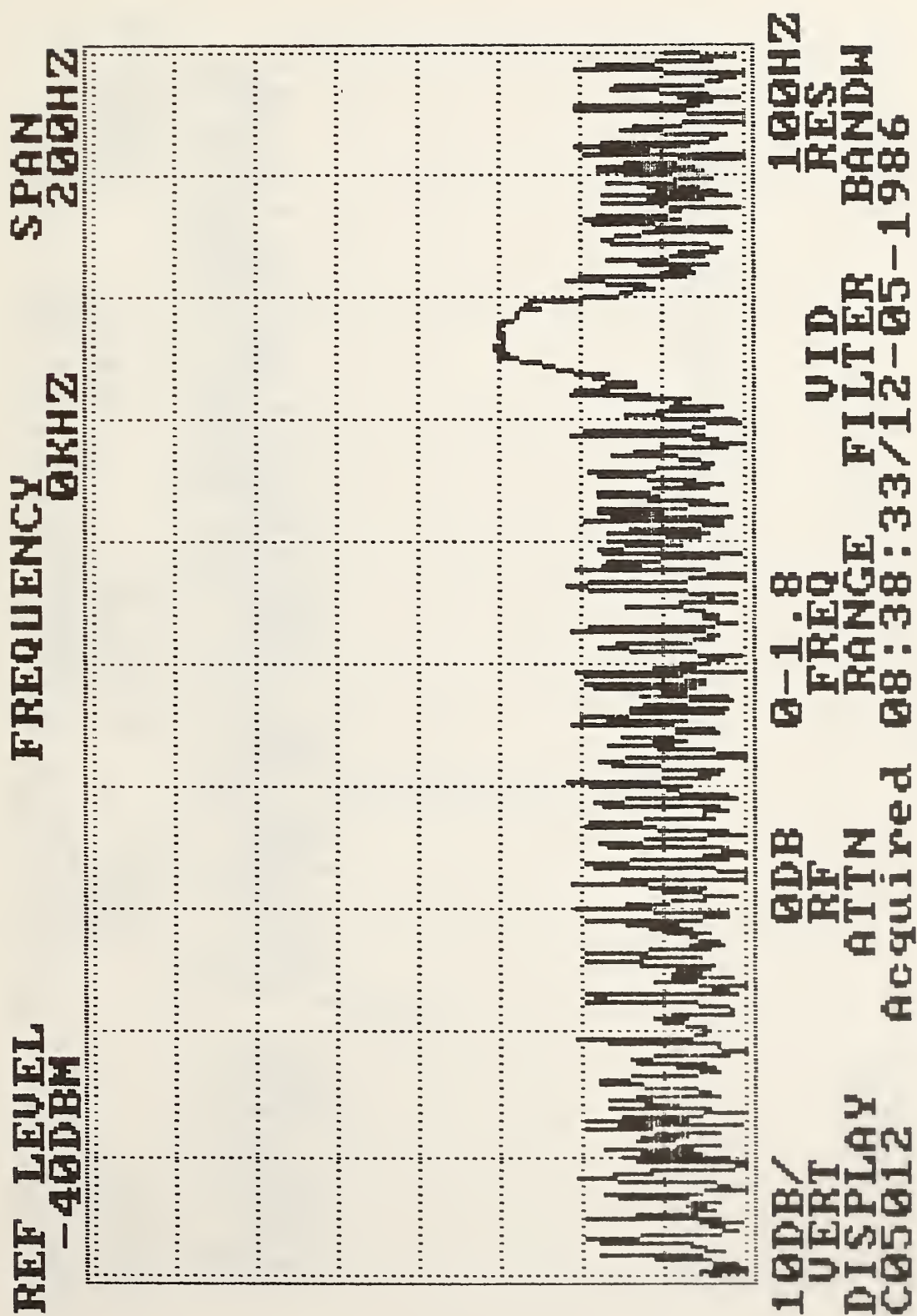


Figure 15. Kiowa Helicopter.

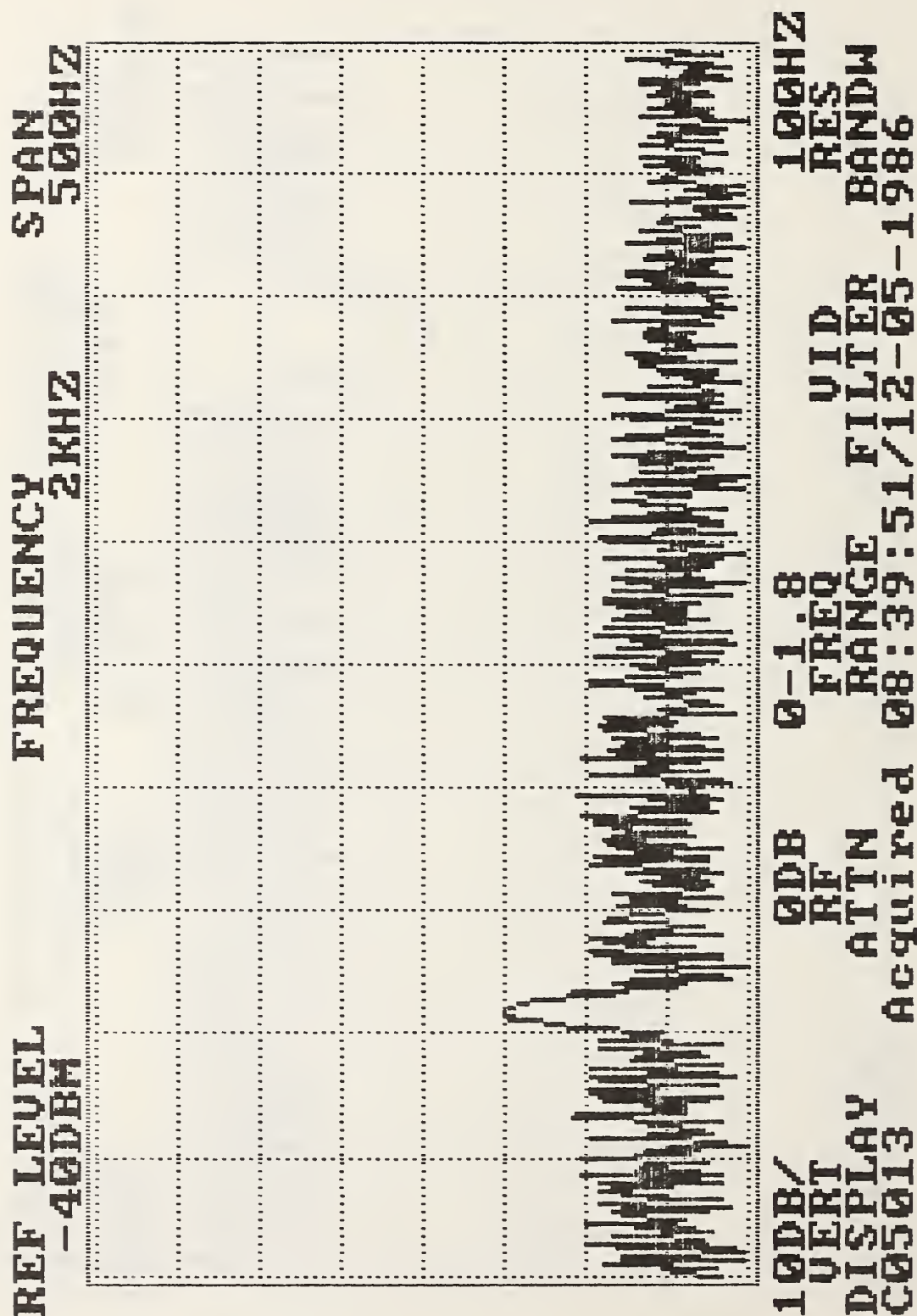


Figure 16. Kiowa Helicopter.

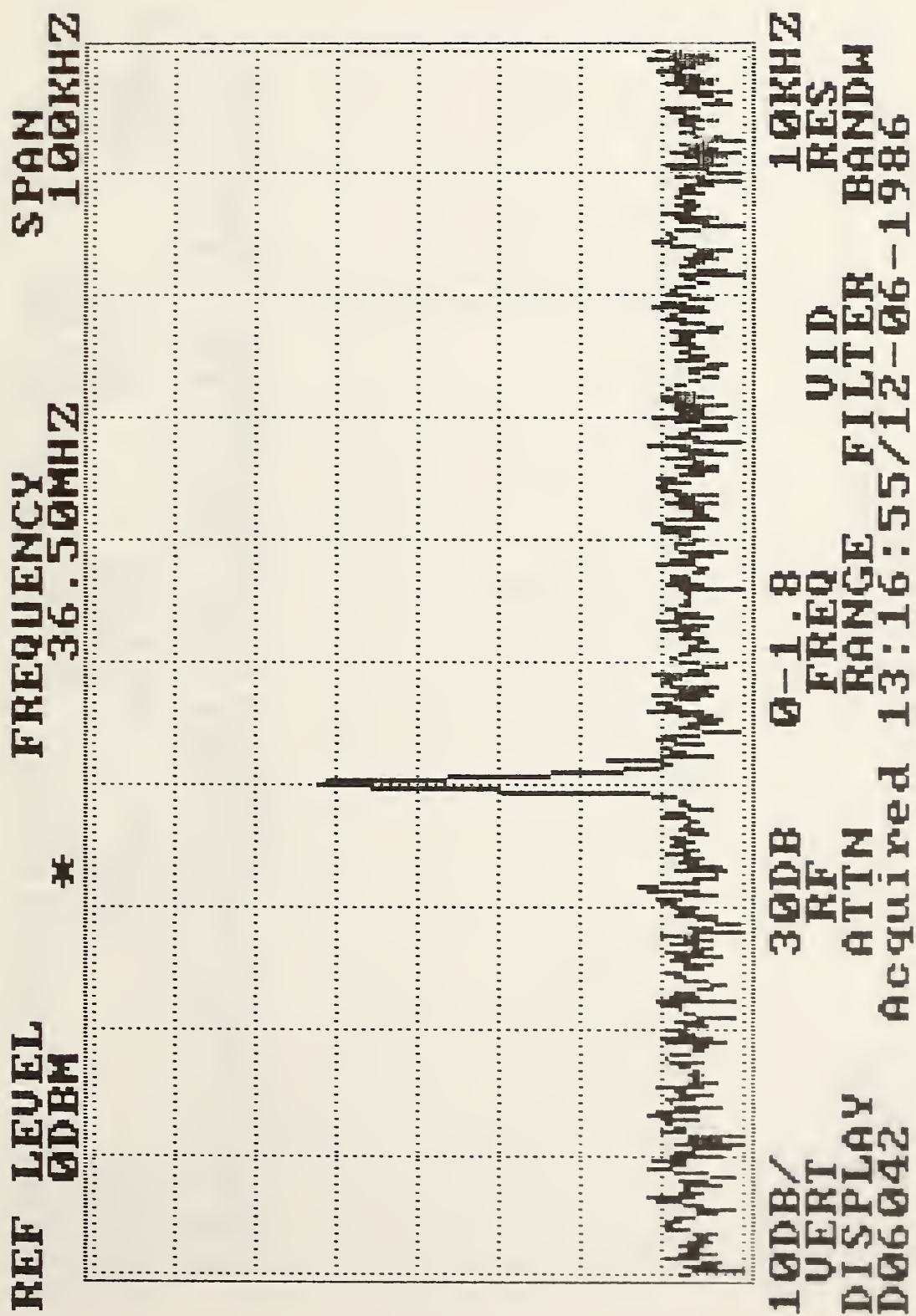


Figure 17. Cobra Helicopter.

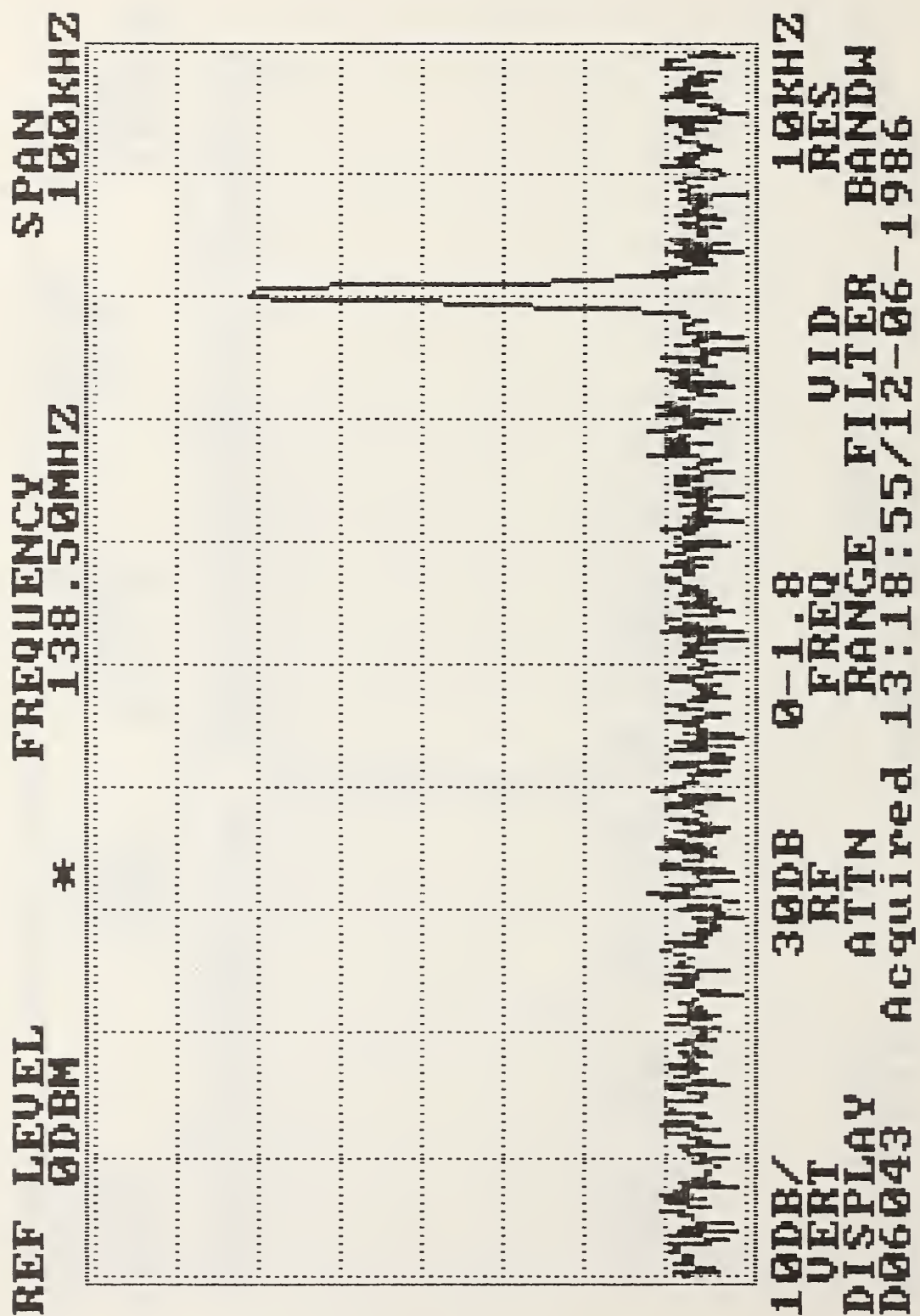


Figure 18. Cobra Helicopter.

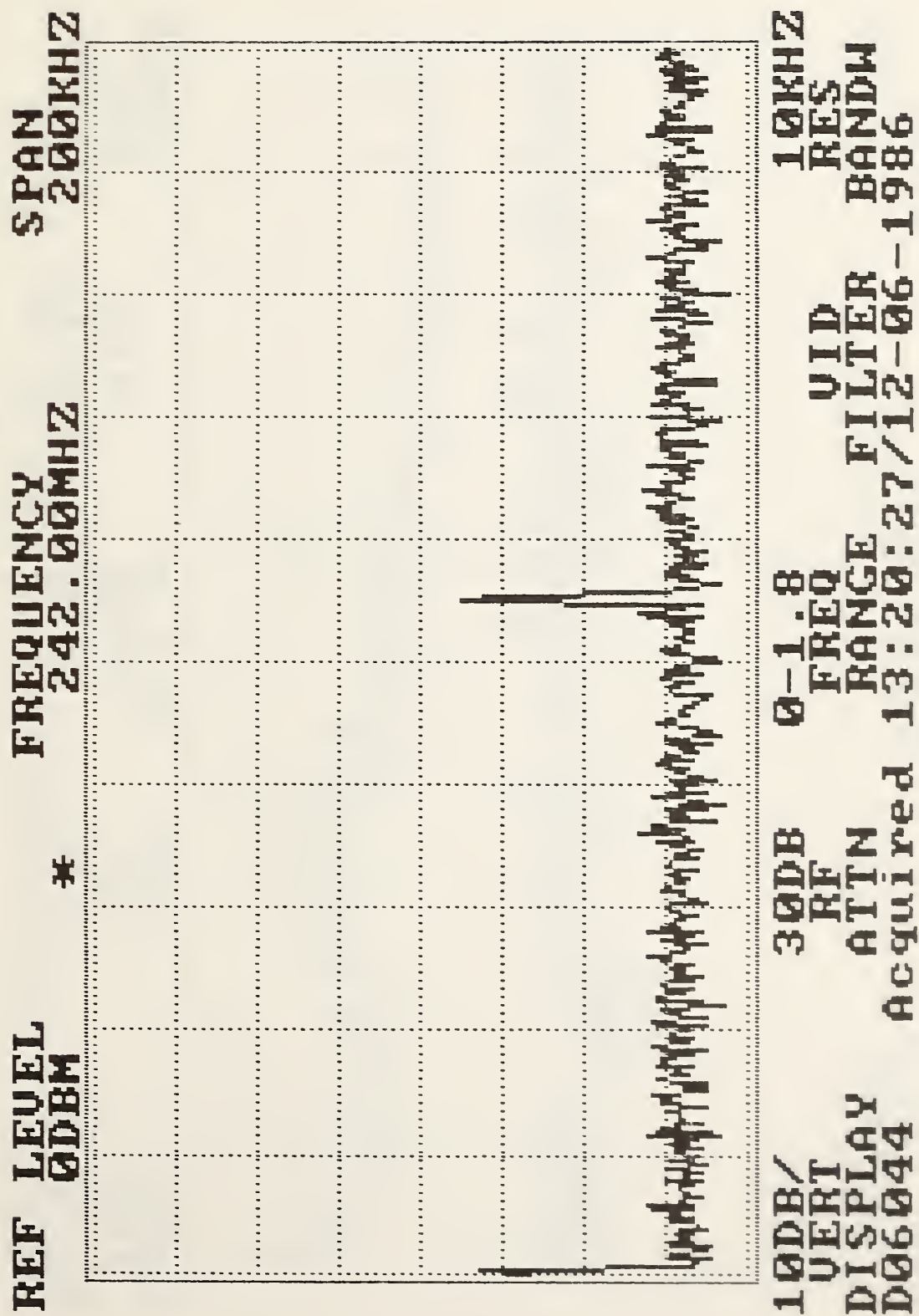


Figure 19. Cobra Helicopter.

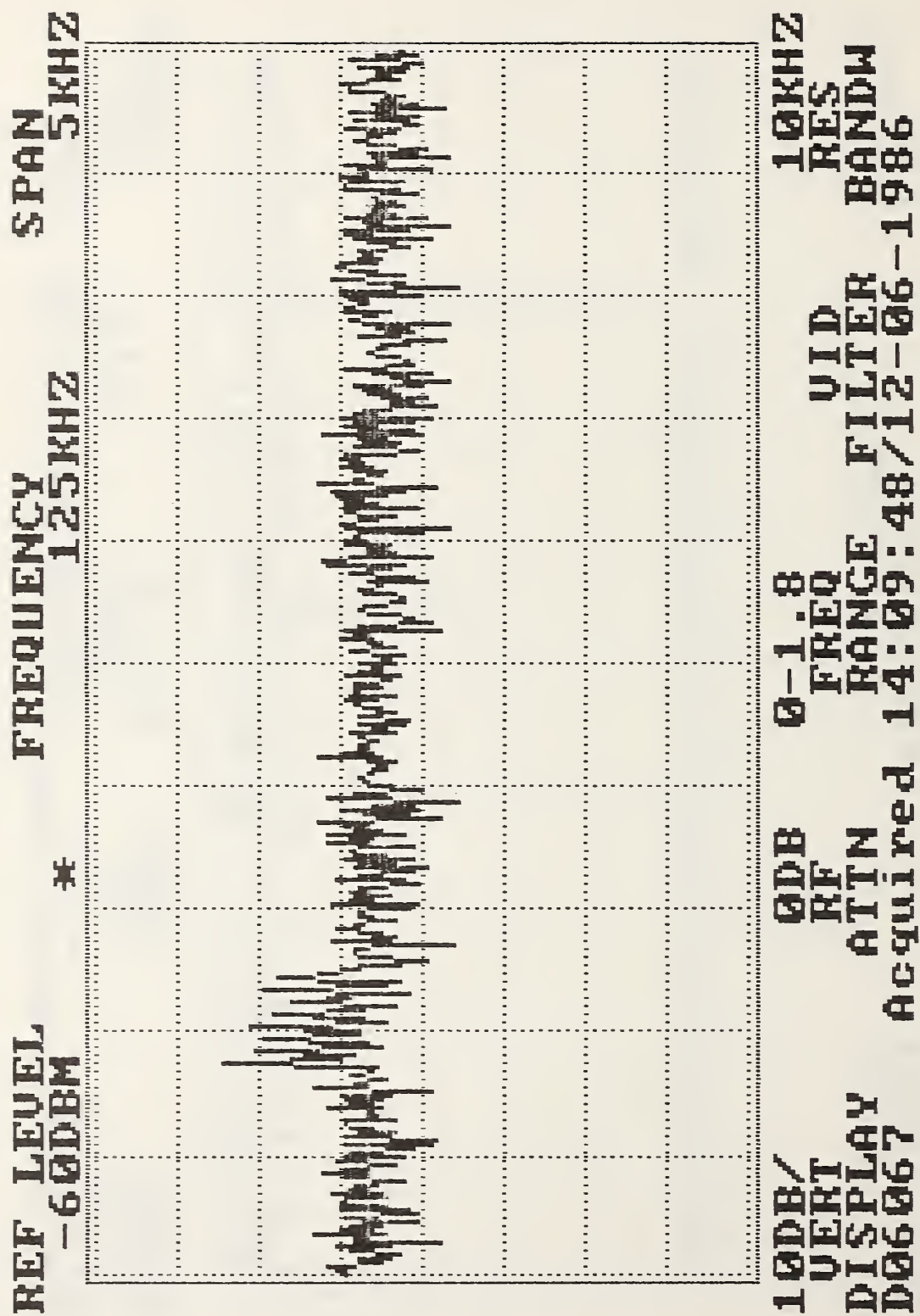


Figure 20. Cobra Helicopter.

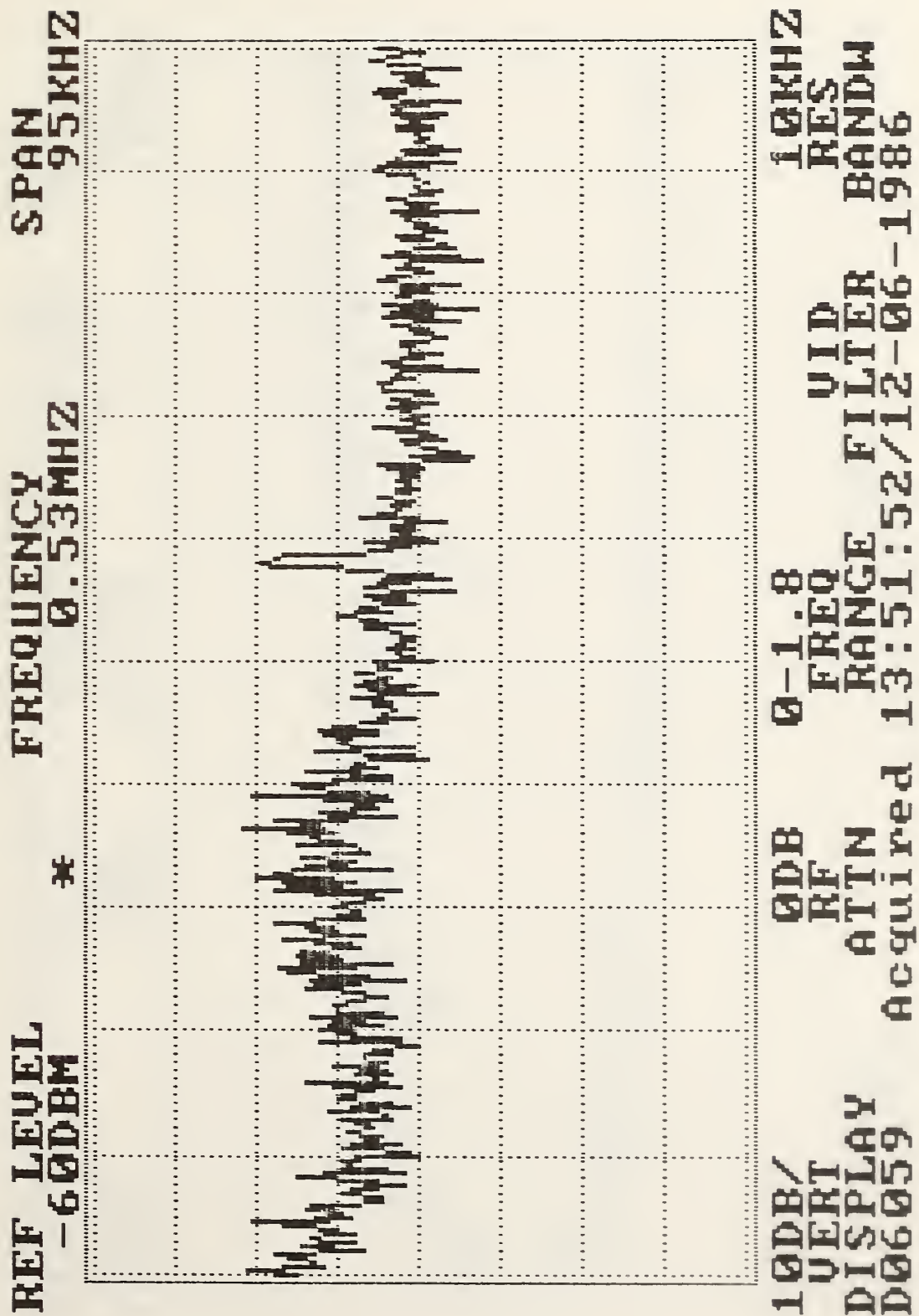


Figure 21. Cobra Helicopter.

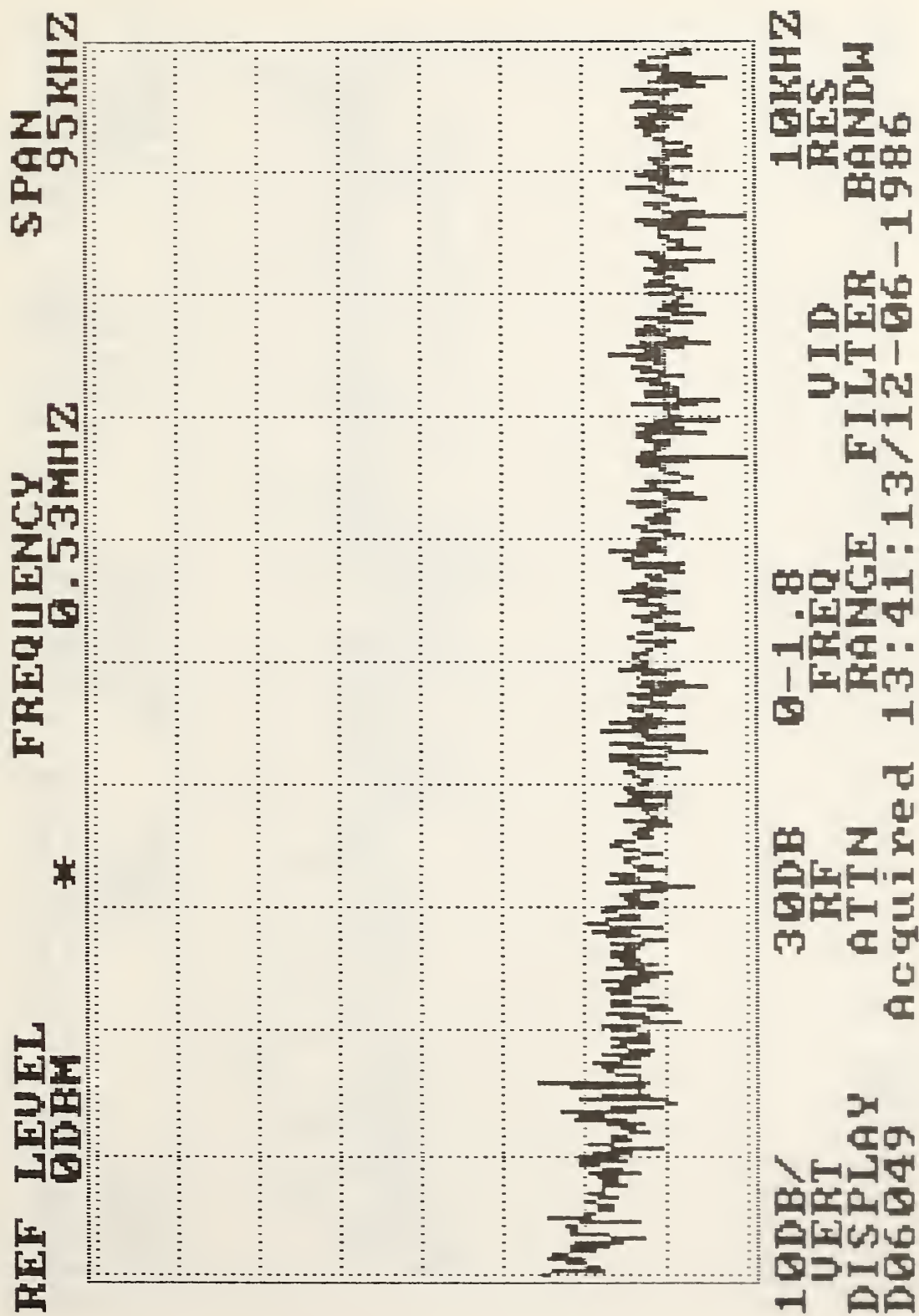


Figure 23. Cobra Helicopter.

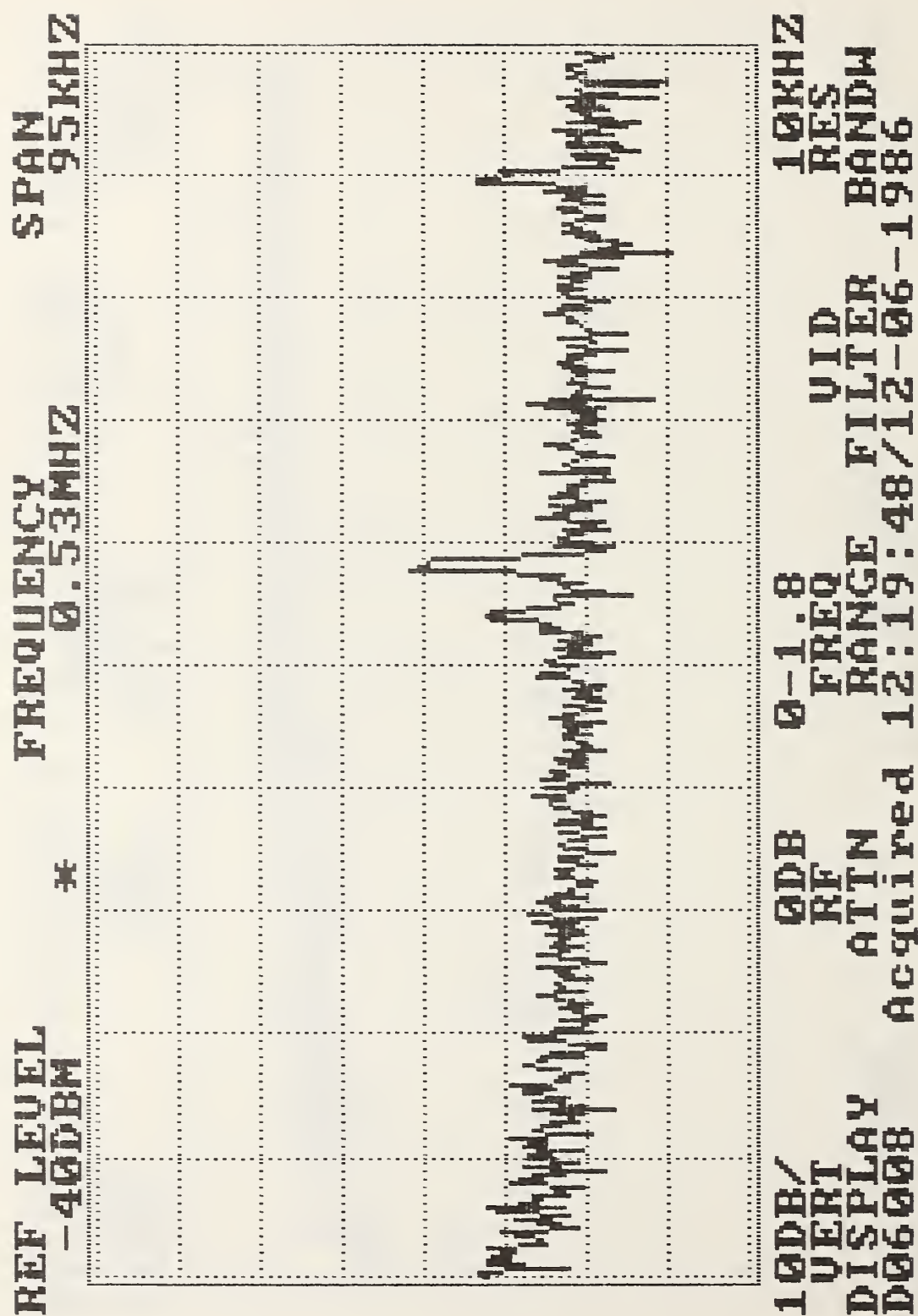


Figure 24. Cobra Helicopter.

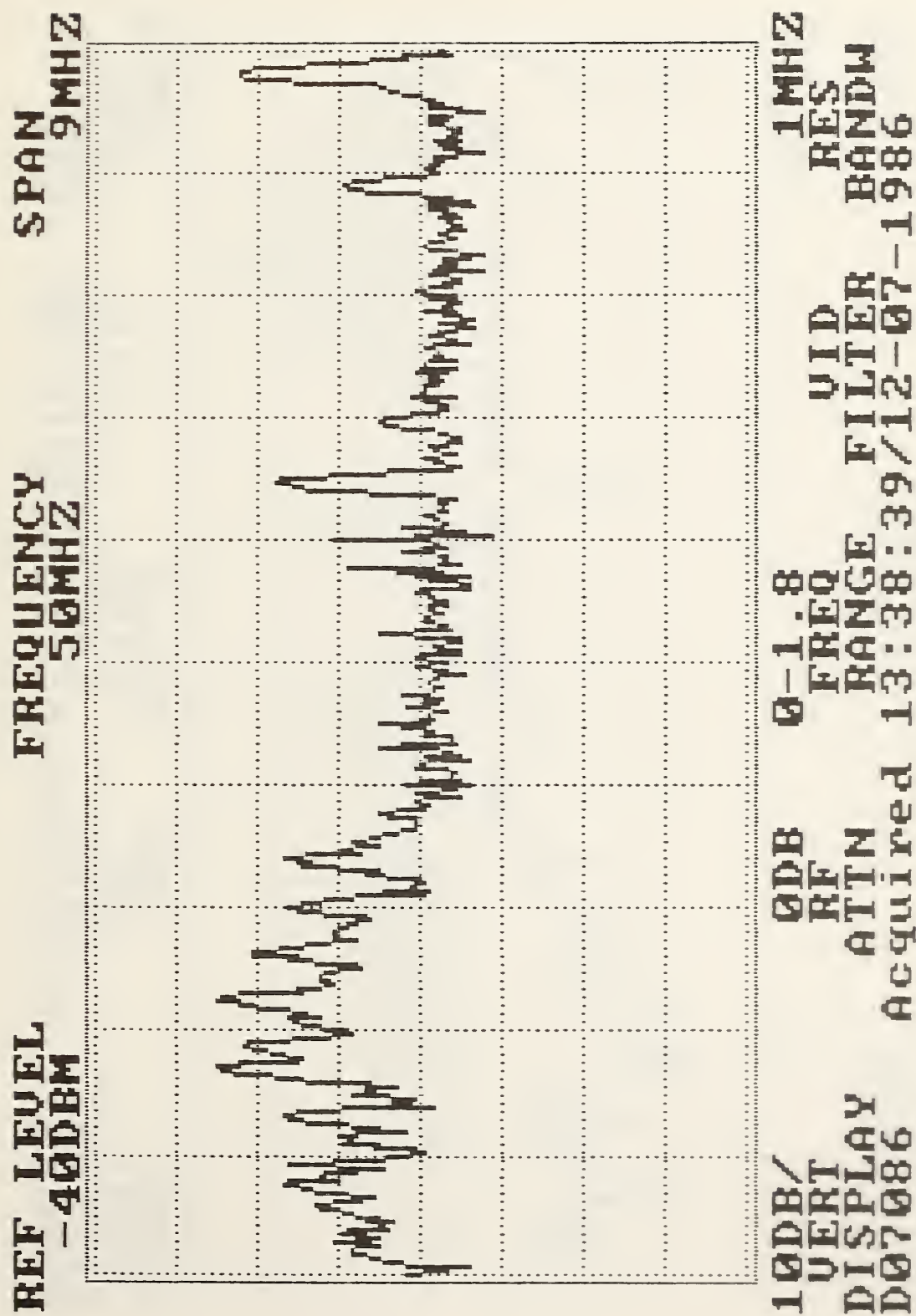


Figure 25. Blackhawk Helicopter.

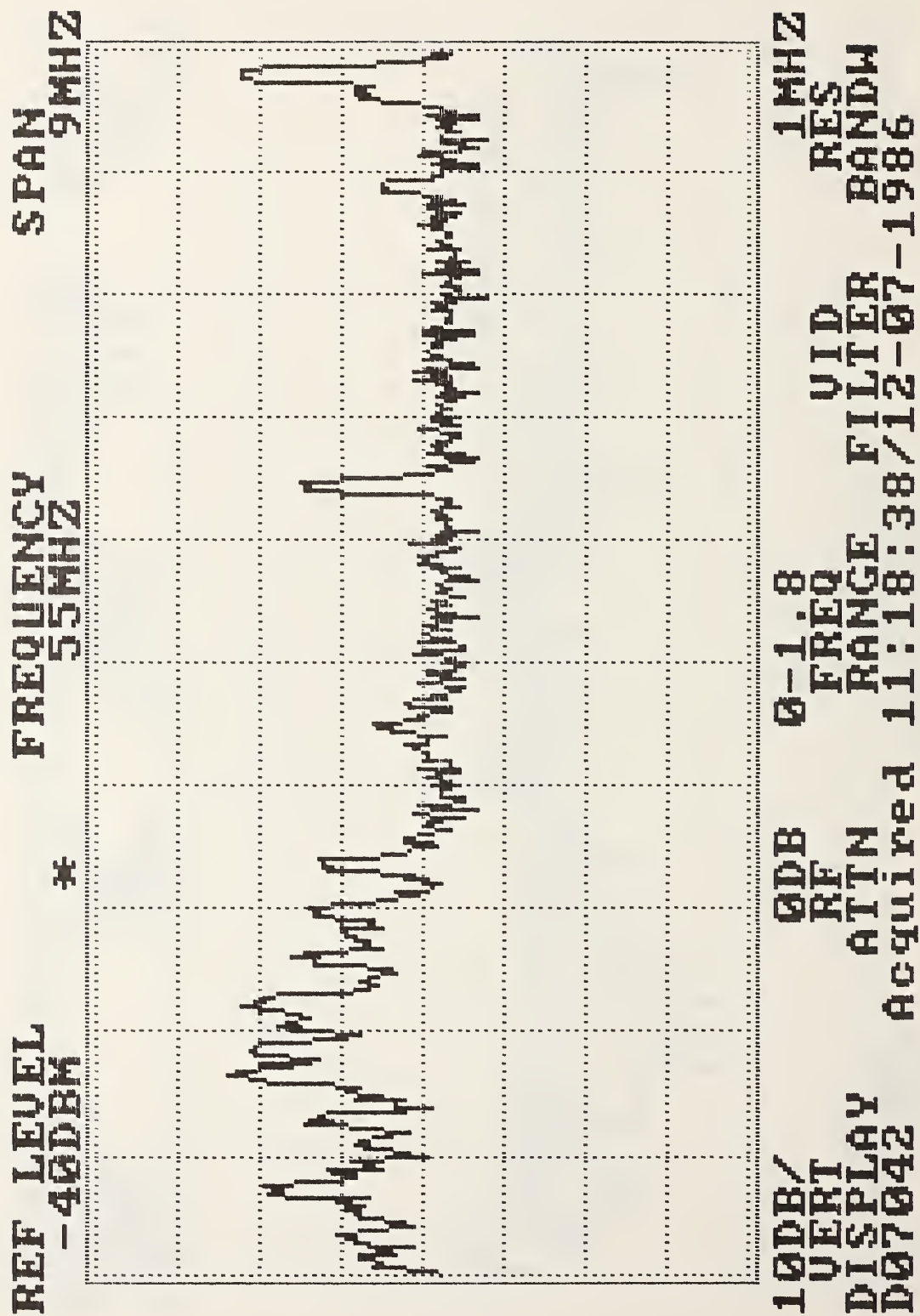
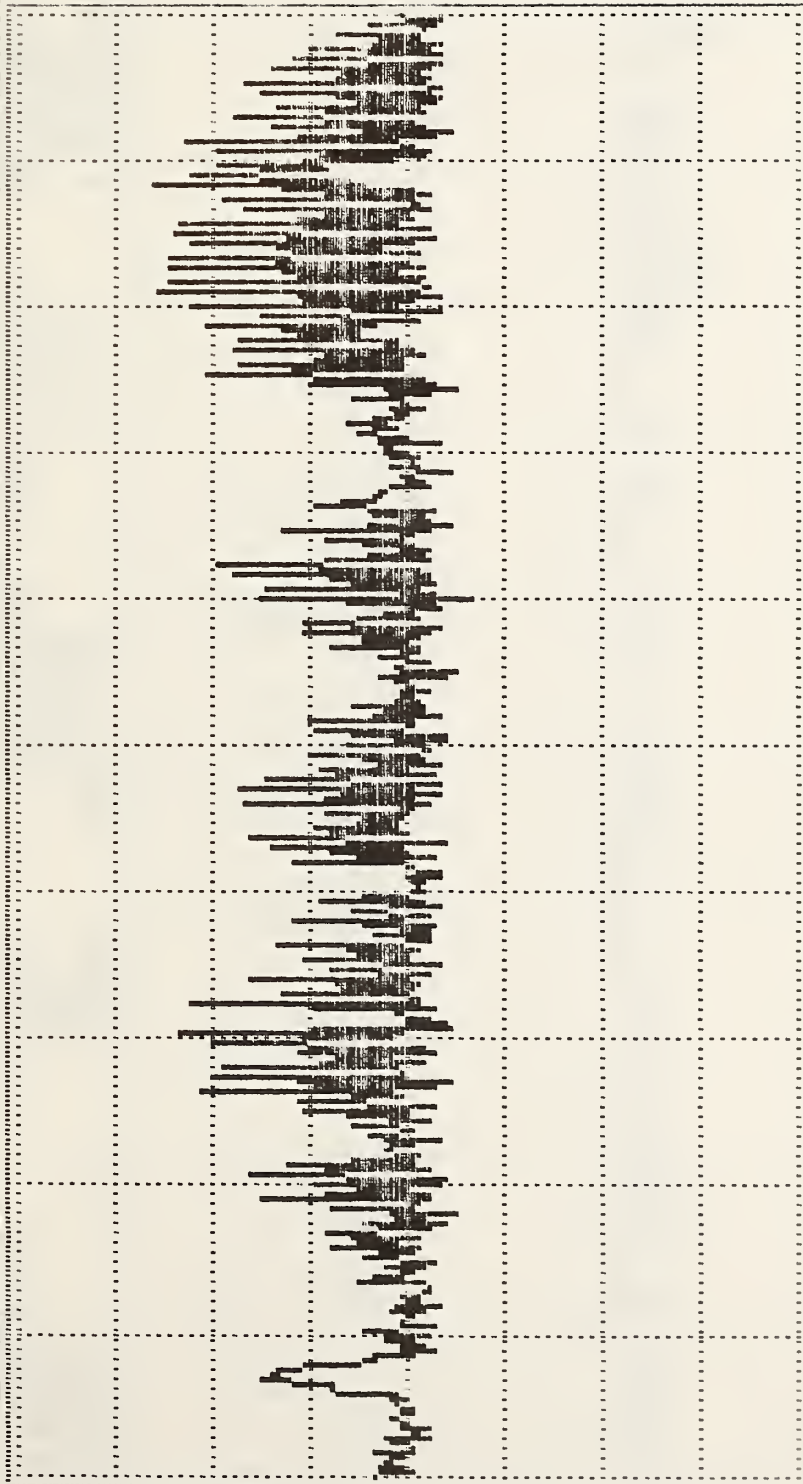


Figure 26. Blackhawk Helicopter.

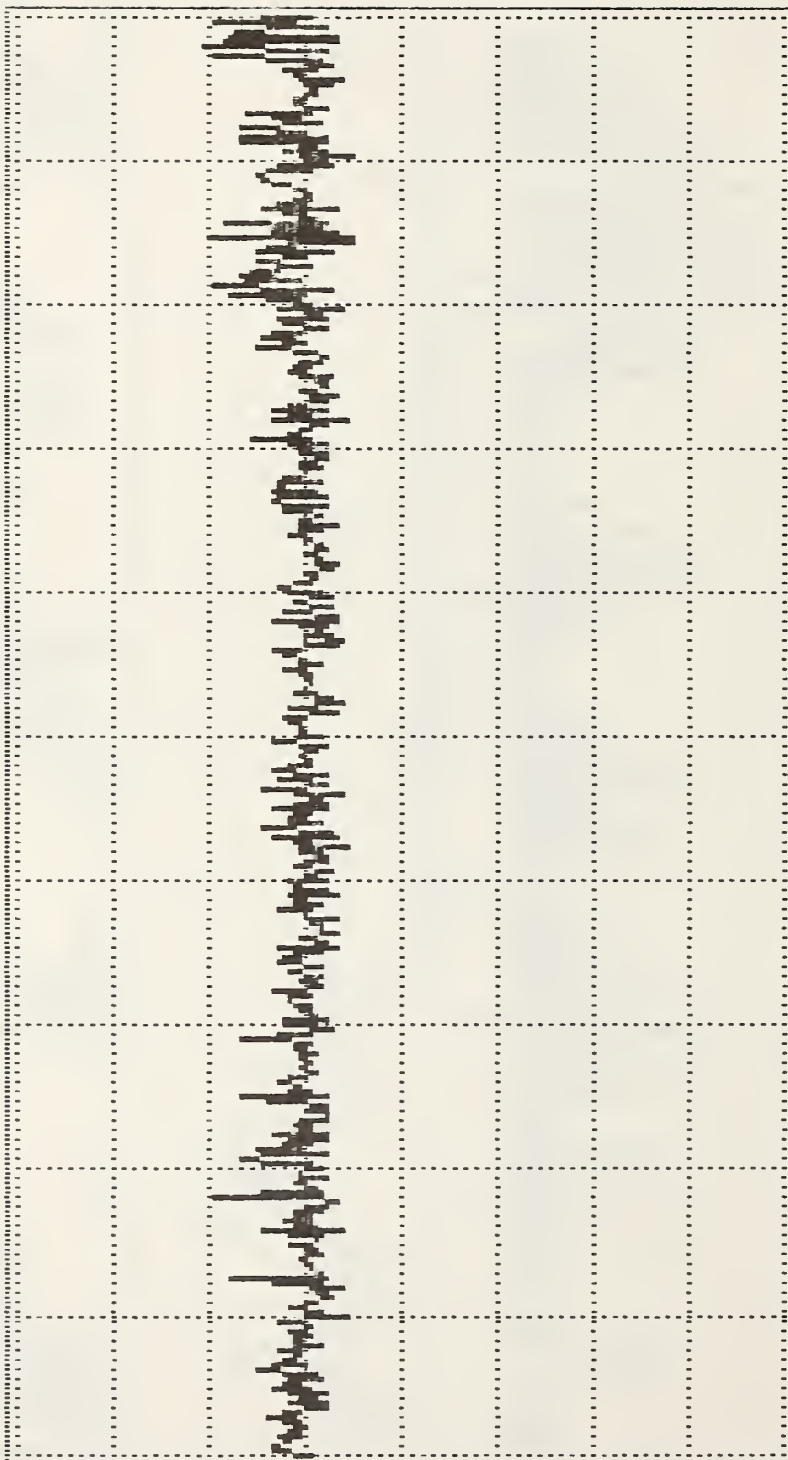
REF LEVEL -50DBM * FREQUENCY 5.5MHZ SPAN 900KHZ



100DB/ T 0DB 0-1.8 100KHZ
 UERTI RF ATN RES
 DISPLAY Acquired 11:32:15/12-07-1986
 D07064 FILTER BANDW

Figure 27. Blackhawk Helicopter.

REF LEVEL FREQUENCY SPAN
 -60DBM 0.0MHZ 900KHZ



10DB/ T QDB 0-1.8 100KHZ
 VERT RF RES
 DISPLAY ATTN RANGE VID BANDW
 D07111 Acquired 13:53:53/12-07-1986

Figure 28. Blackhawk Helicopter.

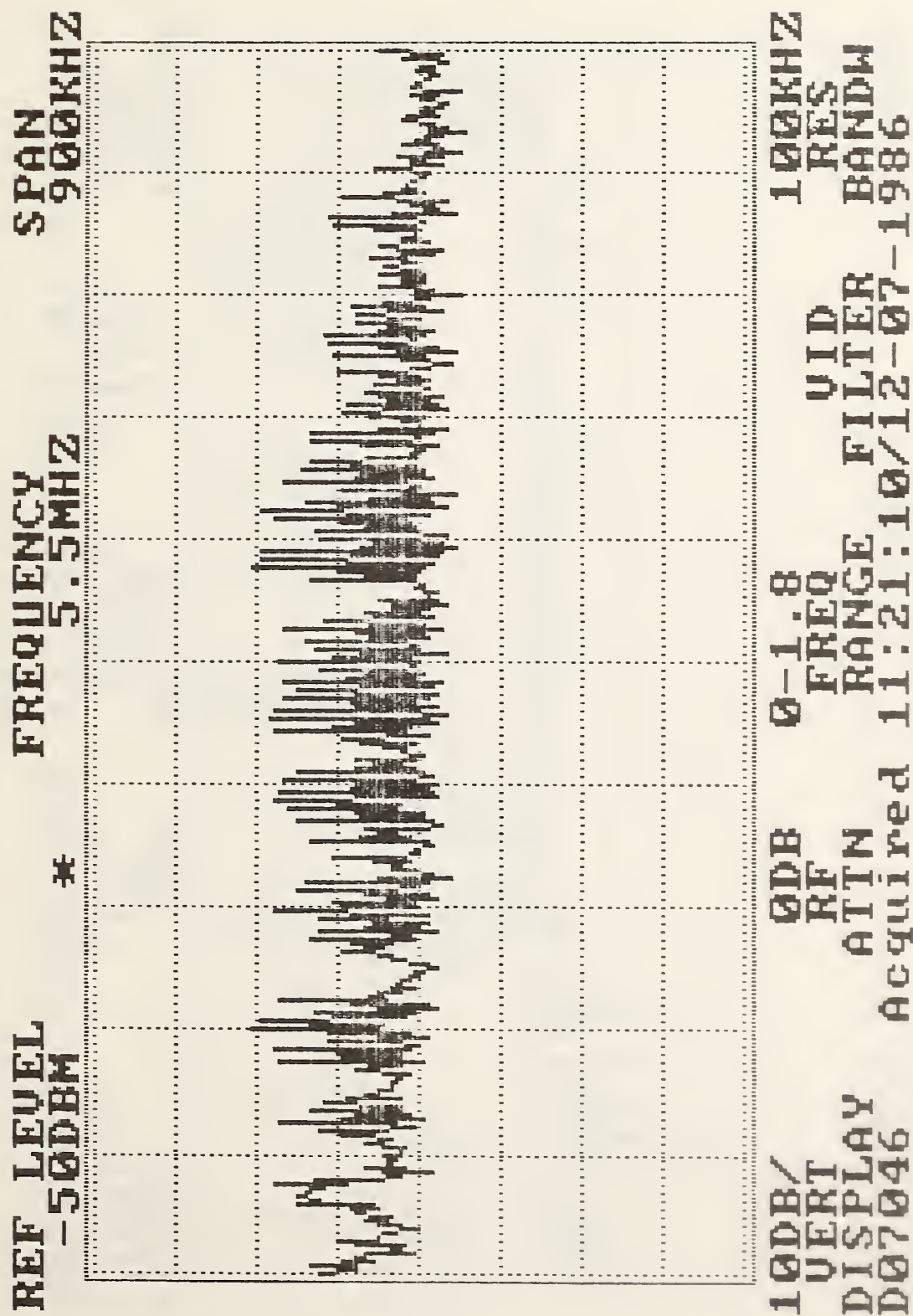


Figure 29. Blackhawk Helicopter.

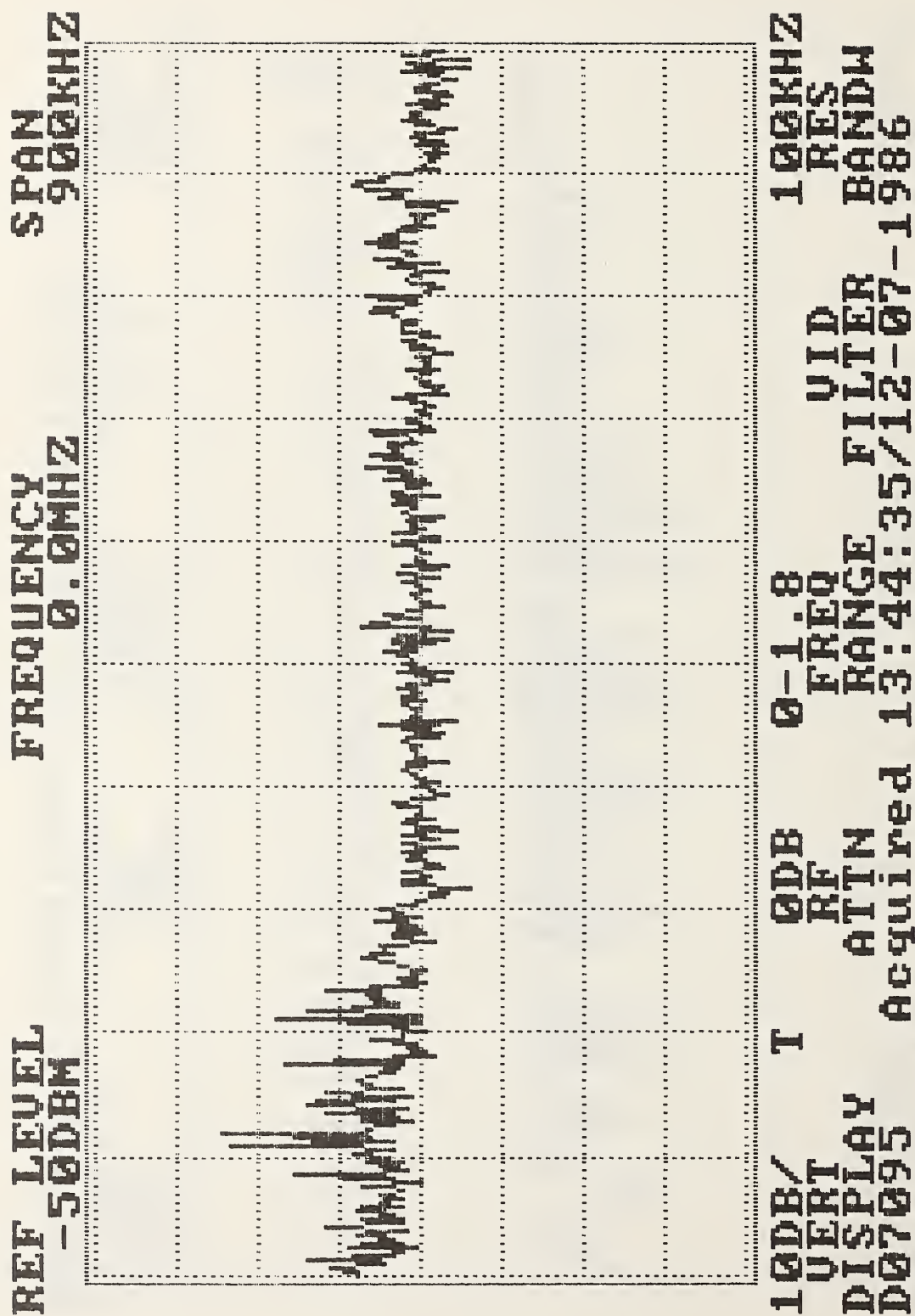
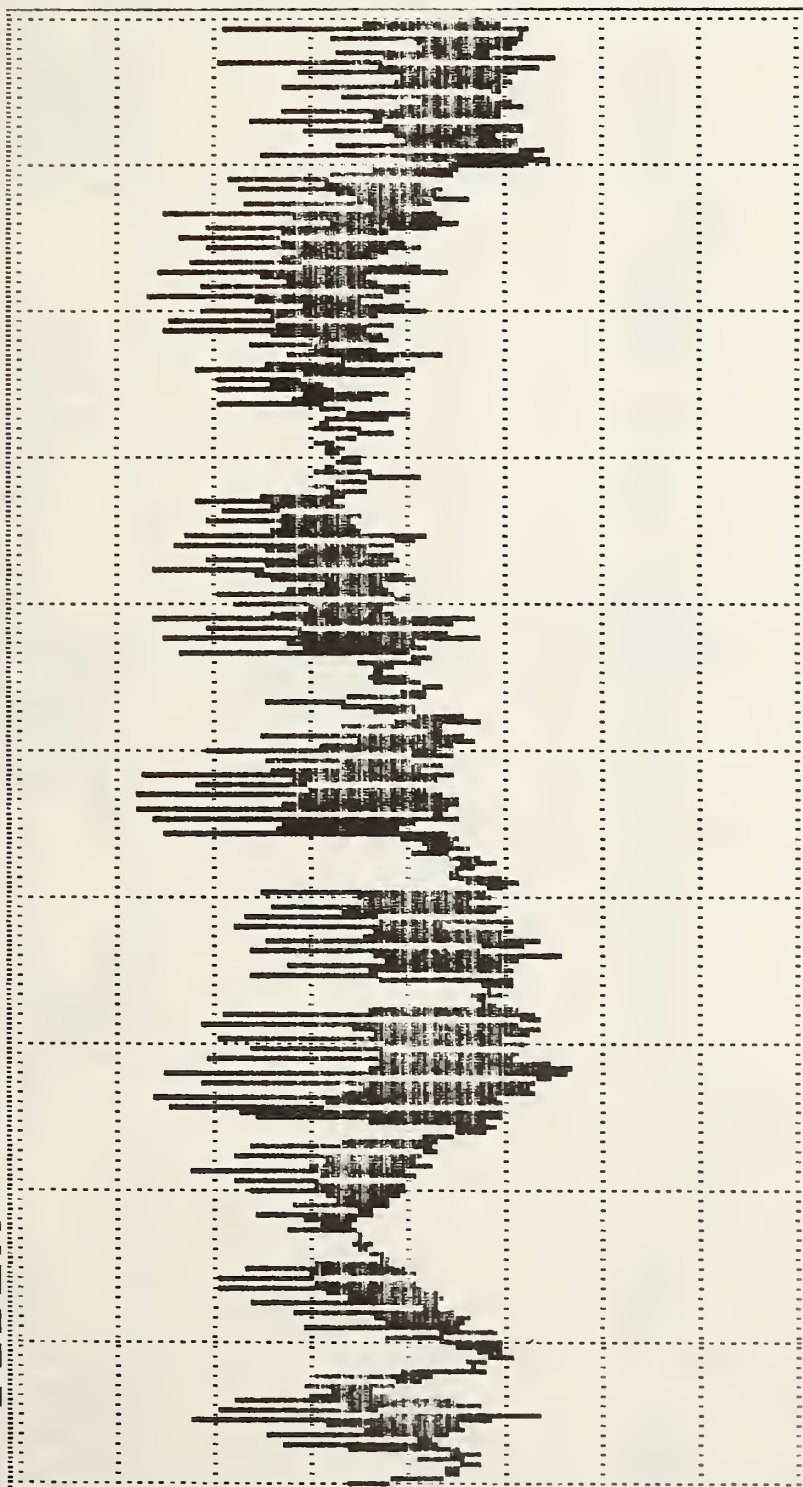


Figure 30. Blackhawk Helicopter.

REF LEVEL -30DBM FREQUENCY 5.5MHZ SPAN 900KHZ



10DB/ 0DB 0-1.8 100KHZ
 UERT RF REQ RES
 DISPLAY ATTN RANGE FILTER BANDW
 D07051 Acquired 11:24:29/12-07-1986

Figure 31. Blackhawk Helicopter.

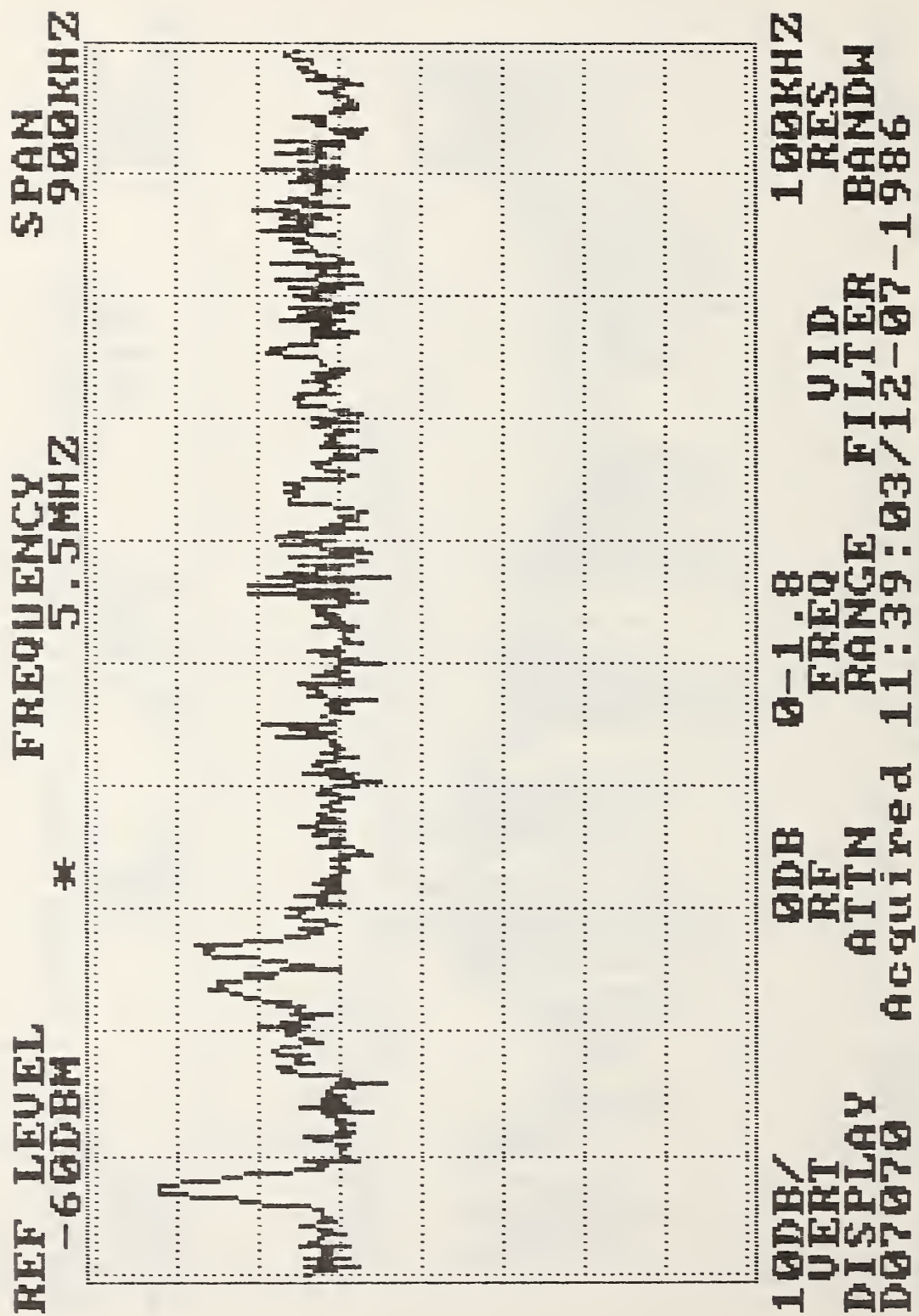


Figure 32. Blackhawk Helicopter.

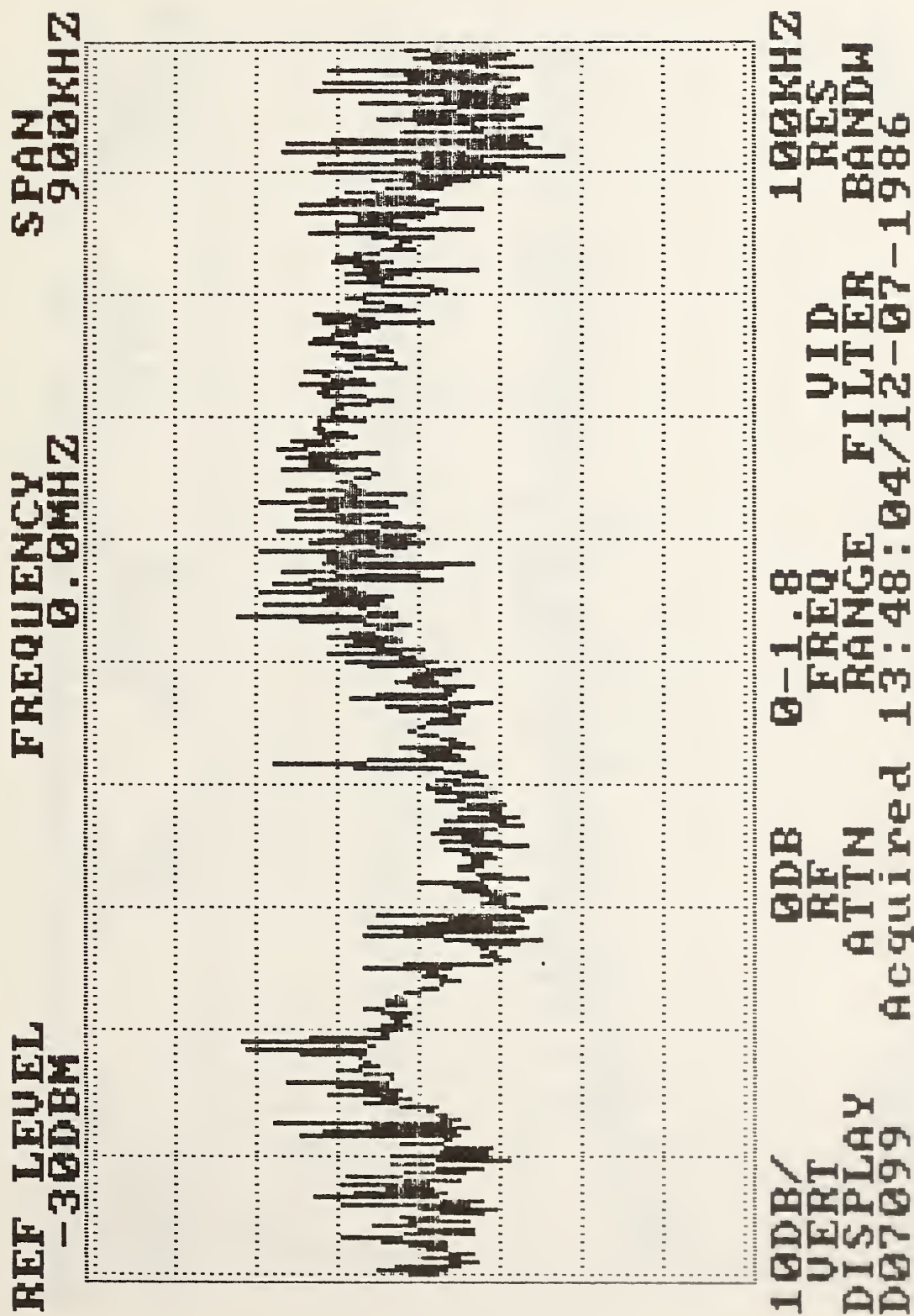


Figure 33. Blackhawk Helicopter.

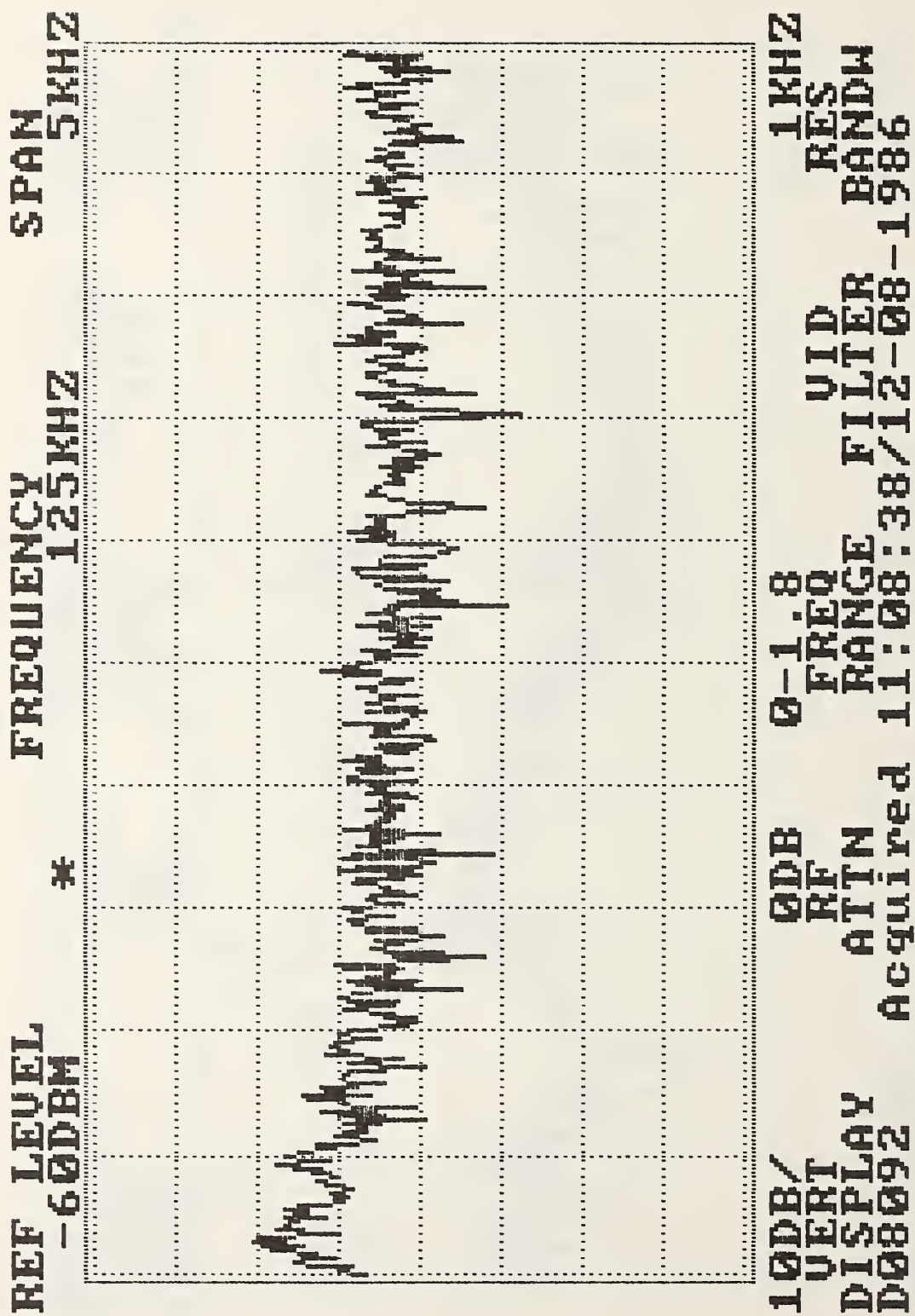


Figure 34. Chinook Helicopter.

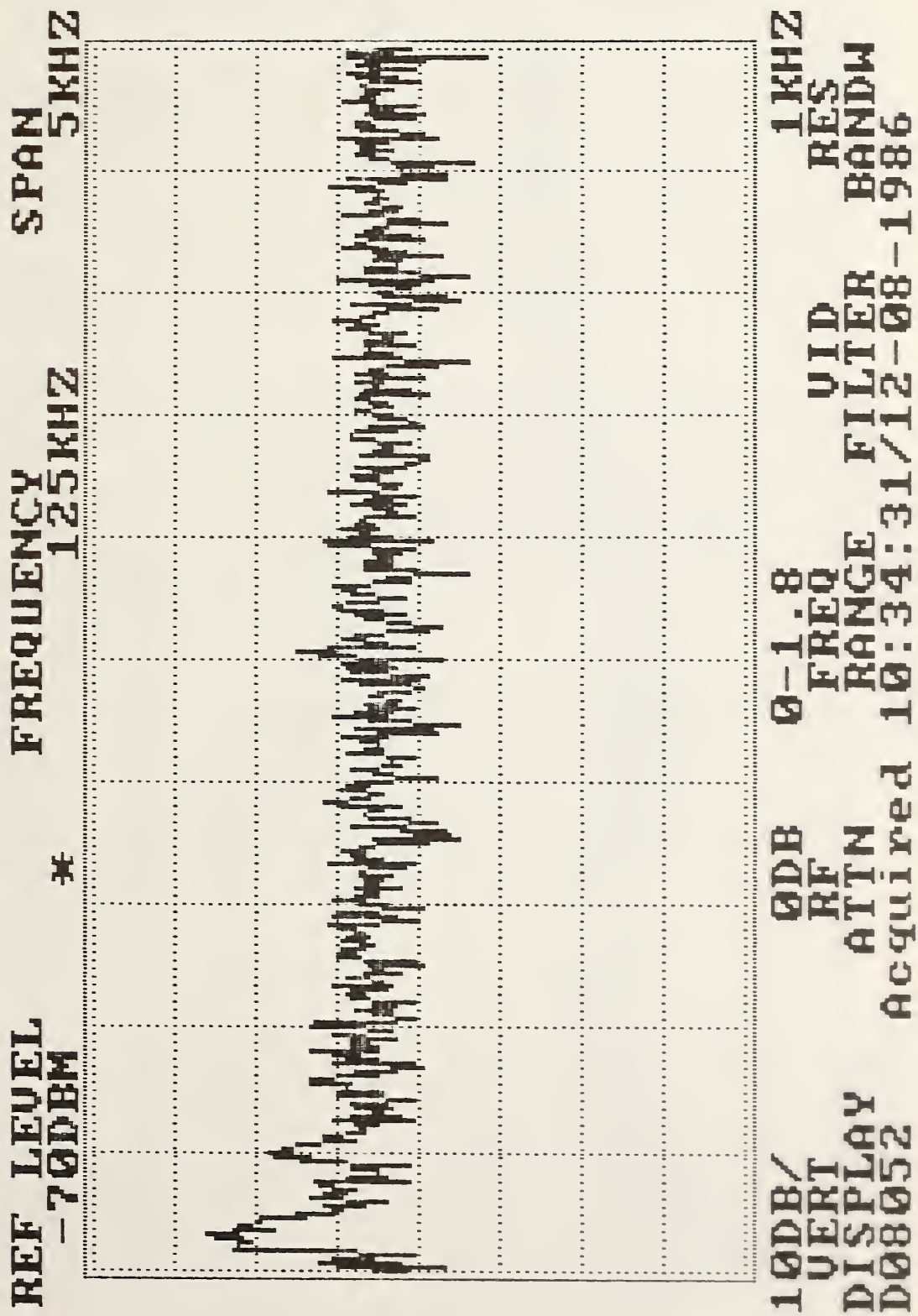


Figure 35. Chinook Helicopter

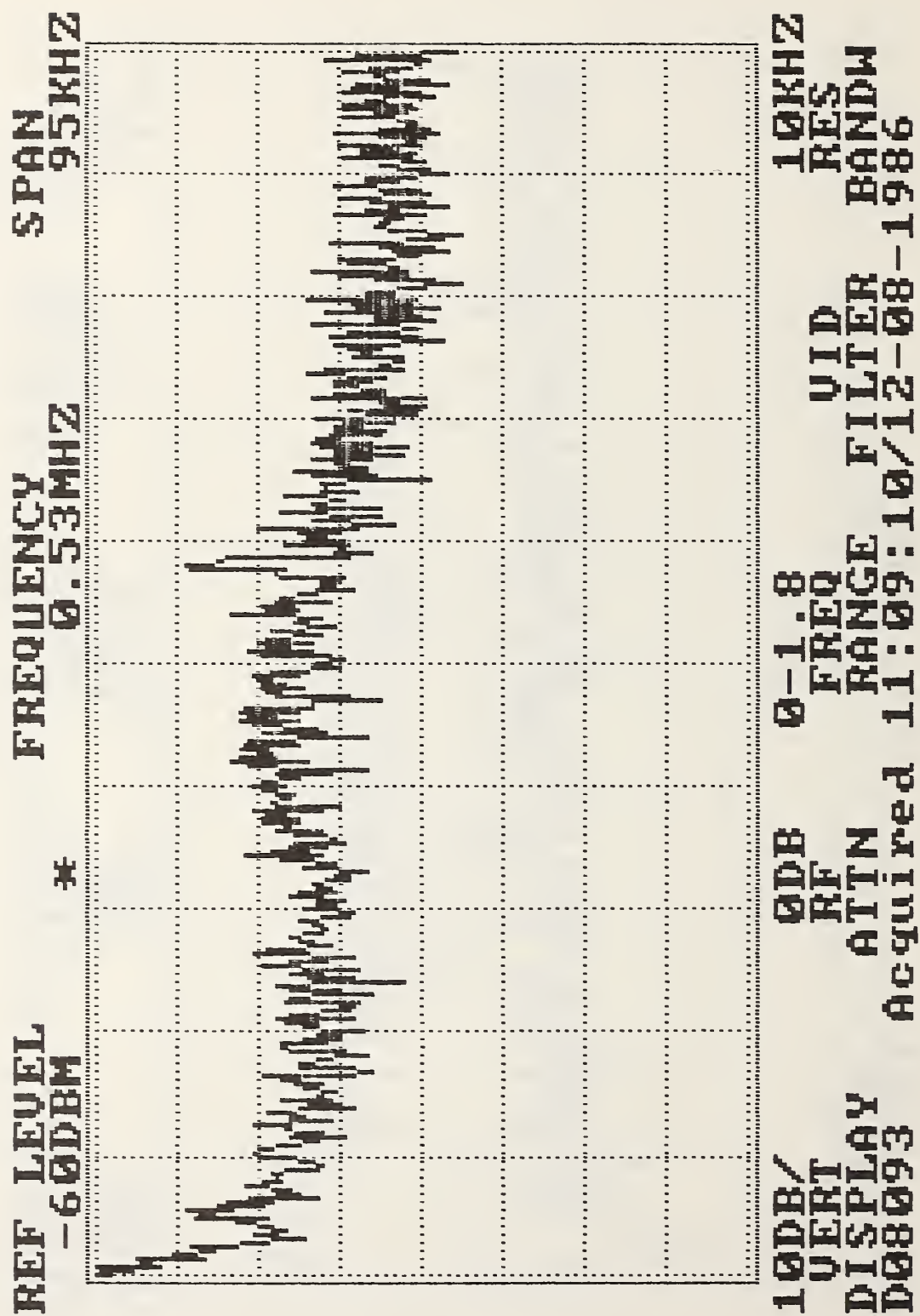


Figure 36. Chinook Helicopter.

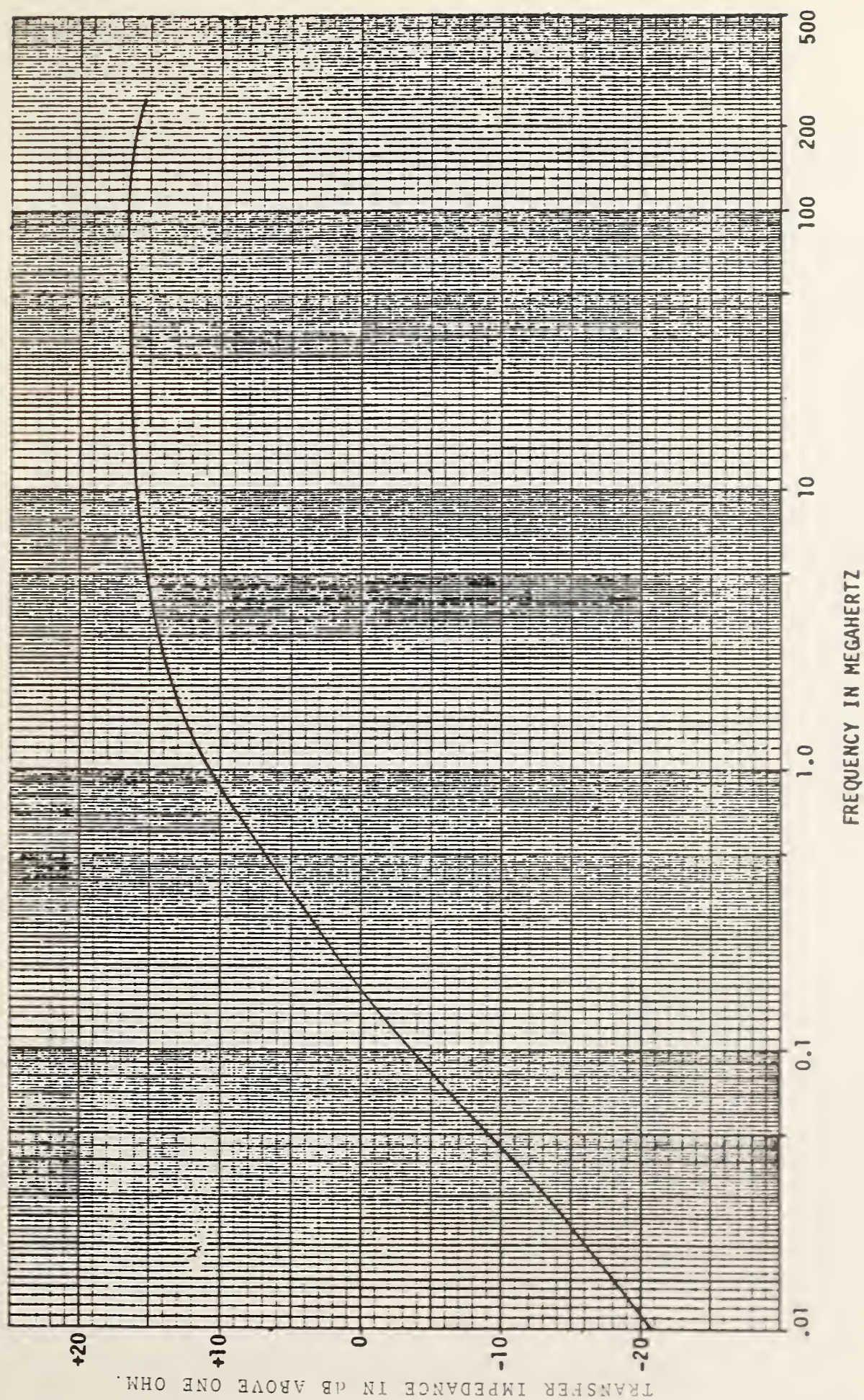


Figure 37 Transfer Function for a small size H-field current clamp.

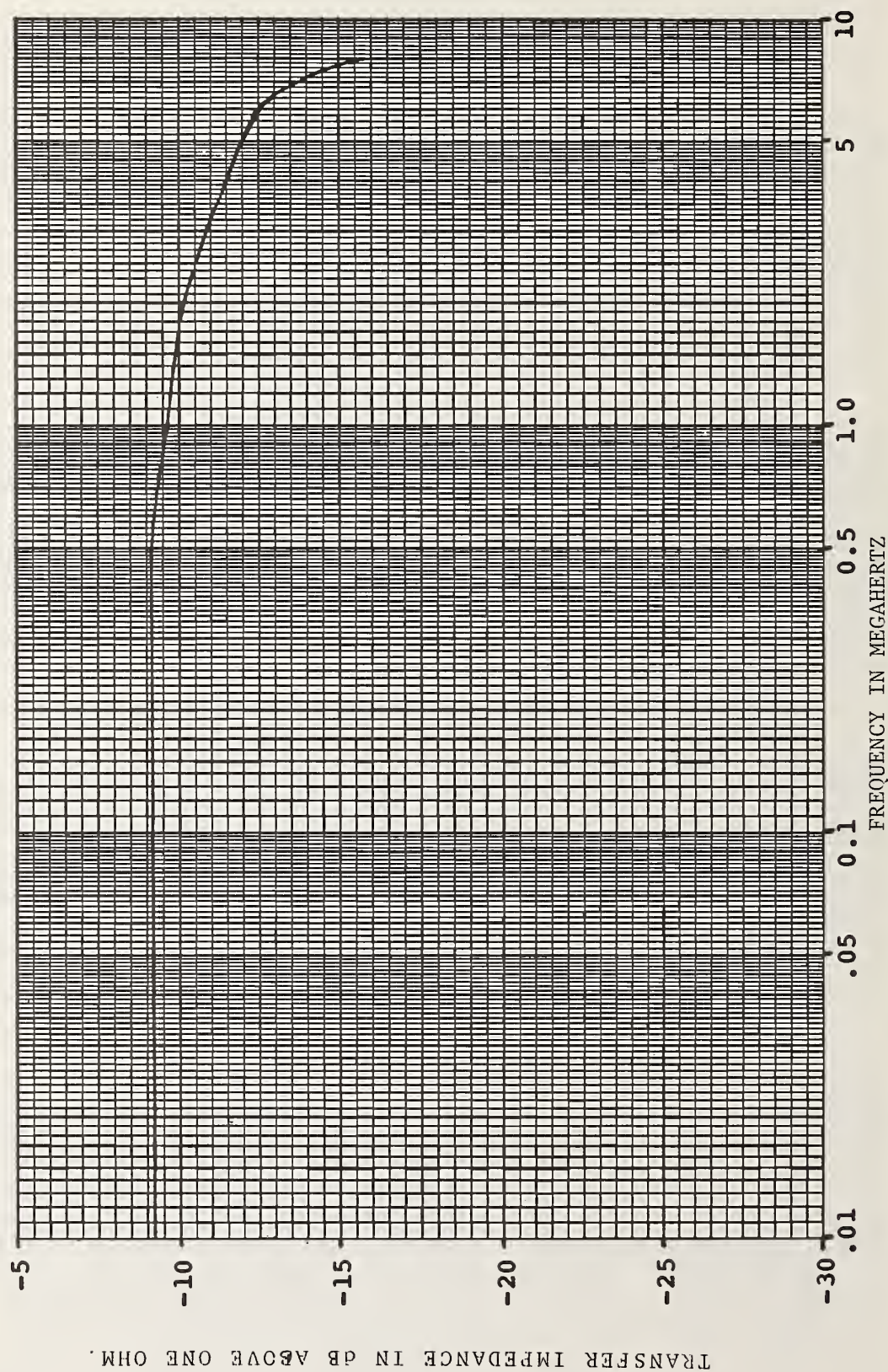
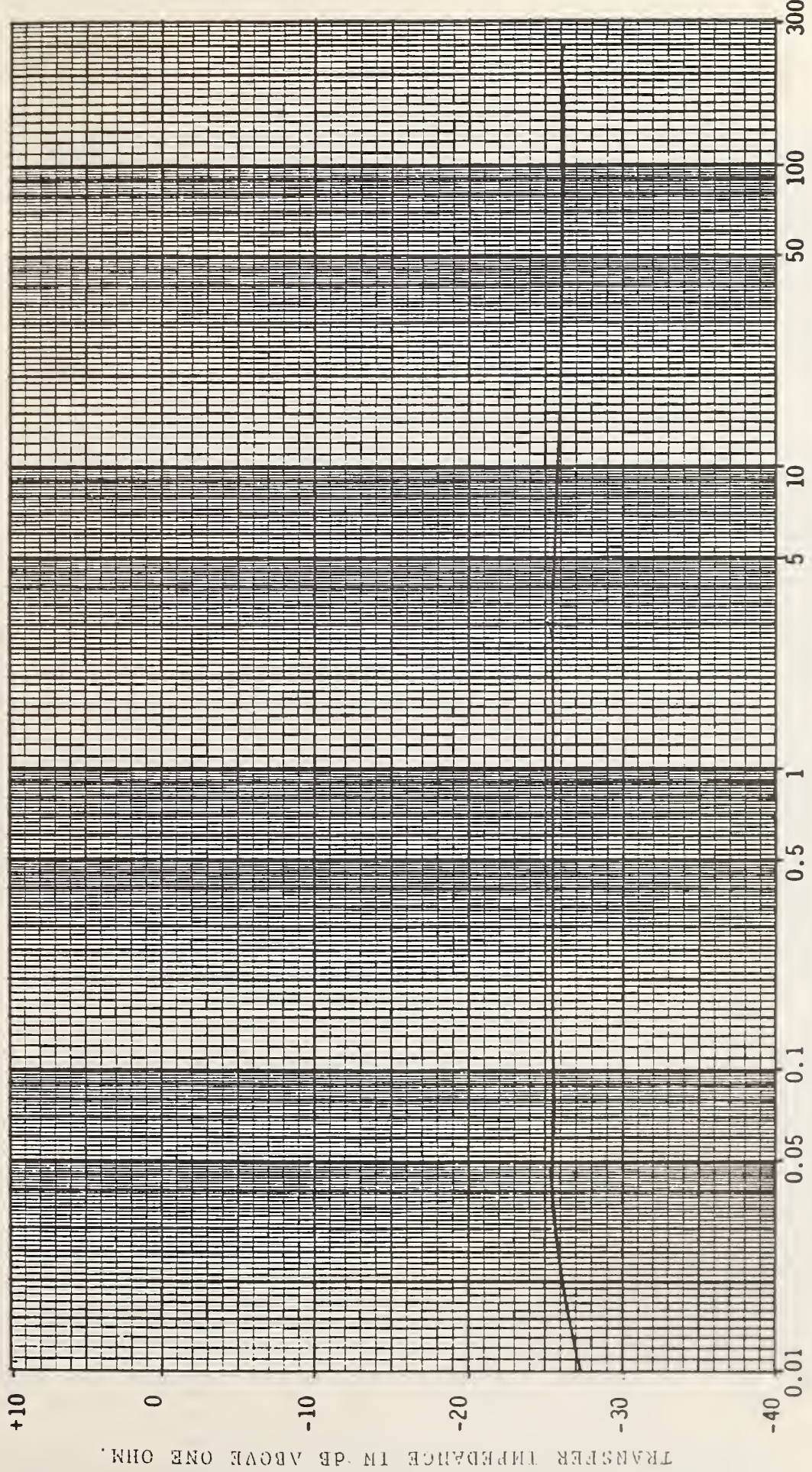


Figure 38. Transfer Function for a medium size H-field current clamp.



TRANSFER IMPEDANCE IN DB ABOVE ONE OHM.

FREQUENCY IN MEGAHERTZ

Figure 39. Transfer Function for a medium size H-field current clamp.

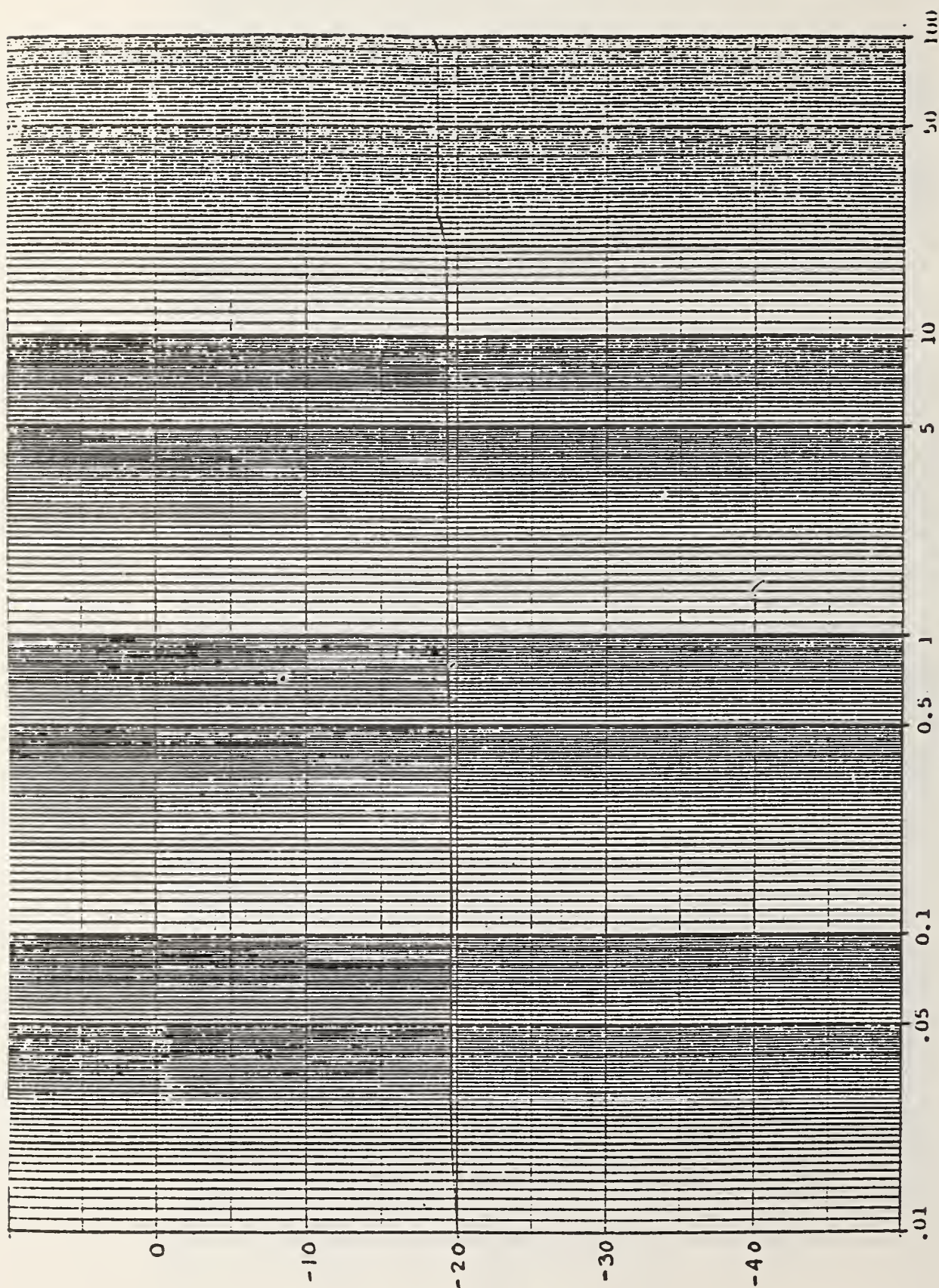


Figure 40. Transfer Function for a medium size H-field current clamp.

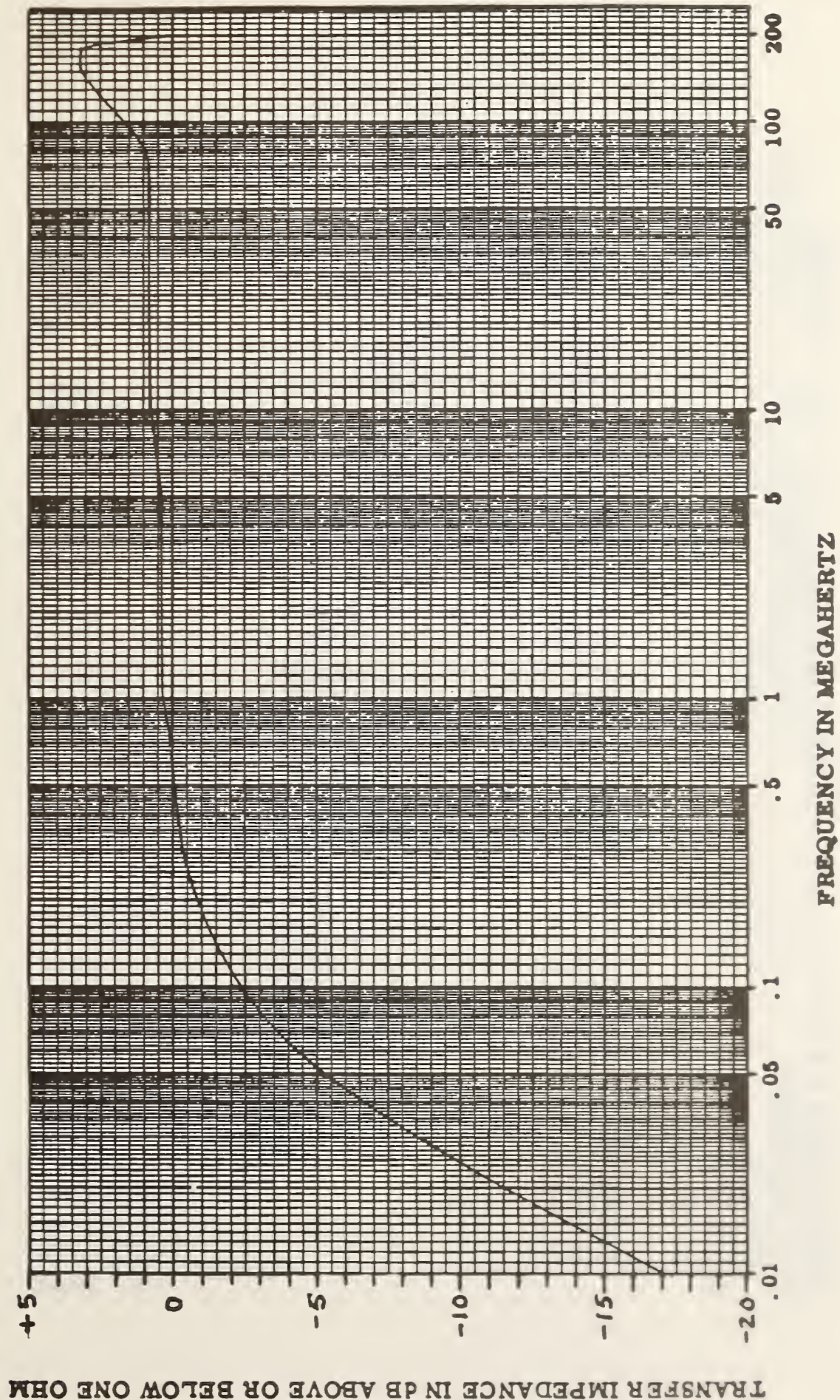
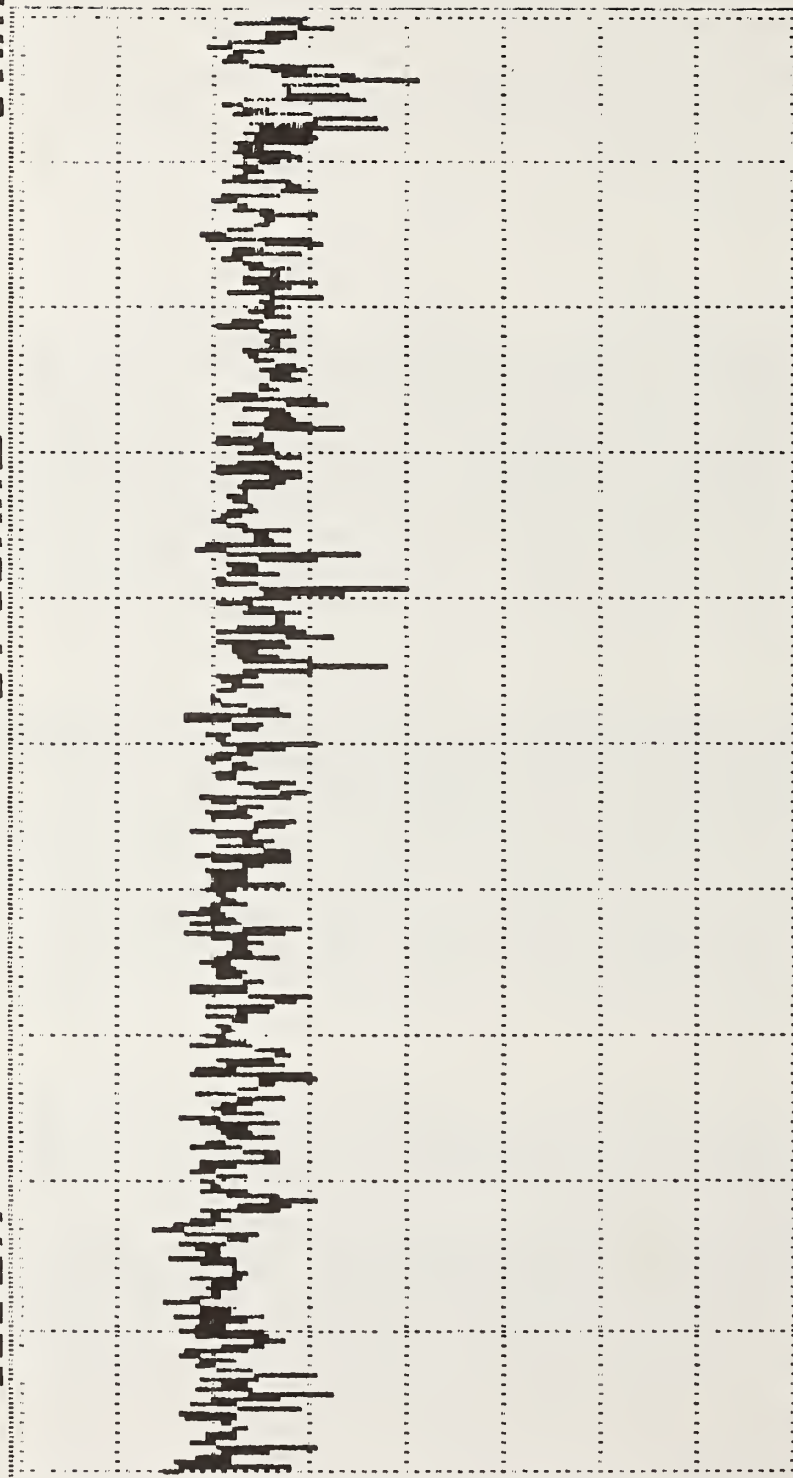


Figure 41. Transfer Function for the large size H-field current clamp.

REF LEVEL FREQUENCY SPAN
 -40DBM -0.40MHZ 5KHZ

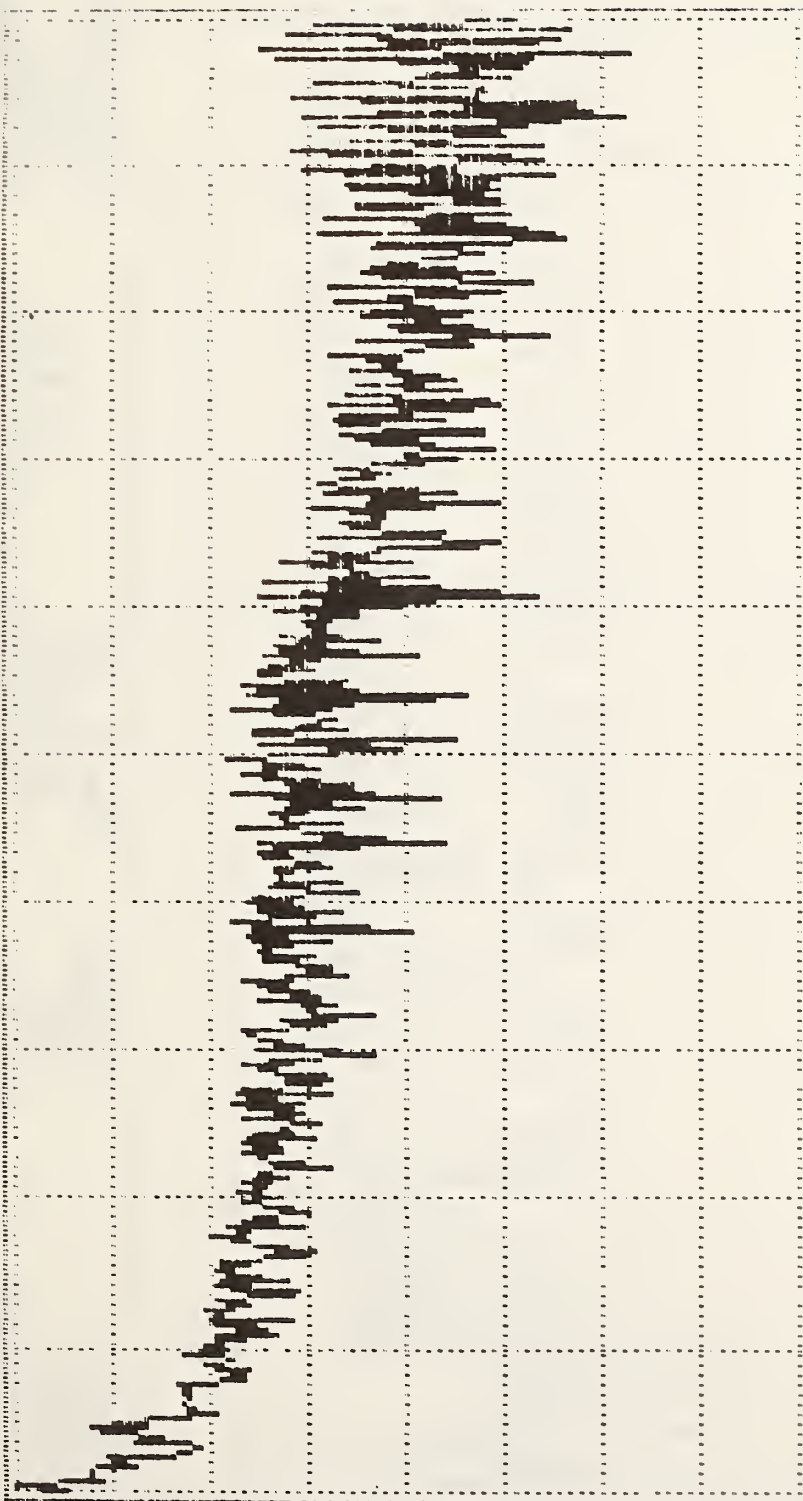


10DB/
 VERT
 DISPLAY
 D08101

0DB 0-1.8 1KHZ
 RF FRQ RES
 ATTN RANGE BANDW
 Acquired 11:15:28/12-08-1986

Figure 42. Chinook Helicopter.

REF LEVEL -30DBM FREQUENCY 0.00MHZ SPAN 95KHZ



10DB/ 0DB 0-1.8 10KHZ
 VERT RF FRÉQ RES
 DISPLAY ATTN RANGE VID BANDW
 D08102 Acquired 11:15:57/12-08-1986

Figure 43. Chinook Helicopter.

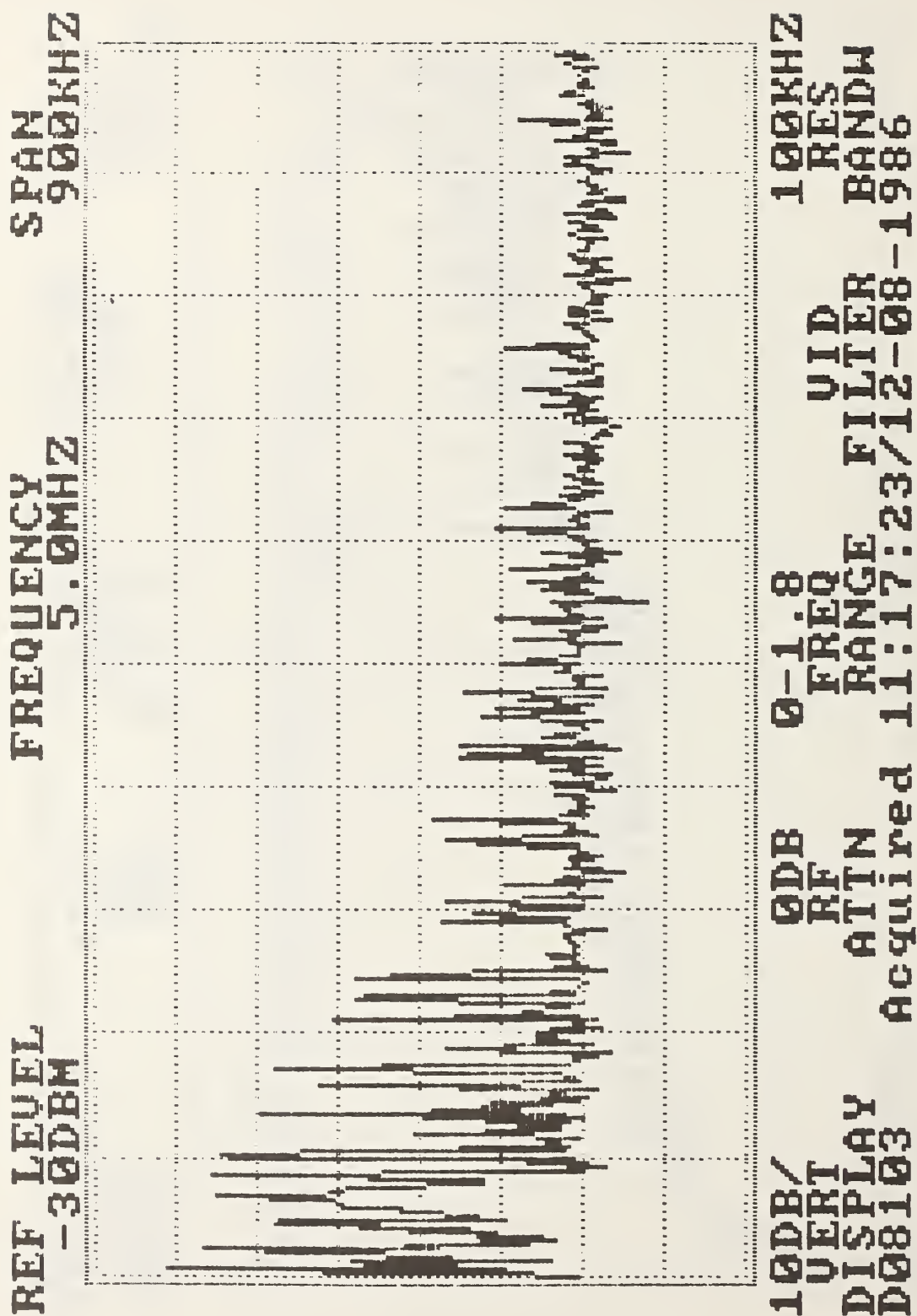


Figure 44. Chinook Helicopter.

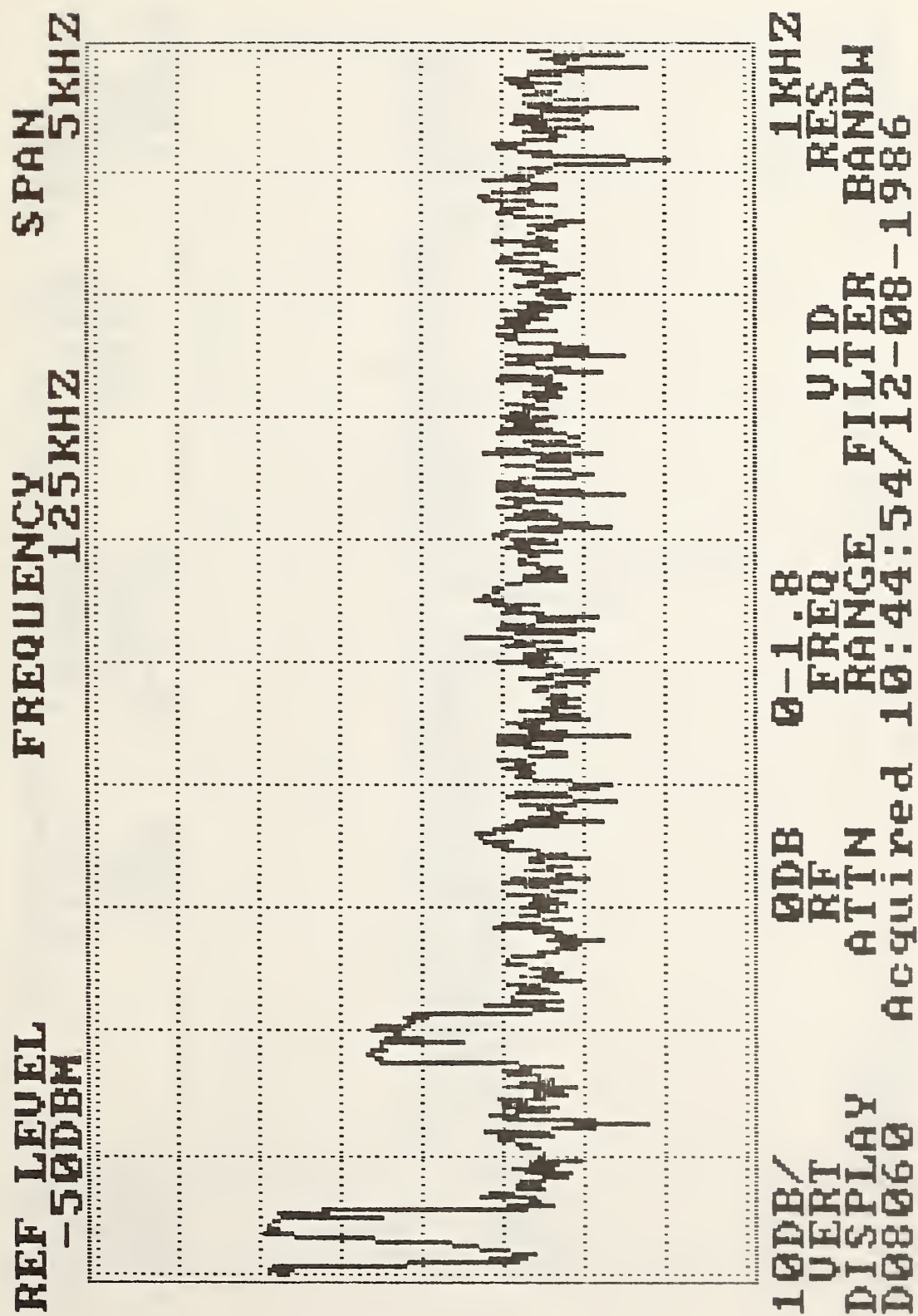


Figure 45. Chinook Helicopter.

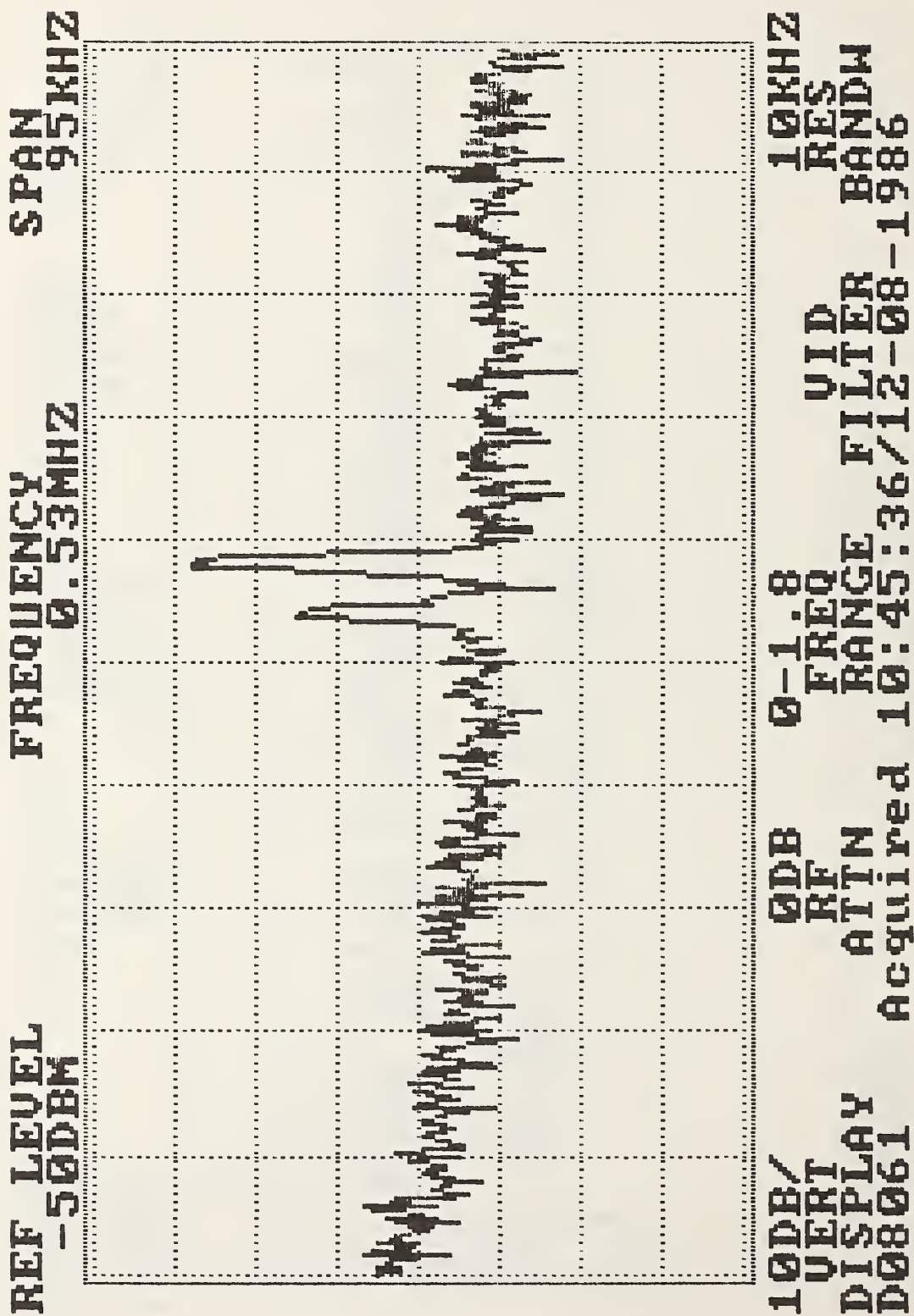
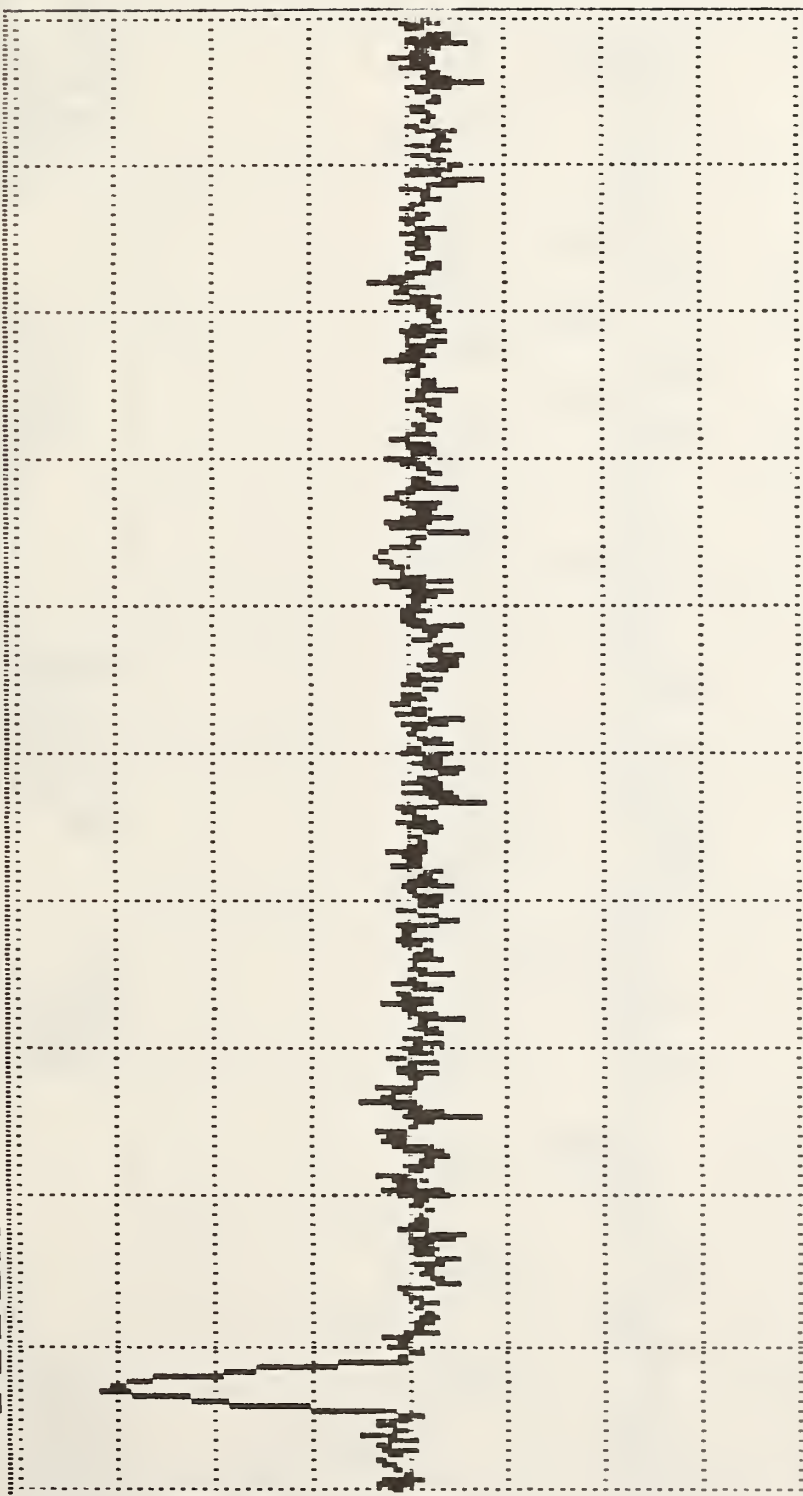


Figure 46. Chinook Helicopter.

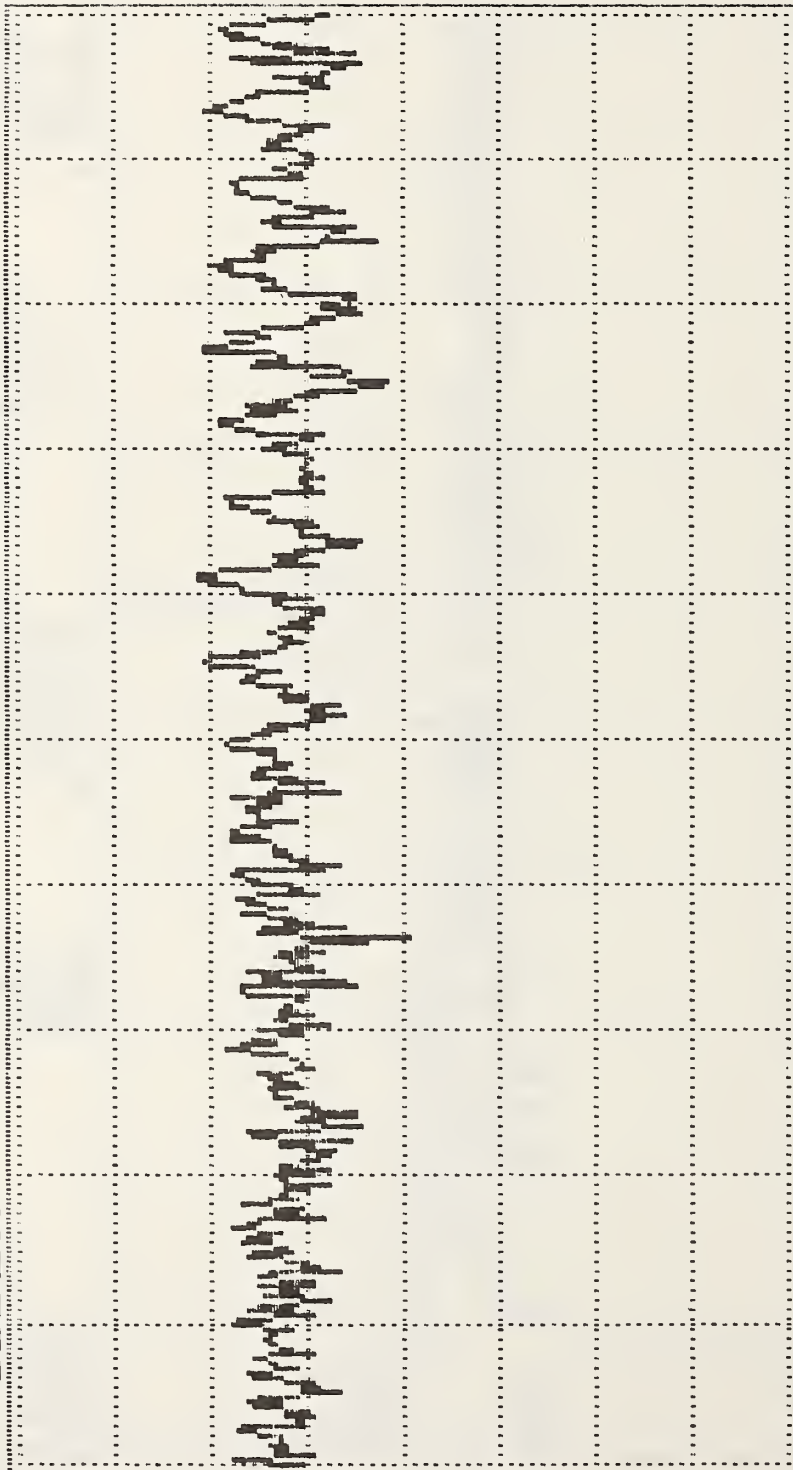
REF LEVEL -50DBM FREQUENCY 5.5MHZ SPAN 900KHZ



10DB/VID 0-1.8 100KHZ
 DISPLAY RANGE RES
 D08062 10:46:20/12-08-1986 BANDW

Figure 47. Chinook Helicopter.

REF LEVEL -40DBM FREQUENCY 125KHZ SPAN 5KHZ



10DB/VERTLAY 0-1.8 1KHZ
 DISPLAY RANGE RES
 D09073 12:54:56/12-09-1986 BANDW

Figure 48. Mohawk Airplane.

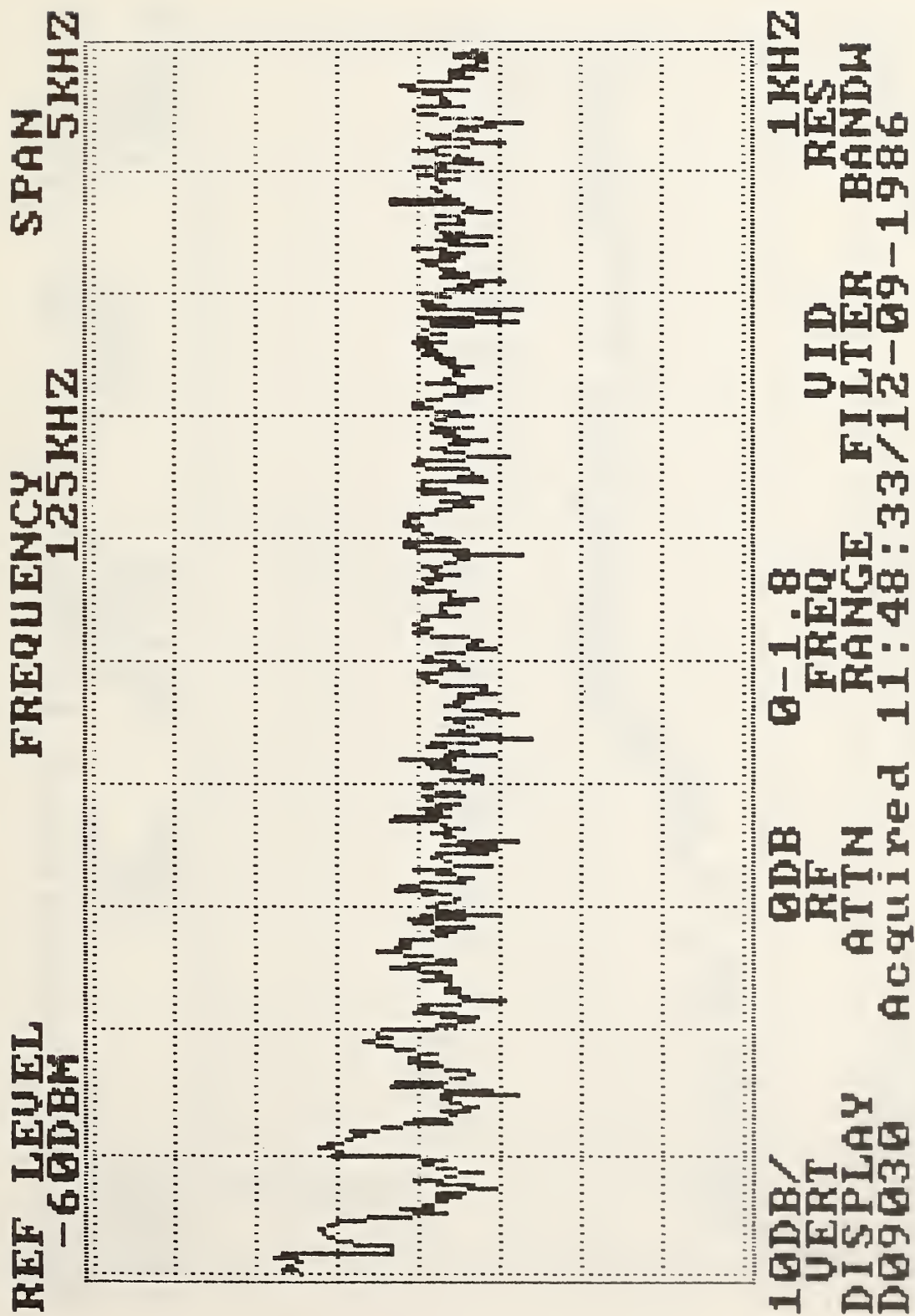


Figure 49. Mohawk Airplane.

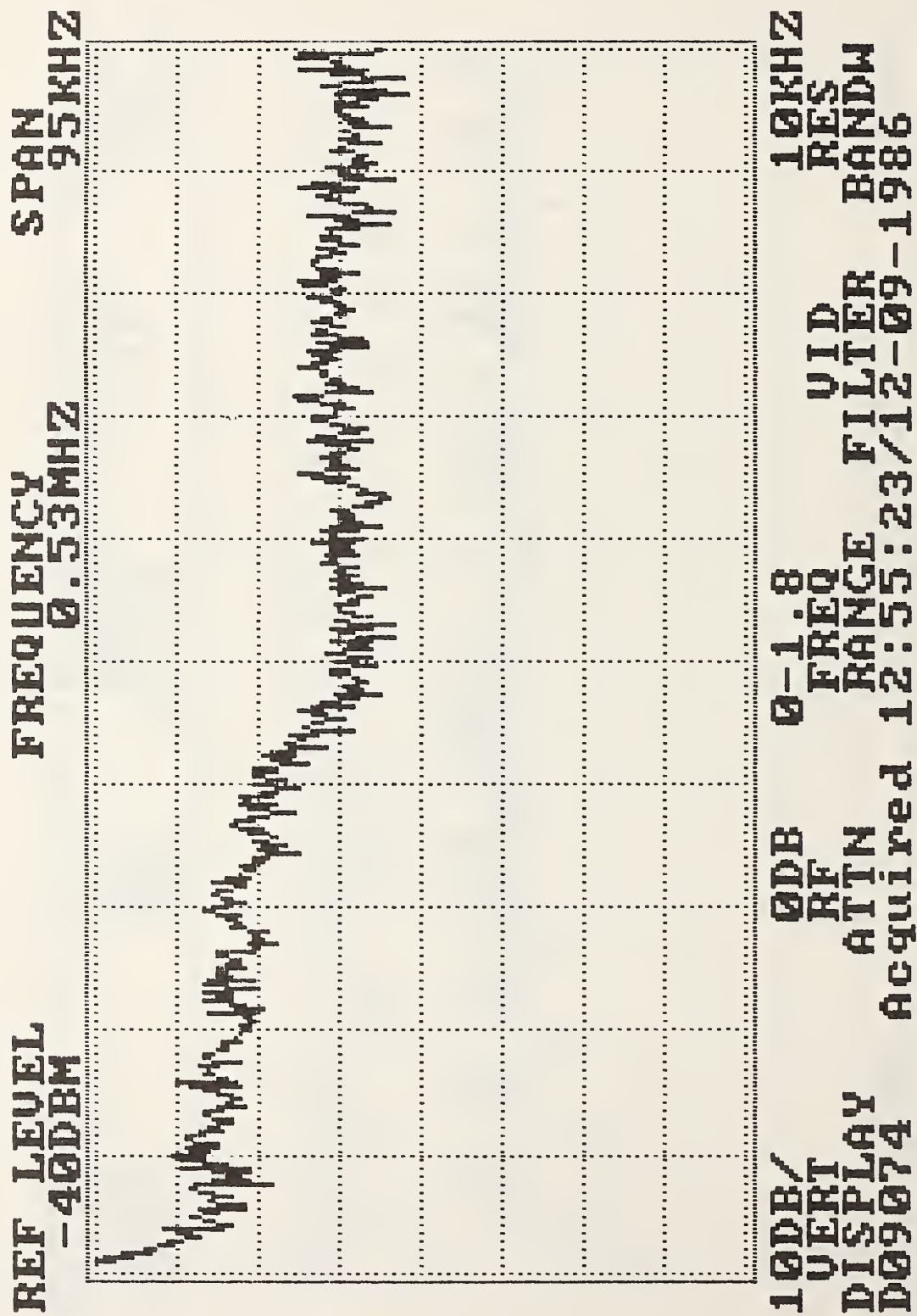
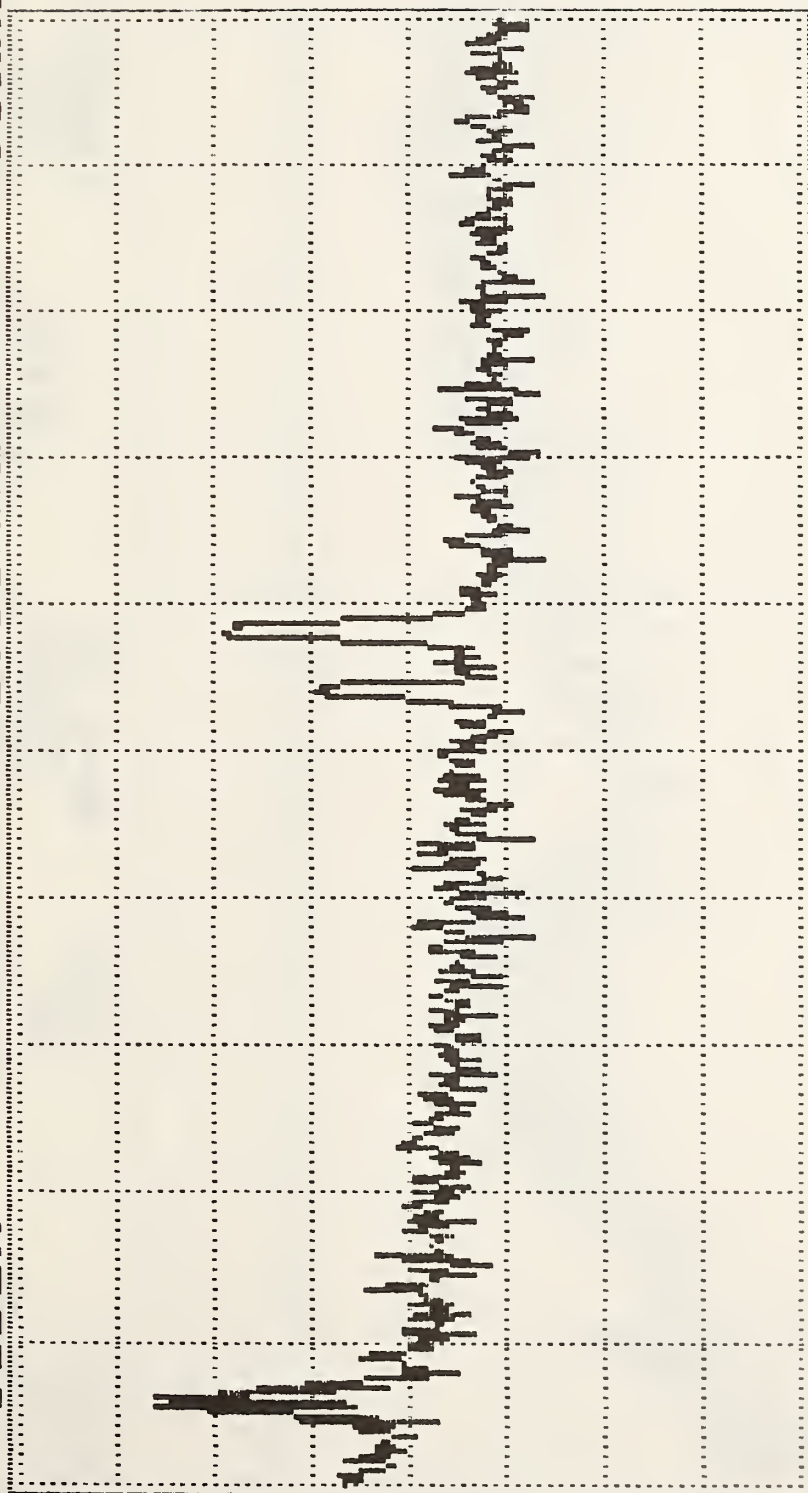


Figure 50. Mohawk Airplane.

REF LEVEL -50DBM FREQUENCY 0.53MHZ SPAN 95KHZ



10DB/VERI 0-1.8 10KHZ
 DISPLAY RF REQ RES
 D09029 ATTN RANGE FILTER BANDW
 Acquired 11:48:04/12-09-1986

Figure 51. Mohawk Airplane.

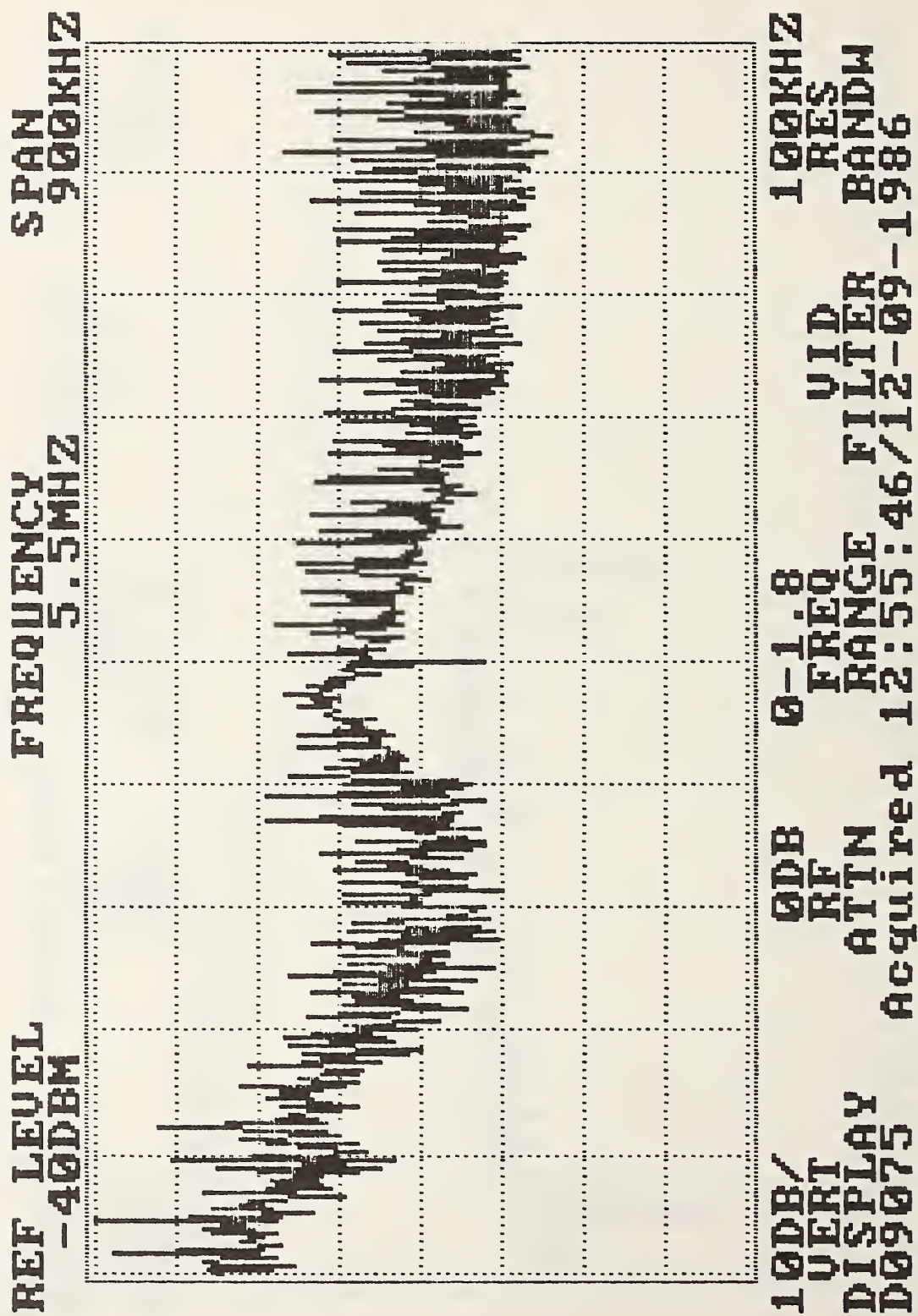
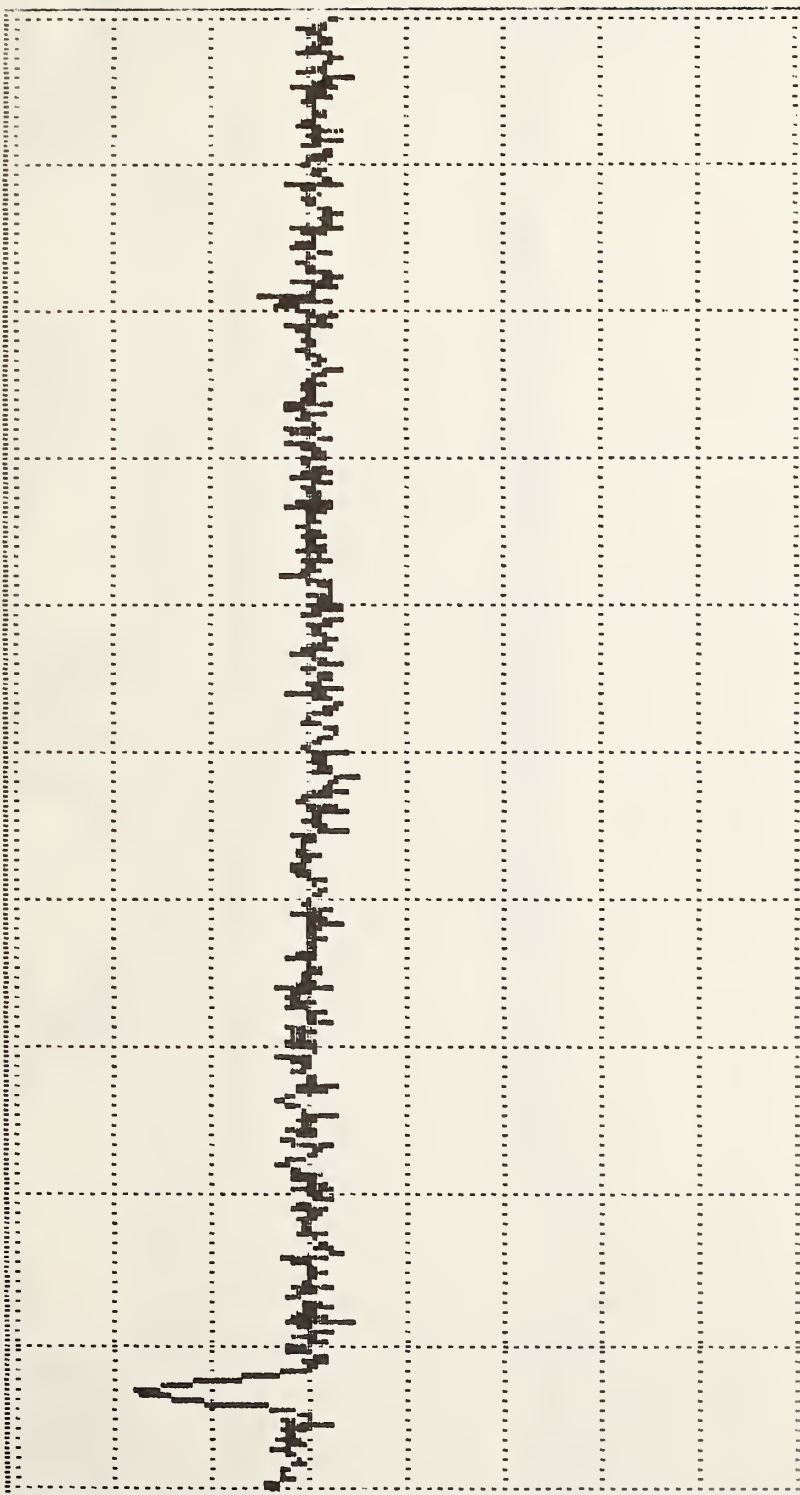


Figure 52. Mohawk Airplane.

REF LEVEL -60DBM FREQUENCY 5.5MHZ SPAN 900KHZ



10DB/VER/ DISPLAY D09028 0DB RF ATTN Acquired 0-1.8 FREQ RANGE 11:47:29/12-09-1986 VID FILTER 100KHZ RES BANDW

Figure 53. Mohawk Airplane.

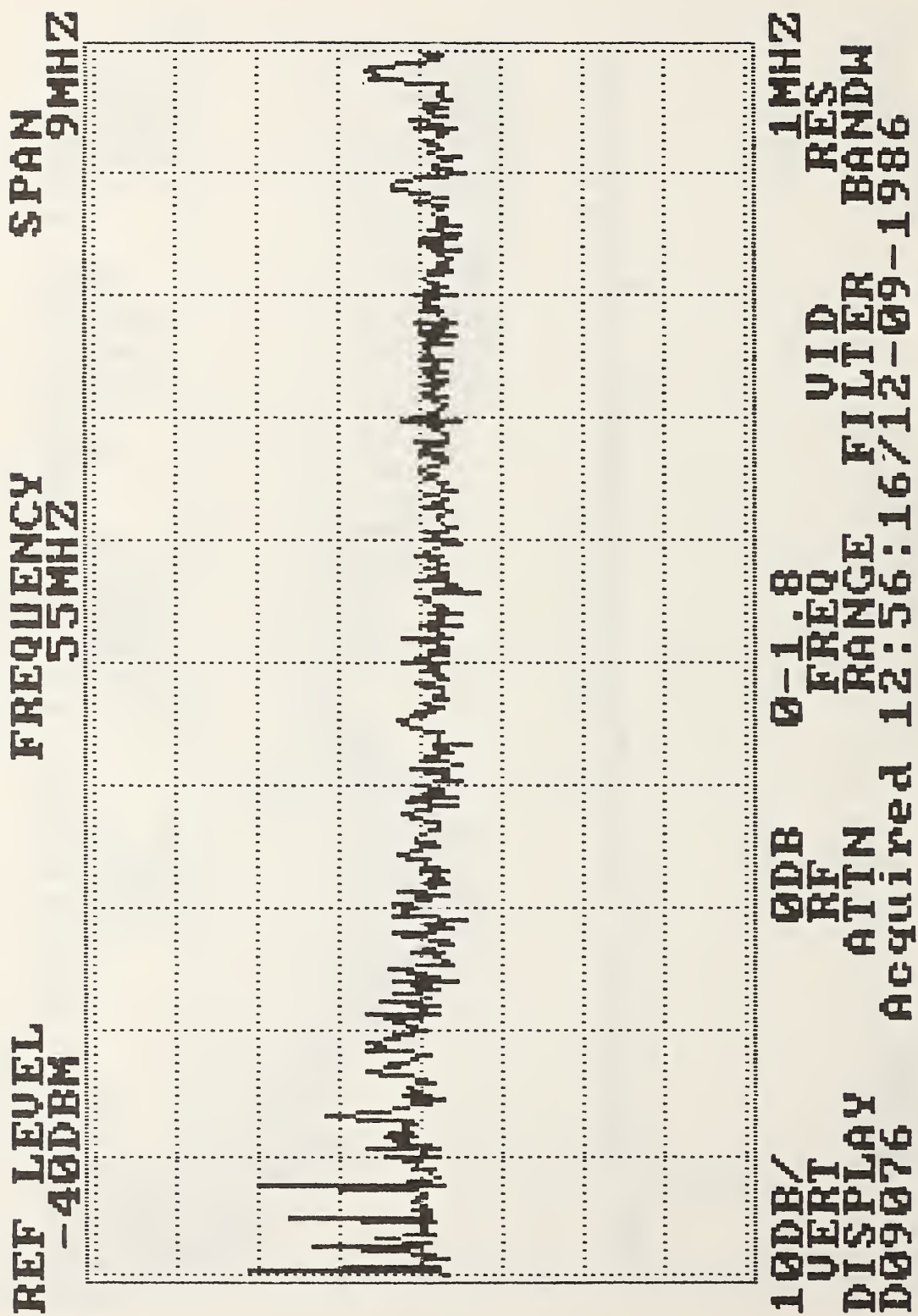
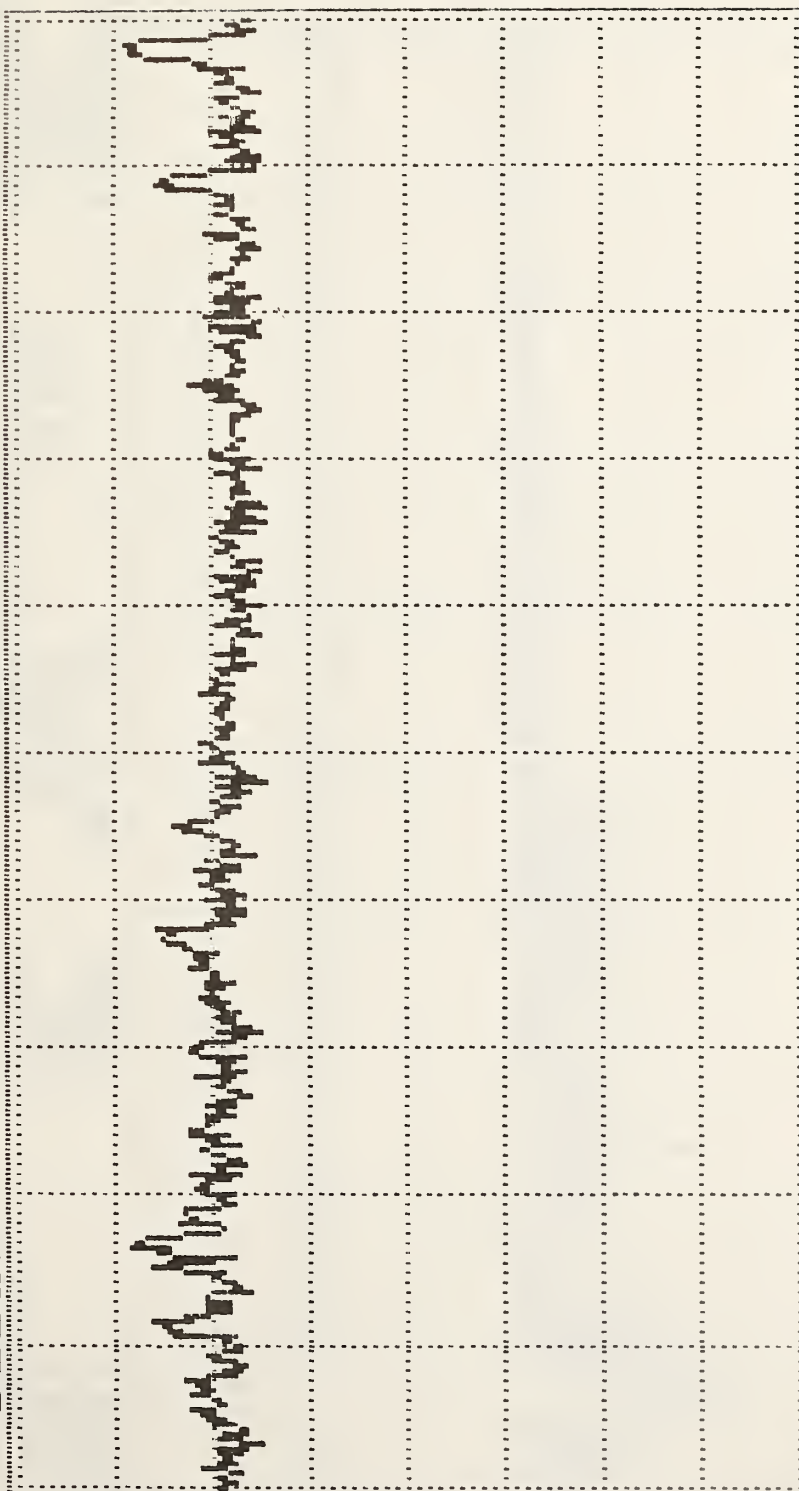


Figure 54. Mohawk Airplane.

REF LEVEL -60DBM FREQUENCY 55MHZ SPAN 9MHZ



10DB/VIDERT DISPLAY D09027 0-1.8 FRQ RANGE 11:47:09-1986 1MHZ RES BANDW

Figure 55. Mohawk Airplane.

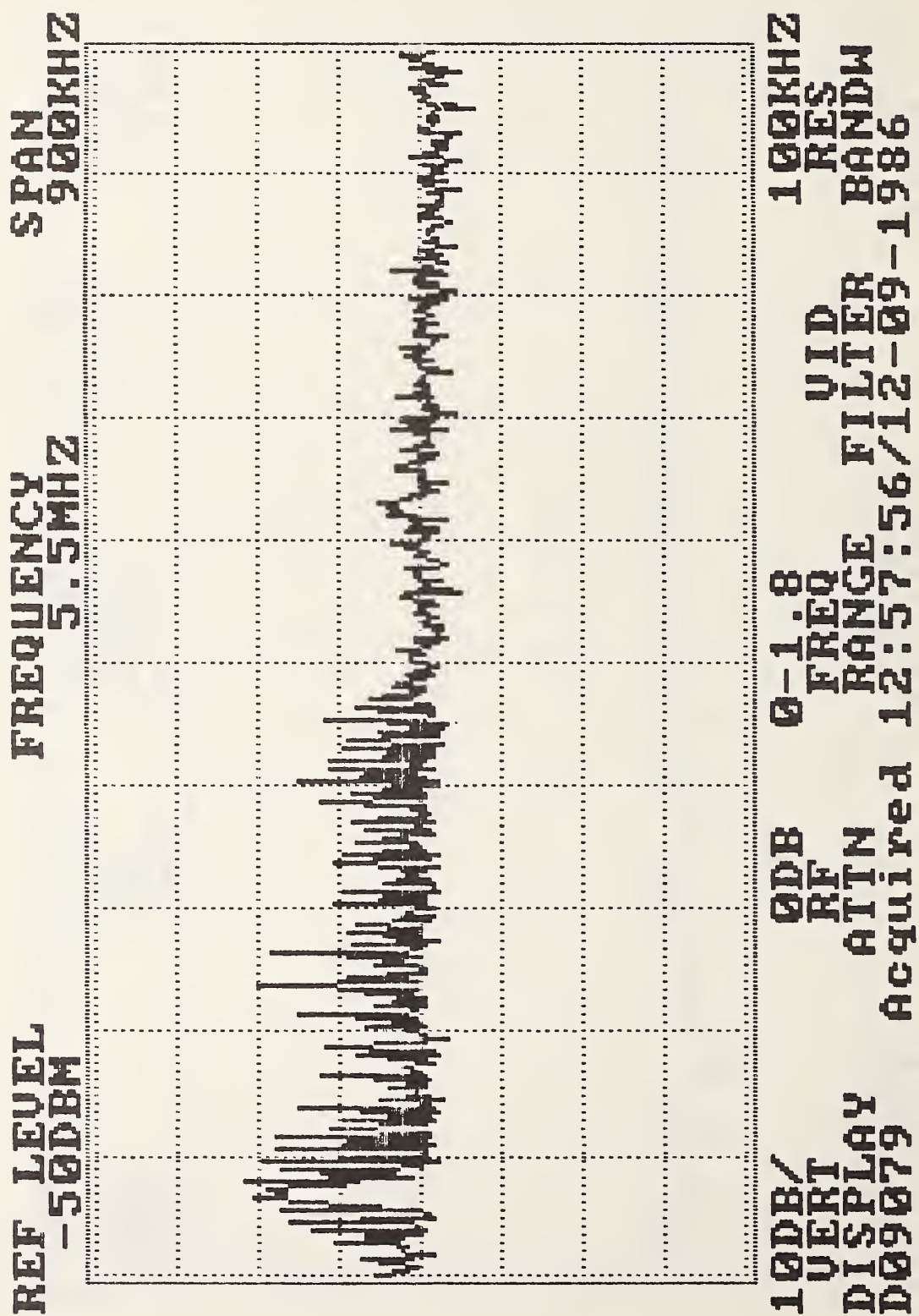
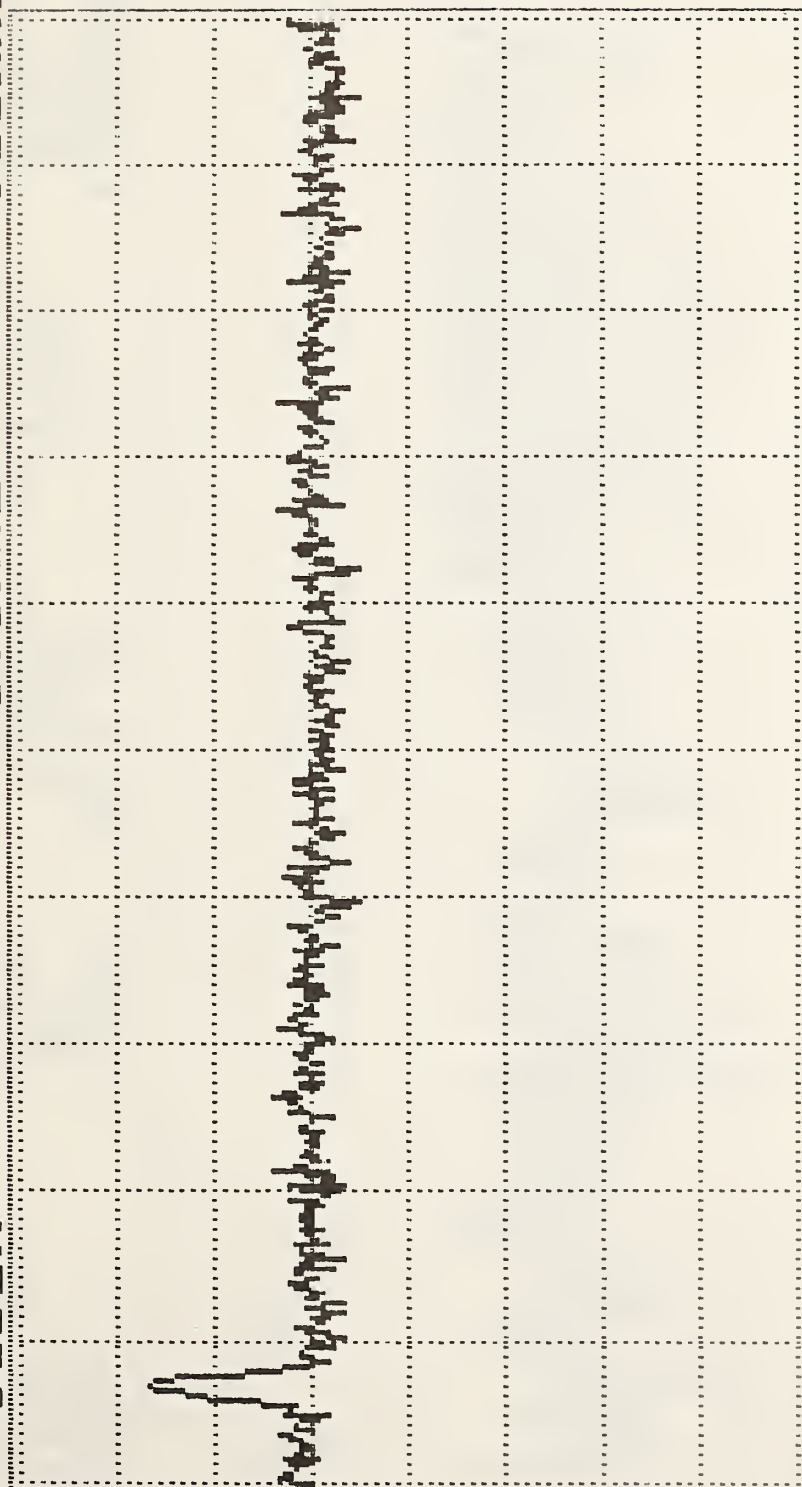


Figure 56. Mohawk Airplane.

REF LEVEL -60DBM FREQUENCY 5.5MHZ SPAN 900KHZ



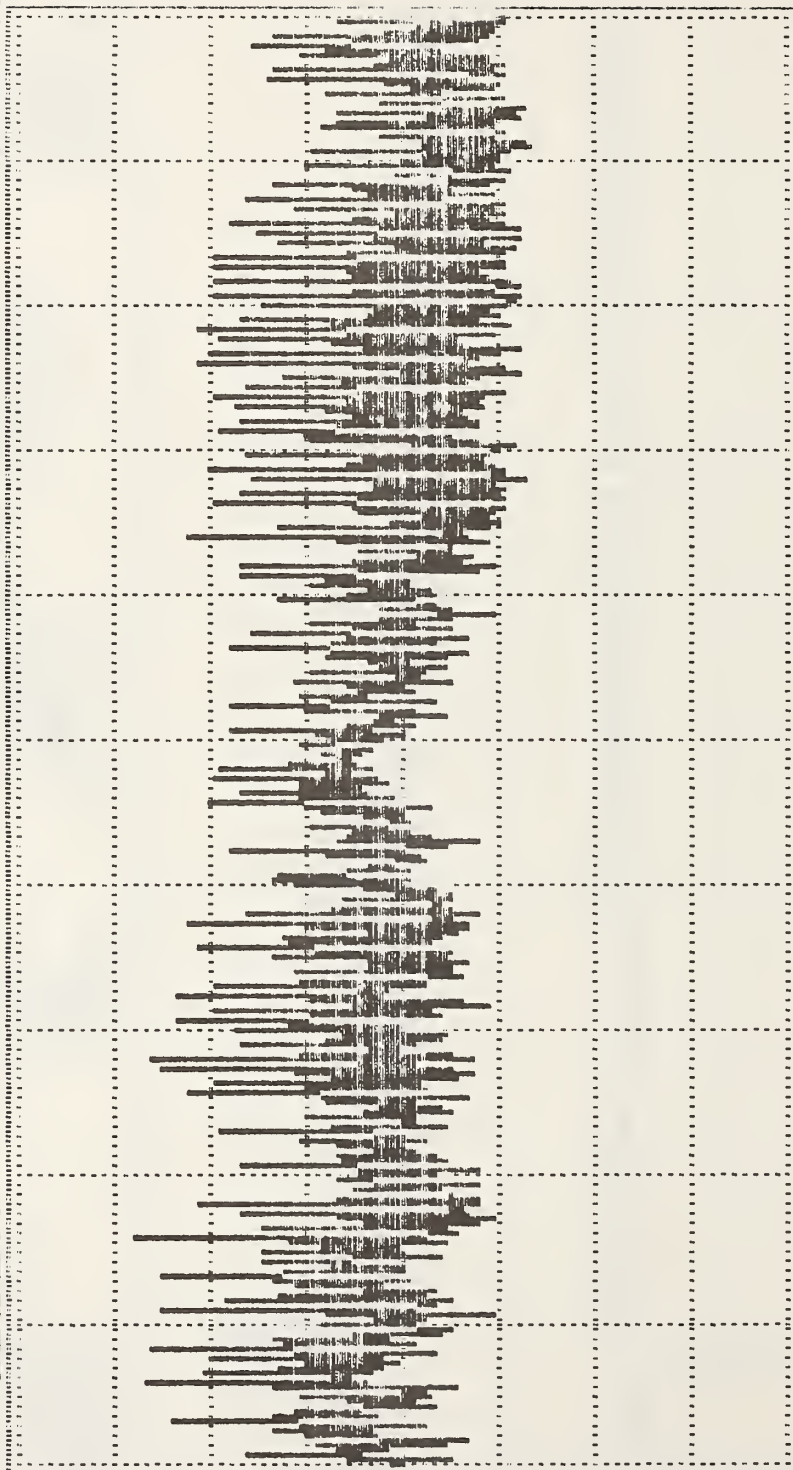
10DB/VID 0-1.8 UID 100KHZ
 DISPLAY RANGE FILTER RES
 D09033 Acquired 11:50:36/12-09-1986 BANDW

Figure 57. Mohawk Airplane.

REF LEVEL
-40DBM

FREQUENCY
5.5MHZ

SPAN
900KHZ



10DB/
OVERLAY
DISPLAY
D09065

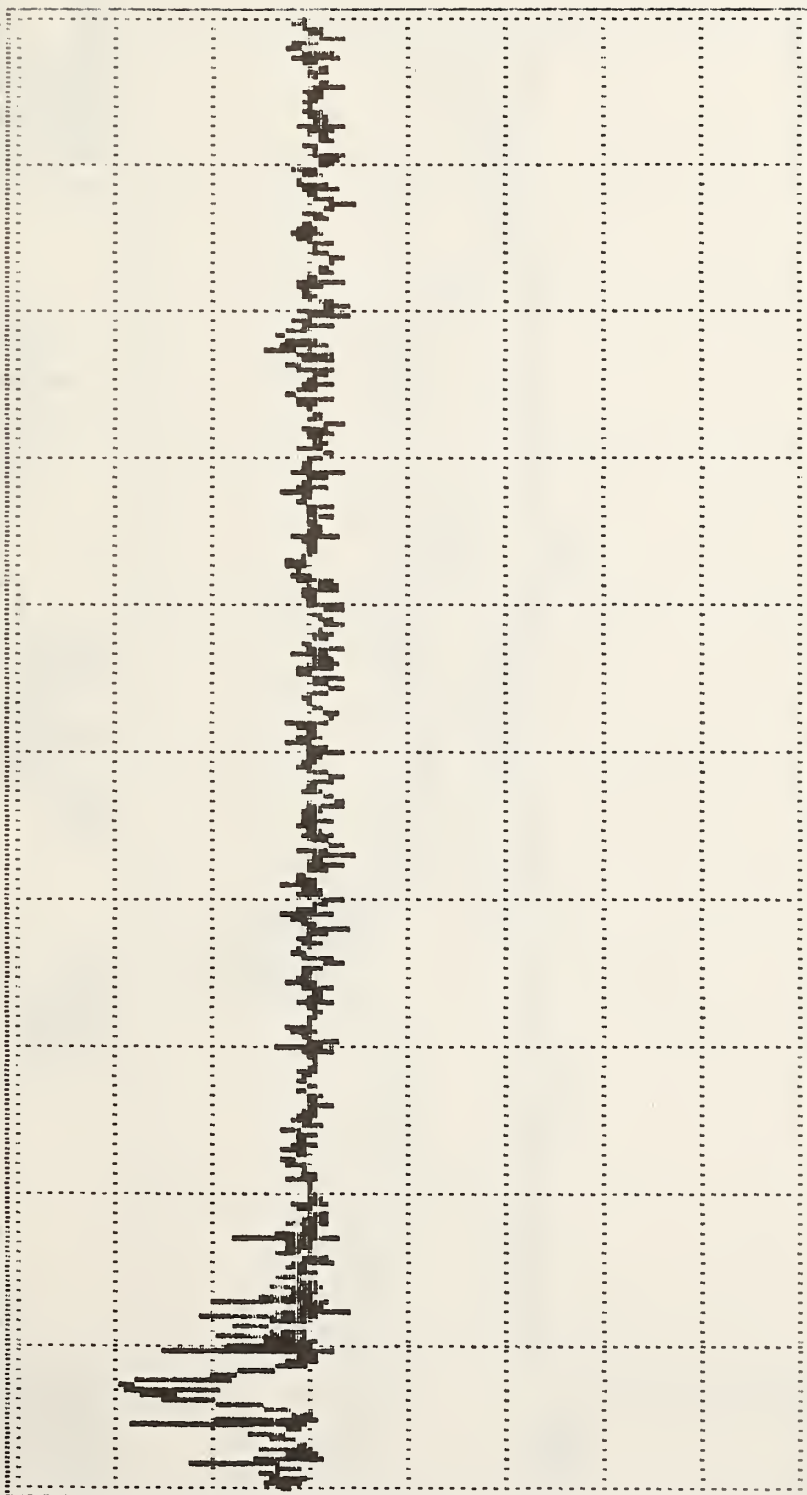
0-1.8
FRQ
RANGE
12:44:26/12-09-1986

0DB
RF
ATTN
Acquired

100KHZ
RES
BANDW
1986

Figure 58. Mohawk Airplane.

REF LEVEL -60DBM FREQUENCY 5.5MHZ SPAN 900KHZ



100DB/VID 0-1.8 100KHZ
 DISPLAY RANGE FILTER RES
 D09061 Acquired 12:42:26/12-09-1986 BANDW

Figure 59. Mohawk Airplane.

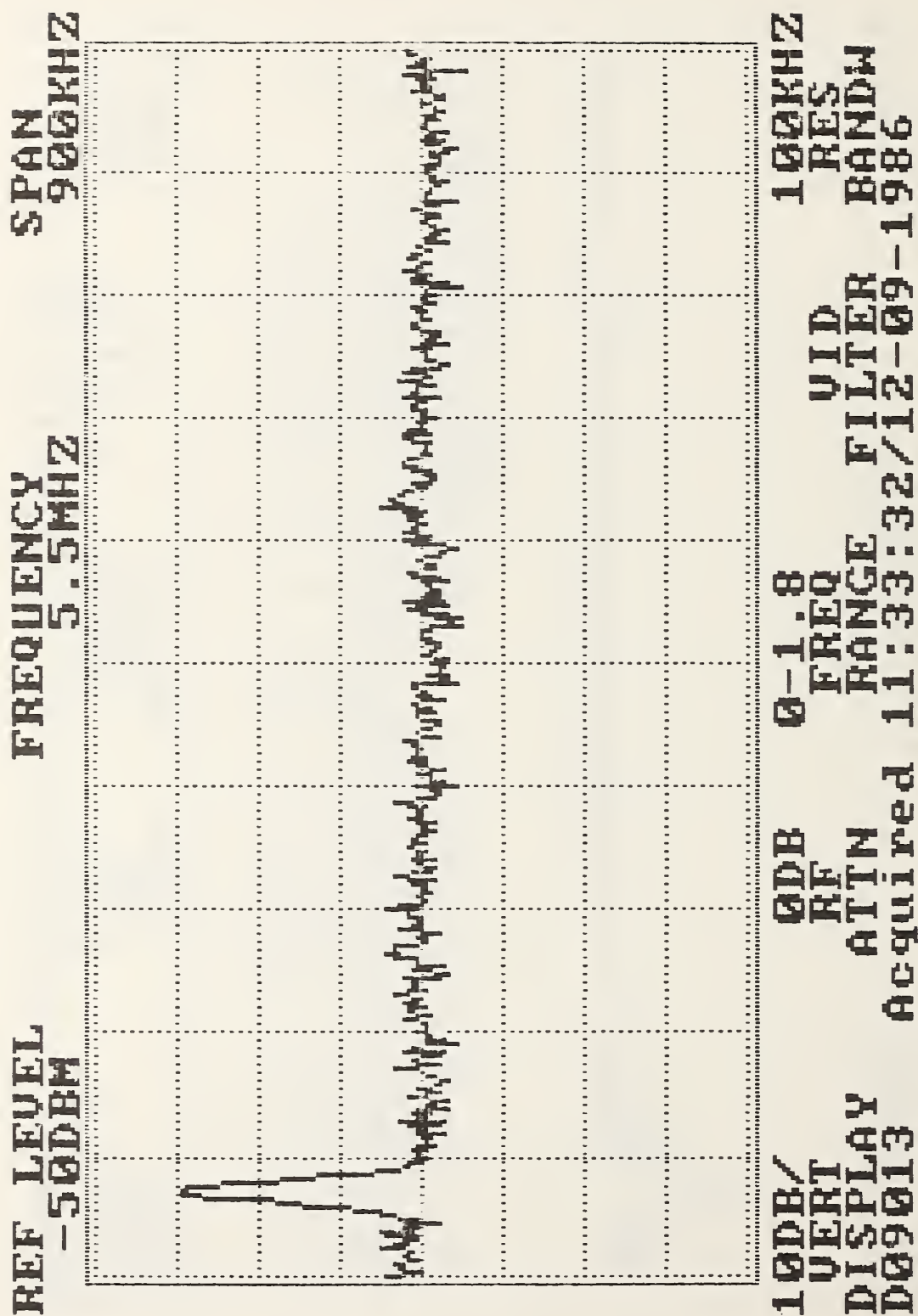
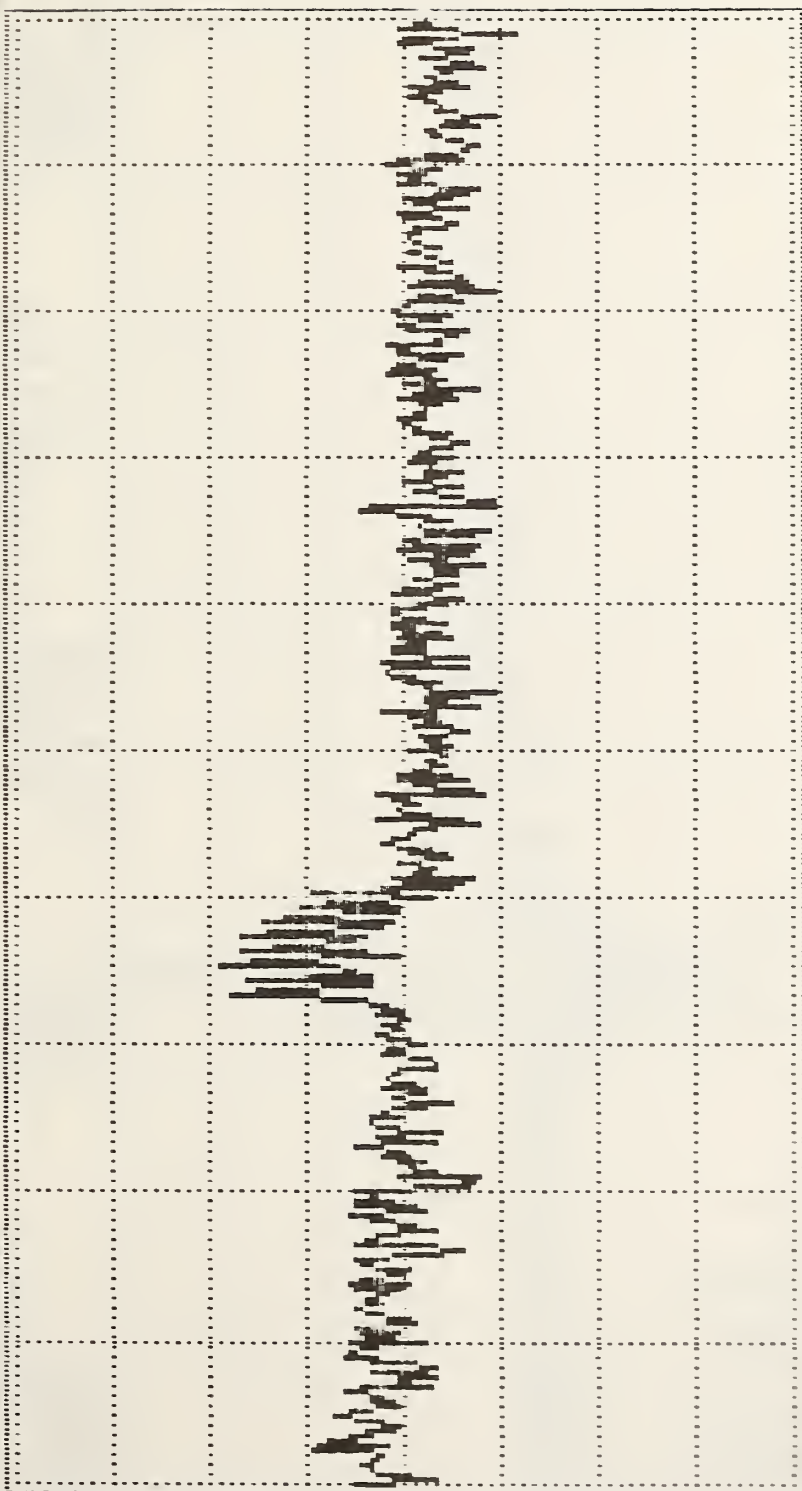


Figure 60. Mohawk Airplane.

REF LEVEL -50DBM FREQUENCY 125KHZ SPAN 15KHZ



10DB/VERT 0-1.8 KHZ RES 10KHZ
 DISPLAY FREQ 125KHZ BANDW 15KHZ
 D09020 ATTN 11:40:56/12-09-1986

Figure 61. Mohawk Airplane.

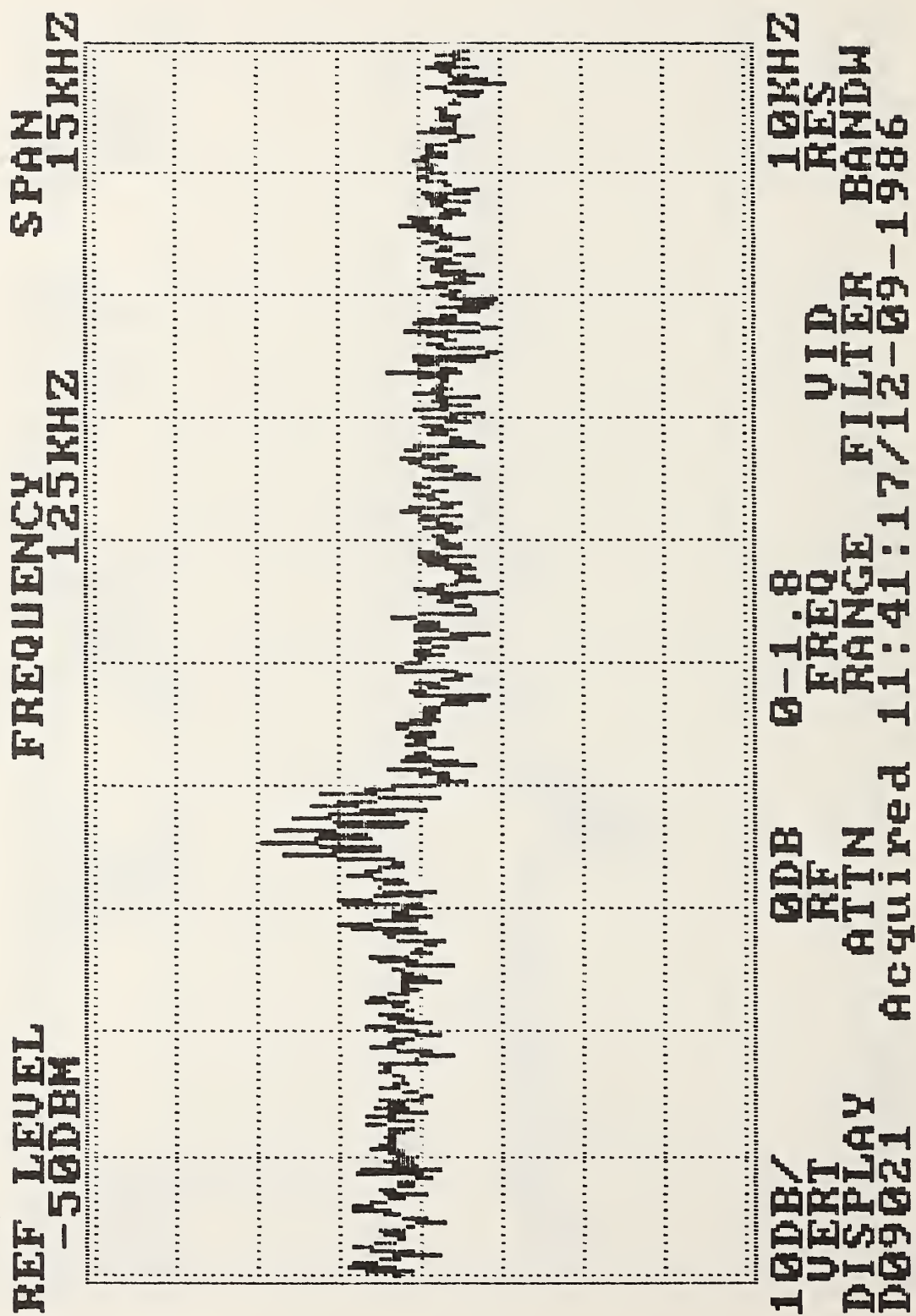


Figure 62. Mohawk Airplane.

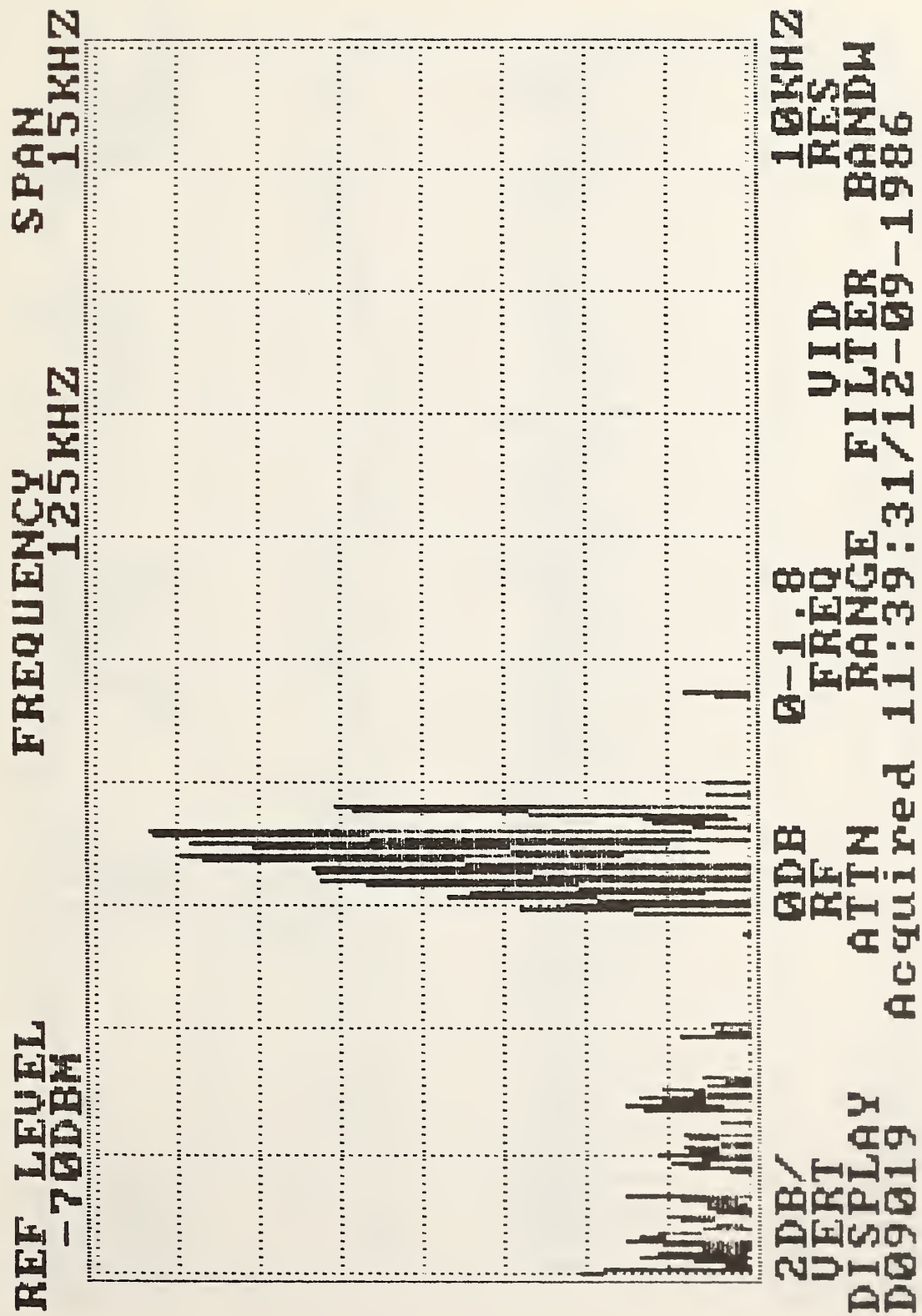


Figure 63. Mohawk Airplane.

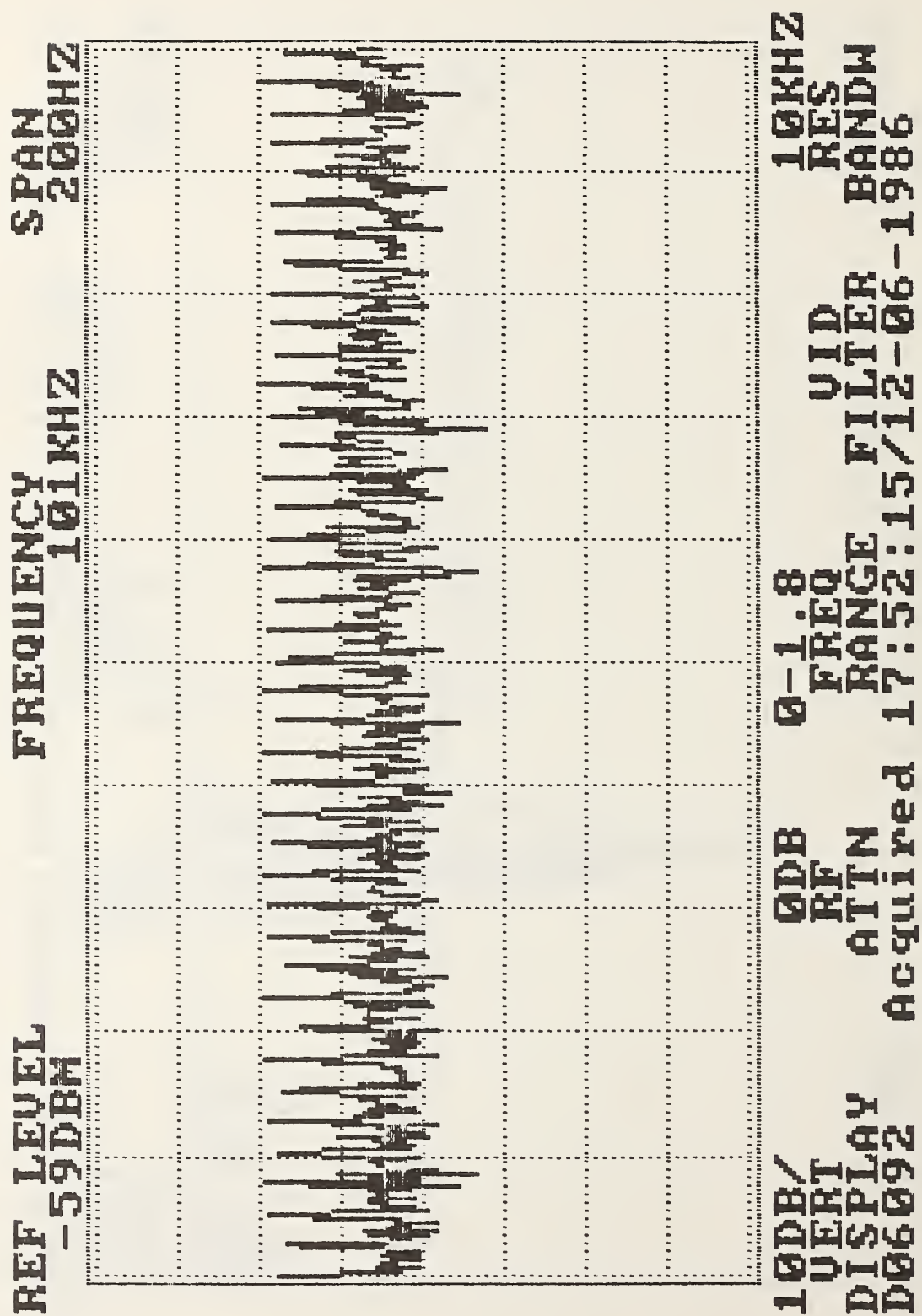


Figure 64. Huey Helicopter No. 1

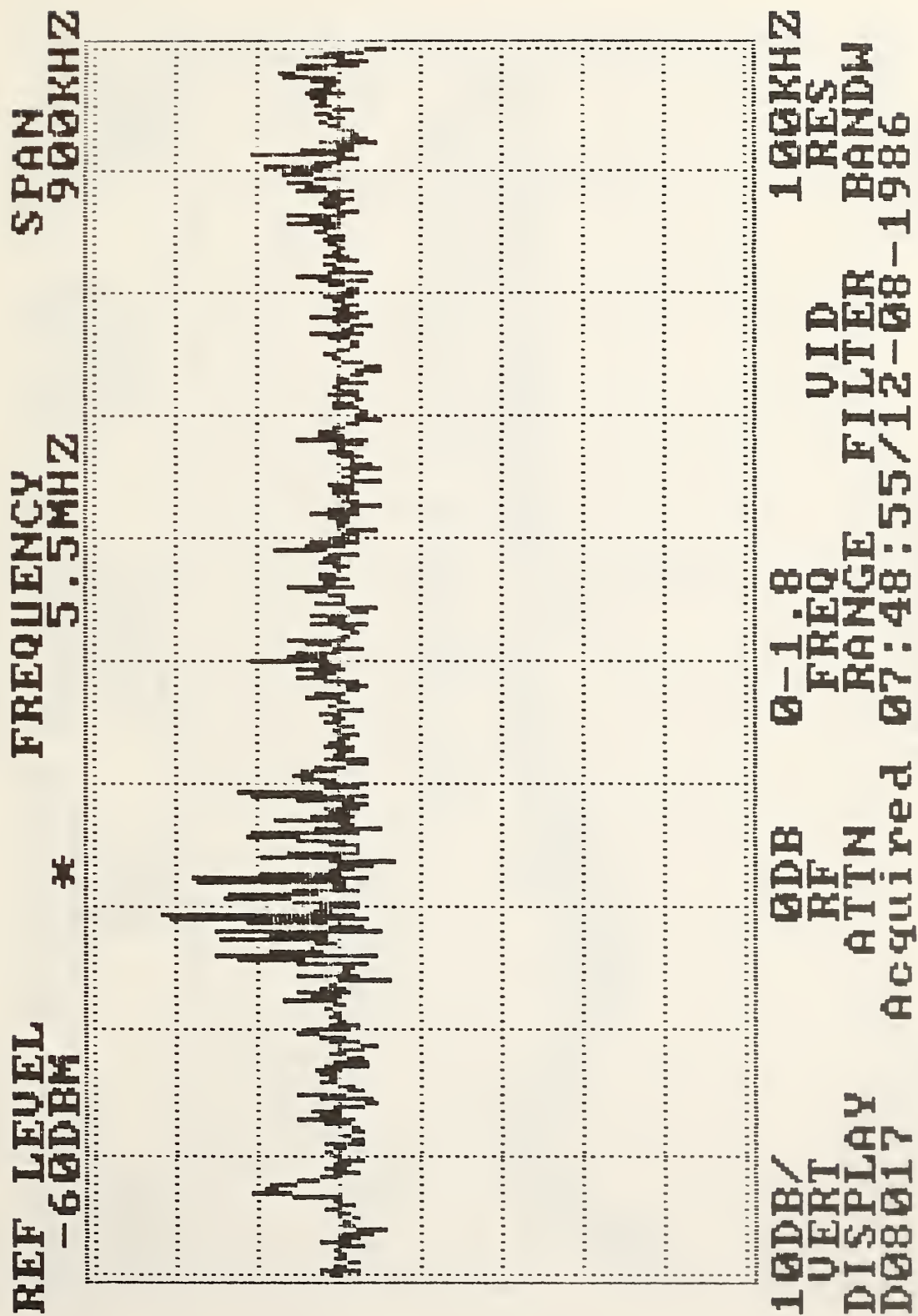


Figure 65. Huey Helicopter No. 2

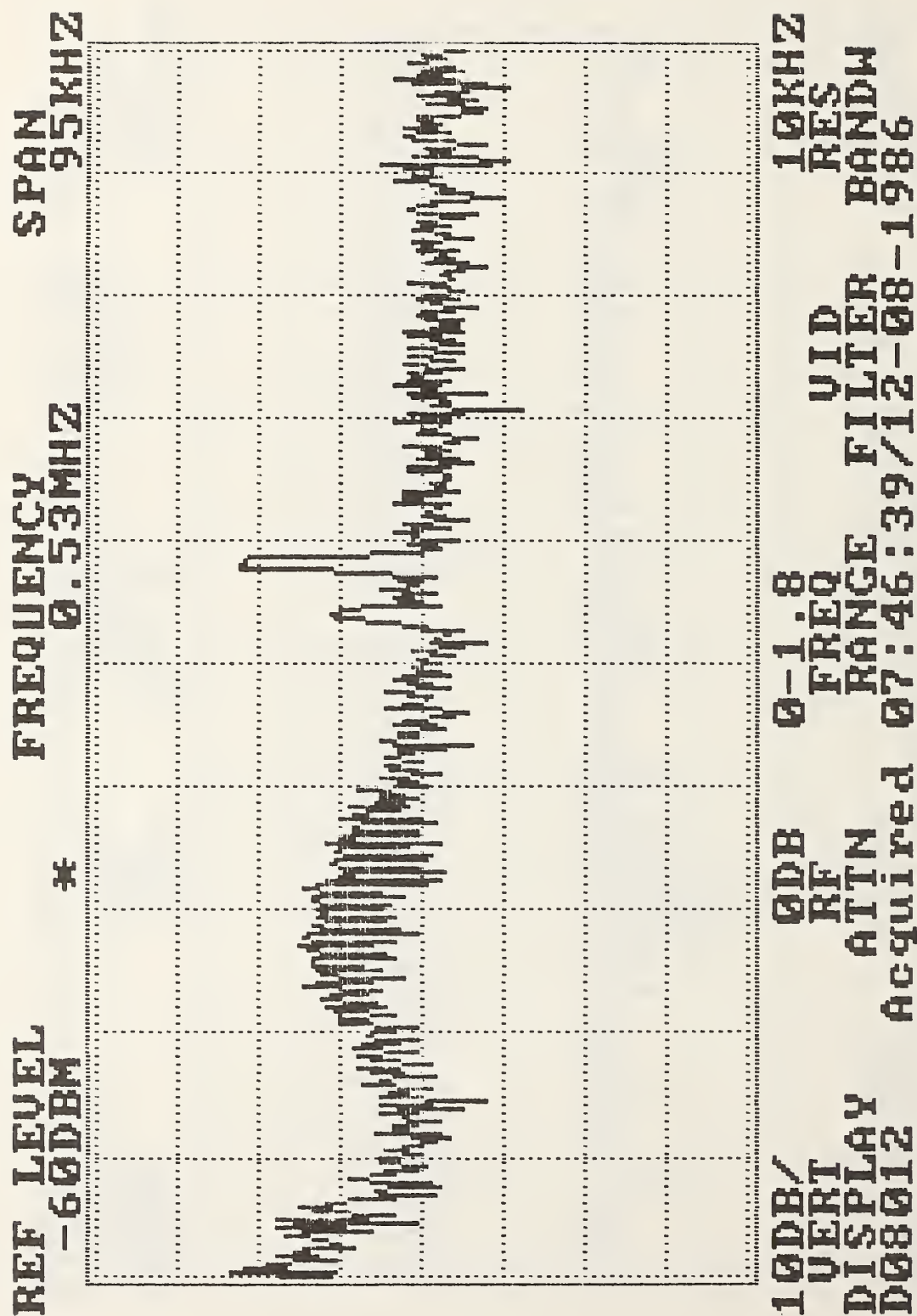


Figure 66. Huey Helicopter No. 2

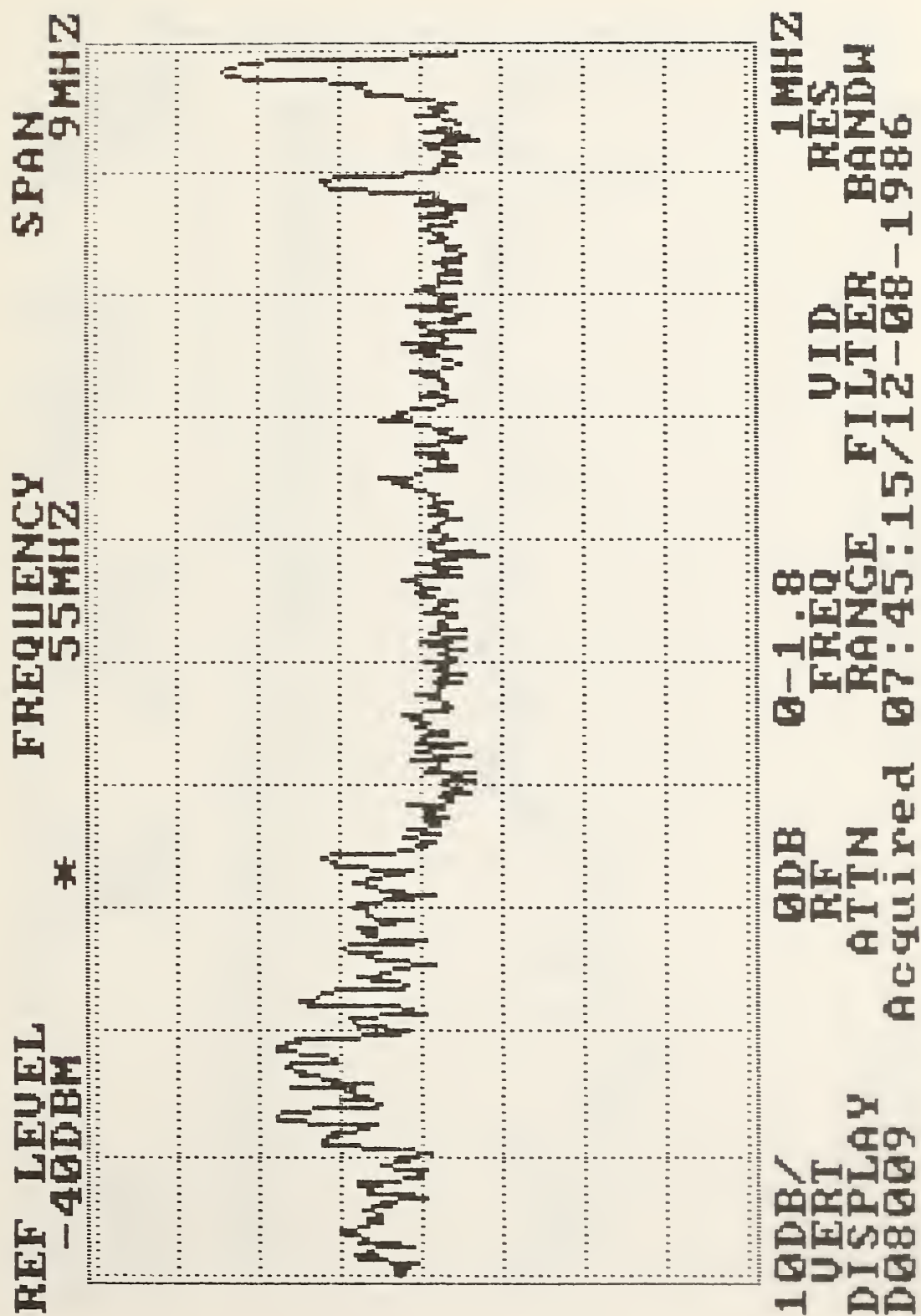
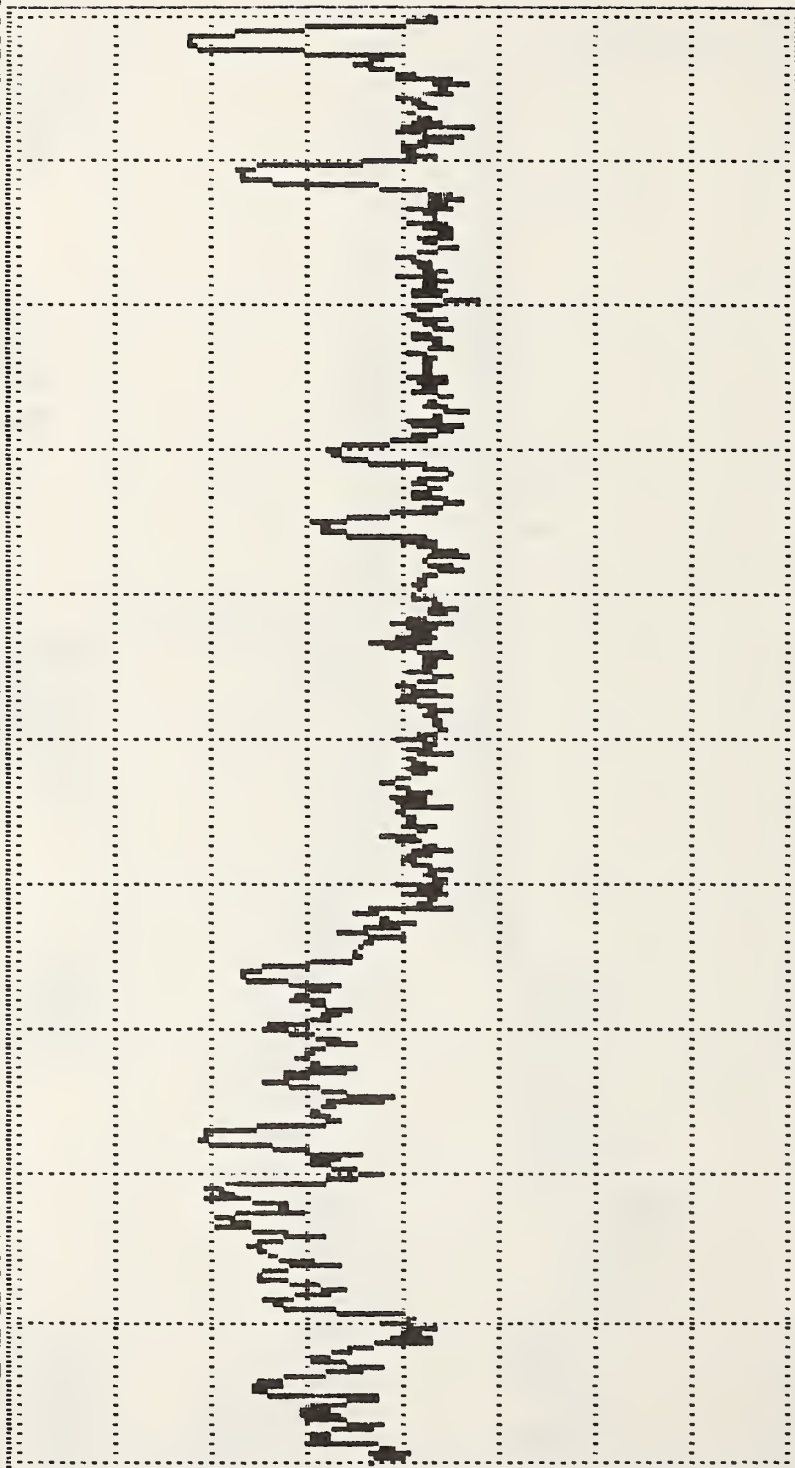


Figure 67. Huey Helicopter No. 2

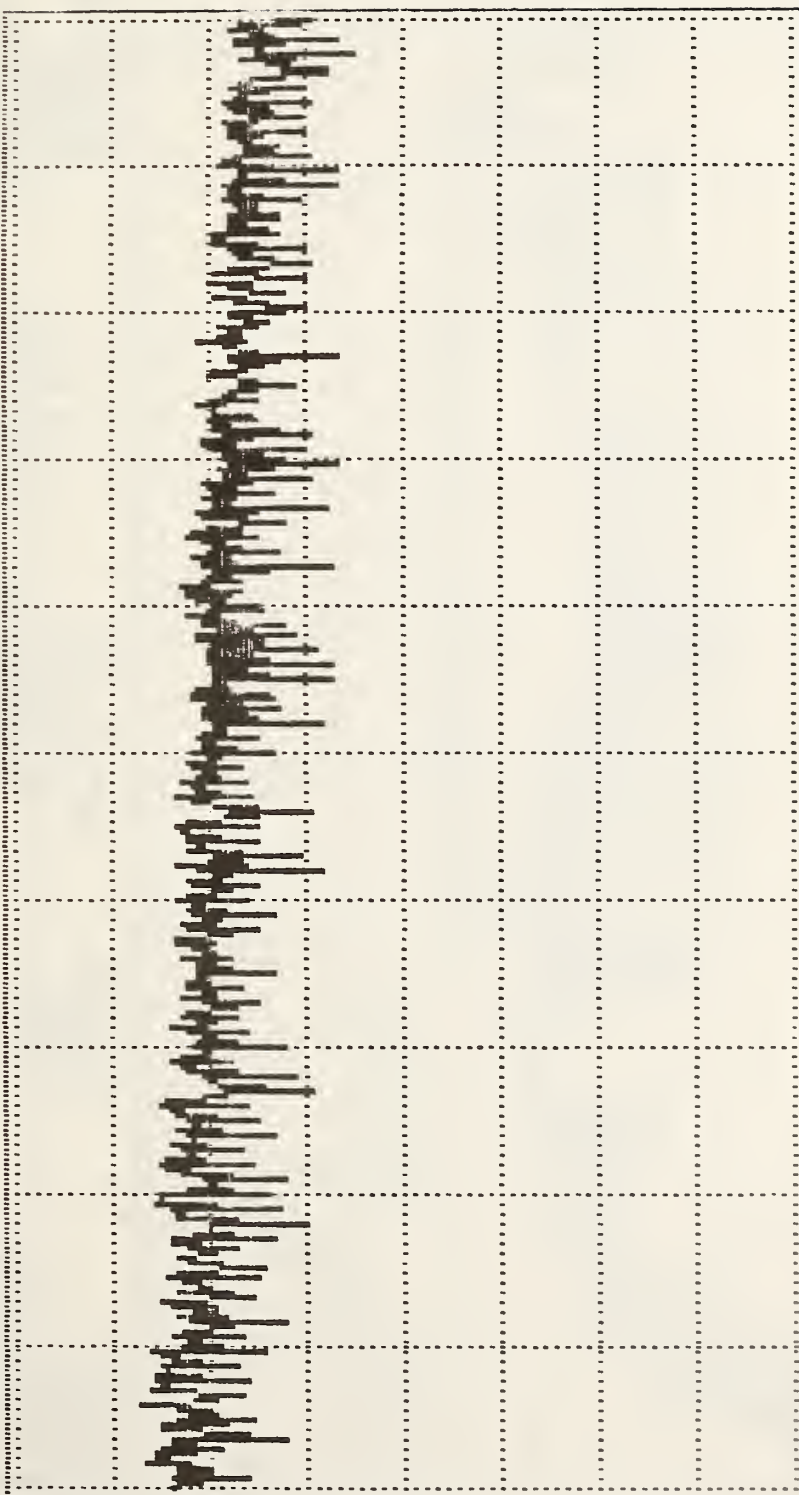
REF LEVEL -40DBM FREQUENCY 50MHZ SPAN 9MHZ



10DB/ 0-1.8 1MHZ
 UERT REQ RES
 DISPLAY RANGE VID BANDW
 D07140 Acquired 16:20:12/12-07-1986

Figure 68. Huey Helicopter No. 2

REF LEVEL -47DBM FREQUENCY 125KHZ SPAN 5KHZ



10DB/VID 0-1.8 10DB RF 10DB RES 1KHZ
DISPLAY RANGE FILTER BANDW
D08174 Acquired 16:28:10/12-08-1986

Figure 69. Huey Helicopter No. 3

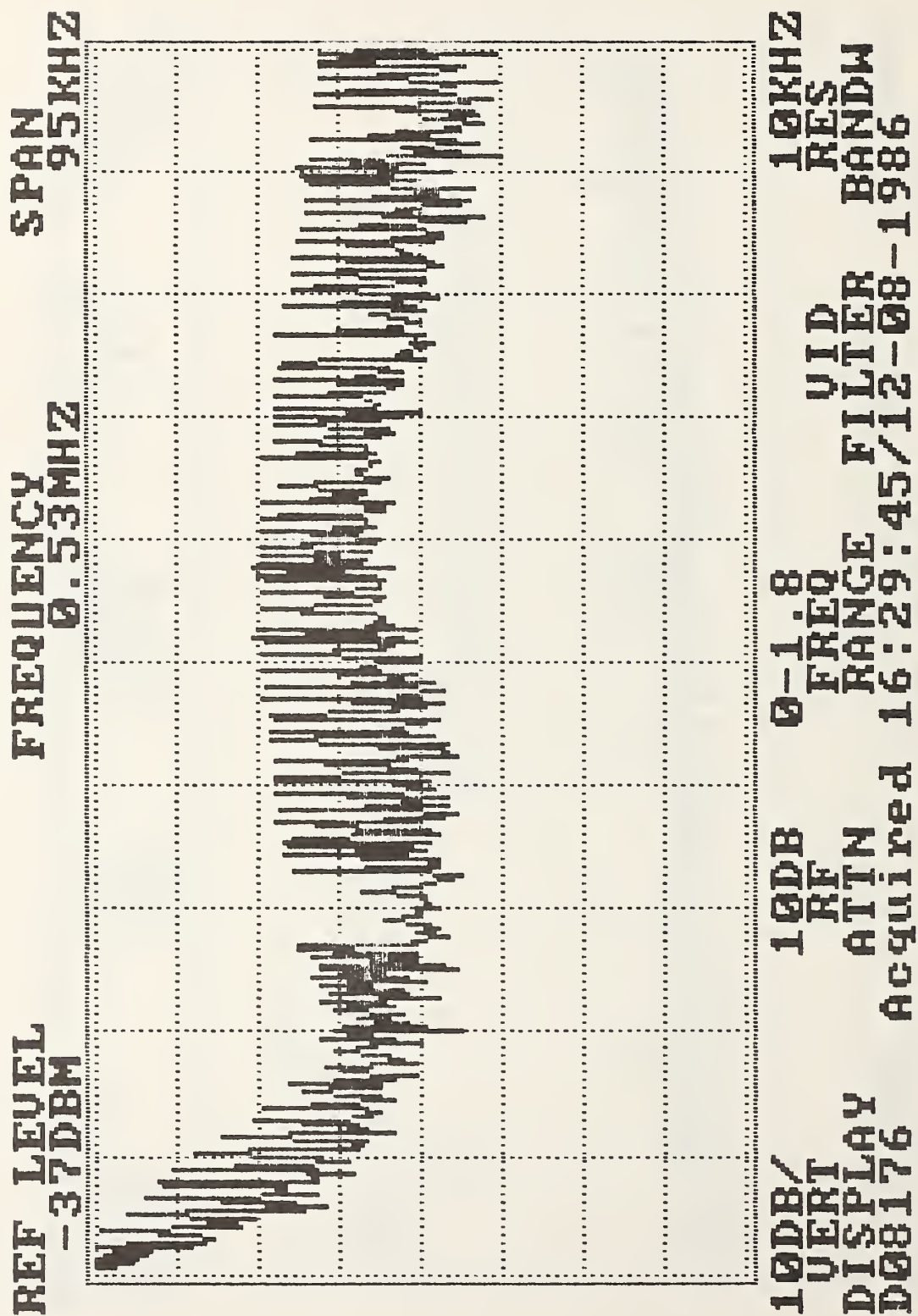


Figure 70. Huey Helicopter No. 3

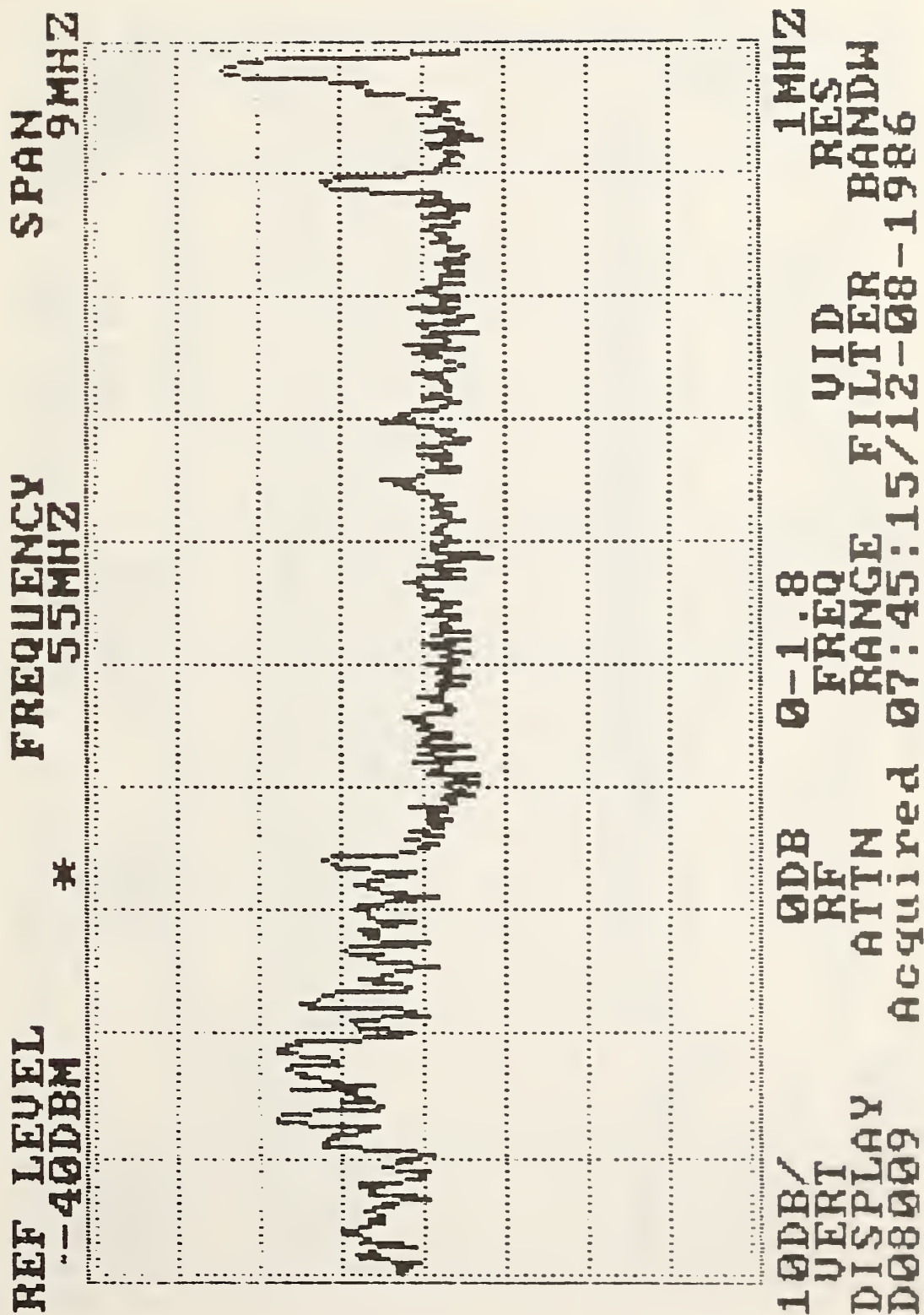


Figure 71, Huey No. 2

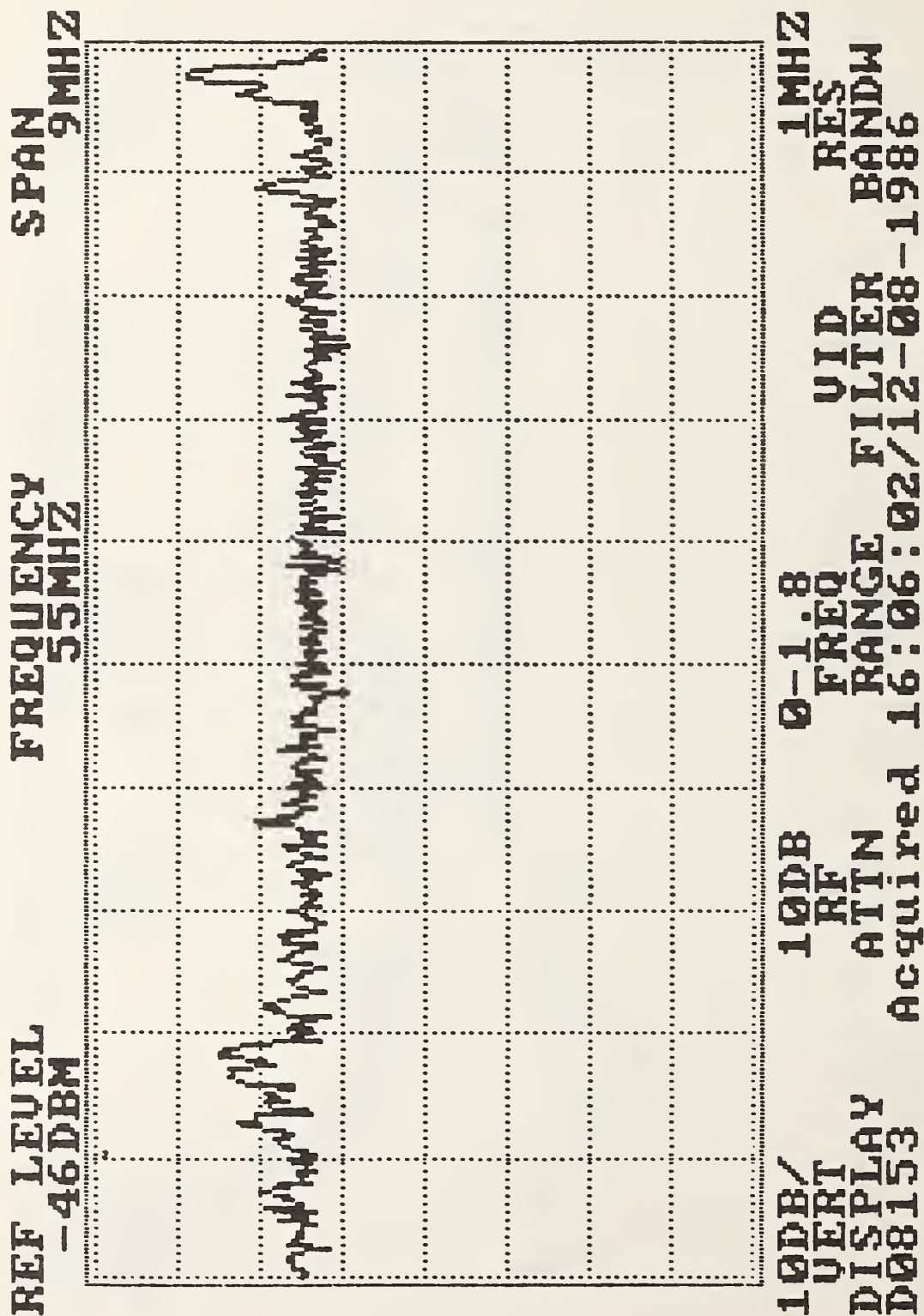


Figure 72, Huey No. 3

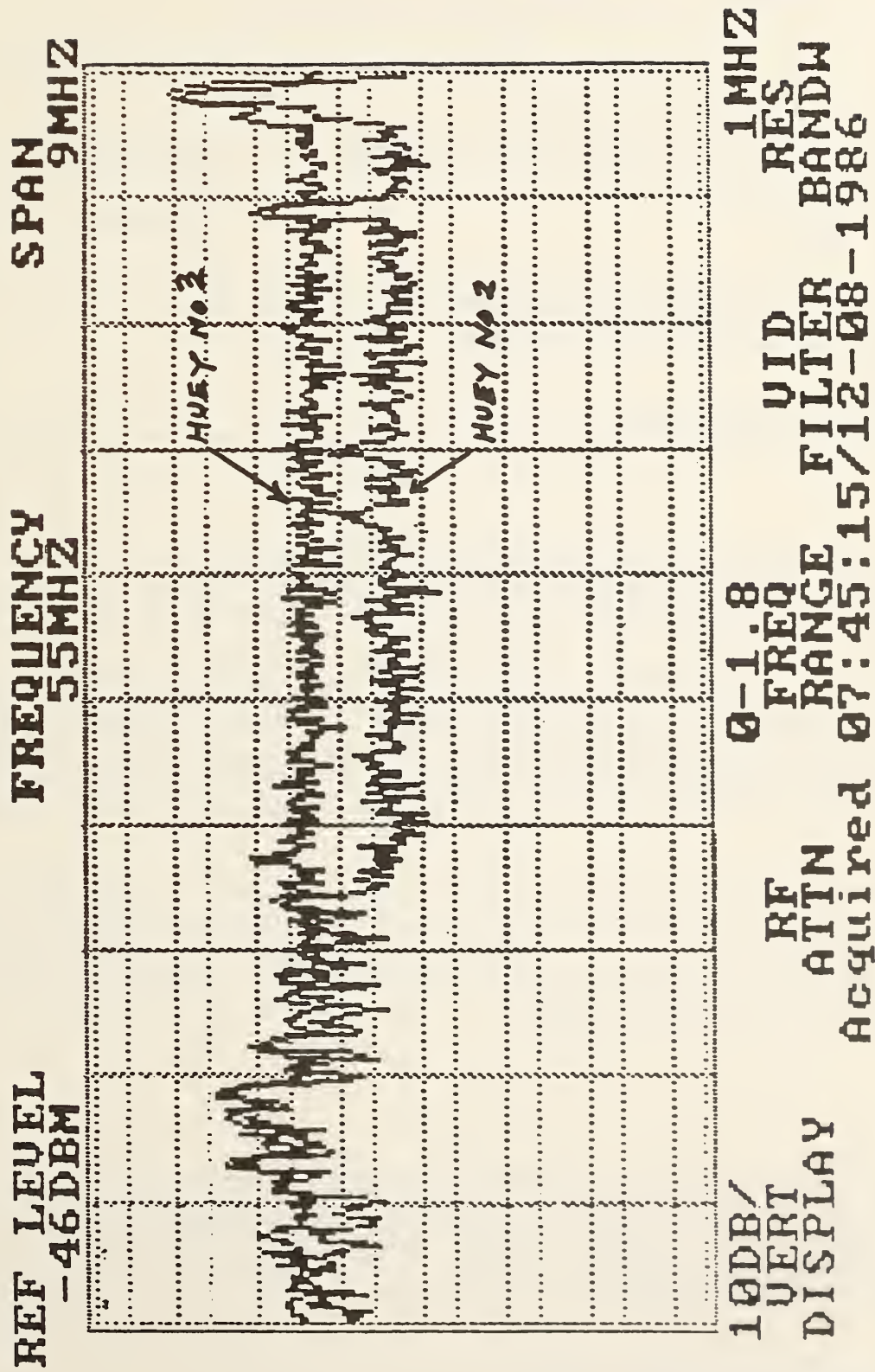


Figure 73, A comparison of the NOISE floor for Hueys No. 2 and No. 3

U.S. DEPT. OF COMM. BIBLIOGRAPHIC DATA SHEET (See instructions)		1. PUBLICATION OR REPORT NO. NBSIR 88-3083	2. Performing Organ. Report No.	3. Publication Date January 1988
4. TITLE AND SUBTITLE AIRCRAFT FIELD DEGRADATION AND ELECTROMAGNETIC COMPATIBILITY				
5. AUTHOR(S) Kenneth H. Cavcey and Dennis S. Friday				
6. PERFORMING ORGANIZATION (If joint or other than NBS, see instructions) NATIONAL BUREAU OF STANDARDS DEPARTMENT OF COMMERCE WASHINGTON, D.C. 20234			7. Contract/Grant No.	8. Type of Report & Period Covered
9. SPONSORING ORGANIZATION NAME AND COMPLETE ADDRESS (Street, City, State, ZIP) U.S. Army Aviation Systems Command (AVSCOM) ATTN: AMSAV-QP 4300 Goodfellow Boulevard St. Louis, Missouri 63120-1798				
10. SUPPLEMENTARY NOTES <input type="checkbox"/> Document describes a computer program; SF-185, FIPS Software Summary, is attached.				
11. ABSTRACT (A 200-word or less factual summary of most significant information. If document includes a significant bibliography or literature survey, mention it here) This paper discusses the first tests undertaken to study the problem of field degradation in army aircraft (helicopters and one fixed wing airplane) due to the deterioration of electronic and electrical systems. The electromagnetic compatibility (EMC) of such systems was investigated by passive measurement of the aircraft as a collection of radio frequency sources. Methods for detection of these sources were developed that included sensitivity to both stationary and nonstationary noise that existed. The collected data were studied to see if there existed any obvious factors derived from the data that one could use to correct potential problems that might affect flight safety. Emphasis was placed upon making such test methods appropriate, inexpensive, and easily performed by army field personnel. In addition, applications to quality control or acceptance testing, as related to the Environmental Stress Screening (ESS) program, were examined.				
12. KEY WORDS (Six to twelve entries; alphabetical order; capitalize only proper names; and separate key words by semicolons) bandwidth; data acquisition; electromagnetic compatibility (EMC); electromagnetic interference (EMI); electromagnetic spectrum ; field probes (or antenna); noise floor; noise sources; spectrum analyzer				
13. AVAILABILITY <input checked="" type="checkbox"/> Unlimited <input type="checkbox"/> For Official Distribution. Do Not Release to NTIS <input type="checkbox"/> Order From Superintendent of Documents, U.S. Government Printing Office, Washington, D.C. 20402. <input checked="" type="checkbox"/> Order From National Technical Information Service (NTIS), Springfield, VA. 22161			14. NO. OF PRINTED PAGES 100 15. Price	

